Dear Dr. Zhang:

Please find below our itemized responses to the reviewer's comments. We have addressed the comments raised by both reviewers, and incorporated their comments / suggestions in the revised manuscript.

Thank you very much for your consideration.

Sincerely,

***Xuejun Liu and Zhaozhong Feng***

On behalf of all co-authors

---

**Anonymous Referee #1**

This paper presented spatial and temporal trends of reactive nitrogen species in air, precipitation and deposition in eastern China. Some of the spatial patterns described in the paper are interesting, such as the higher rural concentrations observed in the northern region compared to the southern region. The paper discusses the need for ammonia emissions policies to reduce reactive nitrogen in air and in deposition. The nitrogen datasets from this ground-based measurement network is valuable; however, a longer dataset needs to be collected before it is suitable for analyzing temporal trends. With only five years of data, this could be the main reason why most of the annual trends were not significant. Another concern that I have is a lack of explanation on the causes of the spatial and temporal trends, which requires analyzing the reactive nitrogen data with other datasets. The discussions seems biased towards ammonia emissions reductions as a more effective means of reducing reactive nitrogen than $NO_x$ and $SO_2$ emissions reductions, but I don't think there is enough evidence in this study supporting this conclusion.

**Response:** Thanks for the referee's thoughtful and critical comments on our manuscript. Below we provide a point-by-point response to the reviewer' comments and how we have addressed them in the revised manuscript (in blue).

**Specific comments**

Line 77: Define Nr since this is the first time that it is mentioned in the paper.

**Response:** $N_r$ has been defined as “reactive nitrogen” occurring in the first time in the text.

Line 83: Be more careful about linking deposition of N to increased greenhouse gas emissions. The referenced article only suggests that the nitrogen cycle is coupled with the carbon cycle and climate variation; however, the latter could be influenced by many factors.

**Response:** We have deleted “increased greenhouse gas emissions” and the referenced article in the revision.

Lines 110-111: The analysis presented by Xu et al. (2015) is quite similar to this study in terms of the measurement network, nitrogen species, time period, and site categories analyzed. The authors should discuss the previous study and explain how this study is different to avoid presenting a duplicate analysis.

**Response:** Thank you for this valuable suggestion. In the revised paper, we have added some sentences to discuss the study of Xu et al., 2015), and explain why the current study is different from the previous one. For details, please see our response to next comment (Lines 148-156).

Lines 148-156: This is where it might be appropriate to discuss the previous study, Xu et al. (2015), and emphasize the new work that will be shown in this study.

**Response**: The main purpose of this study was to reveal spatial-temporal (annual and seasonal) patterns of $N_r$ concentrations and deposition based on a full 5-year (2011-2015) measurement at 27 NNDMN sites in eastern China and its northern and southern parts. It also should be noted that, although the study of Xu et al. (2015) and this study both examined the spatial patterns, the regions divided are different. In contrast, the study of Xu et al., 2015 mainly focused on spatial pattern of N deposition at six regions in China, and did not consider seasonal and annual trends. We have added the following sentences in the revision.

**“**Our previous work (Xu et al., 2015) used multiyear measurements (mainly from Jan. 2010 to Sep. 2014) at the 43 sites in the NNDMN, aiming to provide the first quantitative information on atmospheric $N_r$ concentrations and pollution status across China, and to analyze overall fluxes and spatial variations of N deposition in relation

to anthropogenic $N_r$ emissions from six regions**”.**

Reference:

Xu, W., Luo, X.S., Pan, Y.P., Zhang, L., Tang, A.H., Shen, J.L., Zhang, Y., Li, K.H., Wu, Q.H., Yang, D.W., Zhang, Y.Y., Xue, J., Li, W.Q., Li, Q.Q., Tang, L., Lu, S.H., Liang, T., Tong, Y.A., Liu, P., Zhang, Q., Xiong, Z.Q., Shi, X.J., Wu, L.H., Shi, W.Q., Tian, K., Zhong, X.H., Shi, K., Tang, Q.Y., Zhang, L.J., Huang, J.L., He, C.E., Kuang, F.H., Zhu, B., Liu, H., Jin, X., Xin, Y.J., Shi, X.K., Du, E.Z., Dore, A.J., Tang, S., Collett, J.L., Goulding, K., Sun, Y.X., Ren, J., Zhang, F.S., and Liu, X.J.: Quantifying atmospheric nitrogen deposition through a nationwide monitoring network across China, Atmos. Chem. Phys. 15 (13), 12345–12360, 2015.

Line 170: Suggest using “and” instead of “resulting in” because this sentence suggests there is a relationship between economic development and nitrogen emissions. If there is such relationship, please elaborate.

**Response**: Agree and done.

Lines 220-221: You need to be clearer about what type of deposition the open sampler collects. Why is it only “some” dry deposition? Isn’t the sampler open to the atmosphere which means it is collecting total deposition?

**Response**: We ensure that N deposition collected by continuously-open rain gauge refers to wet/bulk deposition, rather than total deposition. Wet/bulk deposition is generally defined as the sum of wet plus some dusts in non-precipitation period (i.e. sedimentary deposition); while dry deposition includes both gases and particles deposition (in which dust or sedimentary deposition is not included). In fact, the wet/bulk plus dry deposition consists of total N deposition without overestimation.

Although N-containing gases and fine particles can be deposited in the 'dry' form to the sampler funnel, the amount of N captured is negligible compared with the dry deposition to plant canopies (Dämmgen et al., 2005; Sutton and Bleeker, 2013). Thus, it is only “some” or small part dry deposition. To make it clearer, “some” was replaced by “incomplete” in the revision.

References:

Dämmgen, U., Erisman, J. W., Cape, J. N., Grünhage, L., and Fowler, D.: Practical

considerations for addressing uncertainties in monitoring bulk deposition, Environ. Pollut. 134(3), 535–548, 2004.

Sutton, M.A., and Bleeker, A.: Environmental science: the shape of nitrogen to come. Nature 494, 435–437, 2013.

Line 271: The dates here should be January 2011 to 30 September 2014 because you stated in the next sentence that the data after 30 September 2014 were not used.

**Response**: This was a wrong expression in the sentence. Actually, we used the daily IASI-$NH_3$ data from 1 January 2011 to 31 December 2015 for the spatial analysis, and from January 2011 to 30 September 2014 for temporal analysis.

We now state that "The daily IASI-$NH_3$ data (provided by the Atmospheric Spectroscopy Group at Université Libre De Bruxelles, data available at http://iasi.aeris-data.fr/$NH_3$/) from 1 January 2011 to 31 December 2015 was used for the spatial analysis in the present study. For the temporal analysis, we used the IASI_$NH_3$ from 1 January 2011 to 30 September 2014 because an update of the input meteorological data on 30 September 2014 had caused a substantial increase in the retrieved atmospheric $NH_3$ columns."

Lines 347-349: The concentration ranges are not clear. Is it the range of the mean concentration between sites or between years?

**Response**: The ranges of mean concentrations denote the minimum and maximum 5-year mean concentrations of measured five $N_r$ species (i.e., $NH_3$, $NO_2$, $HNO_3$, $pNH_4^+$, and $pNO_3^-$) for each land use type (i.e., urban, rural and background), which can be derived from Table 1. For example, the values of 1.6 ± 0.2 and 10.2 ± 1.0 μg N $m^{-3}$ are 5-year mean concentrations of $HNO_3$ and $NO_2$ at urban sites in eastern China, respectively.

To make it clear, in the revision we now state that "In eastern China, annual mean concentrations of $NH_3$, $NO_2$, $HNO_3$, $pNH_4^+$, and $pNO_3^-$ at the urban sites (averages for the 5-year, 1.6 ± 0.2 (for $HNO_3$) to 10.2 ± 1.0 (for $NO_2$) μg N $m^{-3}$) increased by 18, 70, 33, 23, and 43%, respectively, compared with their corresponding concentrations at the rural sites (1.2 ± 1.0 (for $HNO_3$) to 7.2 ± 0.9 (for $NH_3$) μg N $m^{-3}$); they also increased by 78-118% compared with the concentrations at the

background sites (0.9 ± 0.1 (for $HNO_3$) to 5.2 ± 0.3 (for $NO_2$) μg N $m^{-3}$) (Table 1)."

Lines 350-352: What is the reason for the lower concentrations at urban sites in the northern region?

**Response**: This is mainly due to the fact that the North China Plain (NCP, that is, the plain areas in Beijing, Tianjin, Hebei, Henan, and Shandong provinces) is located in the northern region. The Plain (i.e., NCP) is featured by intensive agricultural production in rural areas, which contributes 30-40% of the total annual $NH_3$ emissions in China (Huang et al., 2012). In addition, the north is dominated by calcareous soils, which favor high soil $NH_3$ volatilization from croplands (Huang et al., 2015). Those emitted $NH_3$ can directly enhance ambient $NH_3$ concentration and also particulate $NH_4^+$ concentrations via chemical reactions between $NH_3$ and acidic gases in the atmosphere (e.g., $H_2SO_4$ and $HNO_3$).

References:

Huang, X., Song, Y., Li, M. M., Li, J. F., Huo, Q., Cai, X. H., Zhu, T., Hu, M., and Zhang, H. S: A high-resolution ammonia emission inventory in China, Global Biogeochem. Cycles 26, GB1030, 2012.

Huang, P., Zhang, J. B., Xin, X. L., Zhu, A. N., Zhang, C. Z., Ma, D. H., Zhu, Q. G., Yang, S., and Wu, S. J.: Proton accumulation accelerated by heavy chemical nitrogen fertilization and its long-term impact on acidifying rate in a typical arable soil in the Huang-Huai-Hai Plain, J. Integr. Agric. 14, 148–157, 2015.

Lines 359-365: I suggest analyzing which nitrogen species was particularly higher between urban and rural sites and between northern and southern regions because this would provide some insight whether the patterns are related to a specific type of emission source.

**Response**: Good point. In the old version, we have made a comparison of annual mean concentration of each $N_r$ species between urban and rural sites, as shown in Table 1. In Results Section, we also stated that "In eastern China, annual mean concentrations of $NH_3$, $NO_2$, $HNO_3$, $pNH_4^+$, and $pNO_3^-$ at the urban sites (1.6 ± 0.2 to 10.2 ± 1.0 μg N $m^{-3}$) were 18-70% and 78-118% higher than their corresponding concentrations at the rural (1.2 ± 1.0 to 7.2 ± 0.9 μg N $m^{-3}$) and background (0.9 ± 0.1

to 5.2 ± 0.3 μg N $m^{-3}$) sites, respectively.". According to suggestion by the reviewer, the sentence was revised to make it clearer, and now reads as "In eastern China, annual mean concentrations of $NH_3$, $NO_2$, $HNO_3$, $pNH_4^+$, and $pNO_3^-$ at the urban sites (averages for the 5-year, 1.6 ± 0.2 (for $HNO_3$) to 10.2 ± 1.0 (for $NO_2$) μg N $m^{-3}$) increased by 18, 70, 33, 23, and 43%, respectively, compared with their corresponding concentrations at the rural sites (1.2 ± 1.0 (for $HNO_3$) to 7.2 ± 0.9 (for $NH_3$) μg N $m^{-3}$); they also increased by 78-118% compared with the concentrations at the background sites (0.9 ± 0.1 (for $HNO_3$) to 5.2 ± 0.3 (for $NO_2$) μg N $m^{-3}$) (Table 1)."

As for comparisons between northern and southern regions, we added the following sentence in the revision.

"Averaged across three land use types, the annual mean $N_r$ concentrations of five $N_r$ species in the north increased to varying extent (by 84% for $pNO_3^-$, 63% for $pNH_4^+$, 57% for $NH_3$, 47% for $NO_2$, and 28% for $HNO_3$) compared with those in the south.".

Lines 371-374: What is the reason for the higher precipitation concentrations in northern rural sites compared to southern rural sites? Is this related to the higher air concentrations of Nr species in northern rural sites?

**Response**: Yes, it is mainly due to significantly ($p$<0.05) higher air concentrations of five $N_r$ species at northern rural sites than at southern rural sites (Table 1), as $NH_4^+$-N and $NO_3^-$-N in precipitation primarily originates from reduced N (e.g., gaseous $NH_3$ and particulate $NH_4^+$) and oxidized N (e.g., gaseous $NO_2$, $HNO_3$, and particulate $NO_3^-$) in air (Wang et al., 2018). Another reason is the "concentration effect" because annual precipitation is much lower in the north (e.g. 400-600 mm per year) than in the south (e.g. 800-1400 mm per year).

Reference:

Wang, H.B., Shi, G.M., Tian, M., Chen, Y.., Qiao, B.Q., Zhang, L.Y., Yang, F.M., Zhang, L.M., and Luo, Q.: Wet deposition and sources of inorganic nitrogen in the Three Gorges Reservoir Region, China, Environ. Pollut., 233, 520-528, 2018.

Lines 383-401: Presenting only the annual trends in the Nr concentrations is not enough. I think that additional analysis with other variables is necessary to attempt to

explain the trends in Nr concentrations (e.g. emissions data). As stated in the introduction, one of the goals of this study is to assess the effectiveness of emissions control measures.

**Response:** We partly agree with the referee. Given that $N_r$ ($NH_3$ and $NO_2$) emissions and concentrations are in different units, and higher $N_r$ concentrations generally result in higher N deposition on an annual timescale, the comparison of $N_r$ emissions with deposition (both are calculated in the unit of kg N $ha^{-1}$ $yr^{-1}$) is more reasonable relative to the comparison between $N_r$ emissions and concentrations. As the main objective of this study is to spatial-temporal patterns of atmospheric inorganic N concentrations and deposition, we presented relevant results of $N_r$ concentrations and deposition in the Results, and put the comparison between $N_r$ emission and deposition in the Discussions (please see Section 4.5 in the old version). Therefore, we keep the analysis as it is.

According to the referee's suggestion, here we also attempt to make the corresponding comparisons using the annual average values on $N_r$ emissions ($NH_3$ and $NO_x$) and air concentrations of $NH_3$ and $NO_2$ at the sixteen sites (details are given in Section 4.5). As shown in Figure 1 below, across all the sites annual mean $NH_3$ emissions and concentrations showed increases of 4 and 20% in 2013-2015 compared with those in 2011-2015, respectively. Correspondingly, annual mean $NO_x$ emissions and $NO_2$ concentrations showed reductions of 18 and 2%, respectively. In addition, there were no significant ($p$>0.05) correlations between $NH_3$ emissions and concentrations, and between $NO_x$ emissions and concentrations during 2011-2015.

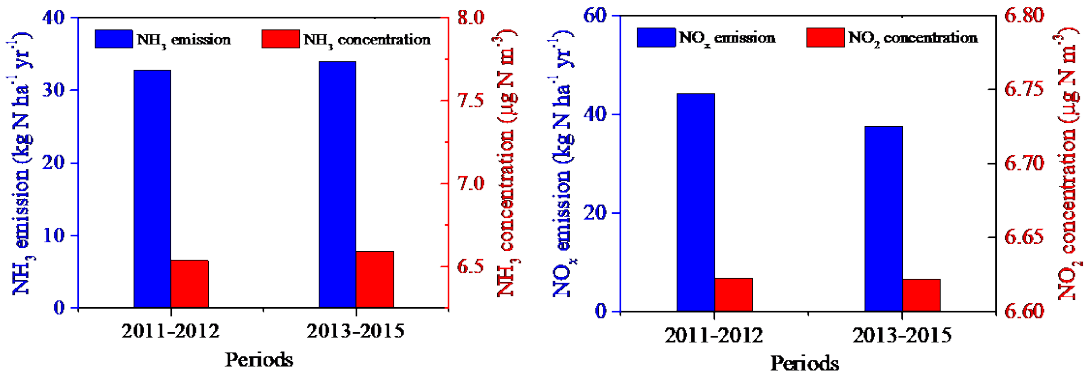

Figure 1. Comparisons of $NH_3$ emissions and $NH_3$ concentrations, and $NO_x$ emissions and $NO_2$ concentrations between the periods 2011-2012 and 2013-2015.

Lines 411-416: Any relationships between precipitation concentration and air concentration trends?

**Response:** Based on analysis of annual averages at the sixteen sites with continuous and simultaneous measurements of dry and wet/bulk N deposition during 2011-2015 (site names are given in Fig. S6 and Table S1), a positive relationship (r=0.62, *p*=0.27) was found between $NH_4^+$-N concentrations in precipitation and air concentrations of reduced $N_r$ (the sum of $NH_3$ and particulate $NH_4^+$), whereas a negative relationship (r= -0.85, *p*=0.07) was found between $NO_3^-$-N concentration in precipitation and air concentration of oxidized $N_r$ (the sum of $NO_2$, $HNO_3$, and particulate $NO_3^-$). We think that those findings are acceptable. This is because that $NH_3$ is locally deposited and relatively high $NH_3$ concentration generally distributed near emission sources. In contrast, local oxidized $N_r$ concentration can be affected by atmospheric transport from nearby regions. No significant correlations between precipitation concentration and air concentration are mainly due to relatively small changes in $NH_3$ and $NO_x$ emissions (Fig. 12) and annual mean precipitation amount (from 800 to 951 mm, Fig. S14) during 2011-2015.

Lines 422-436: What is the reason for the seasonal trends? E.g. changes in emissions, meteorology, and/or air mass patterns? I think these other factors need to be analyzed in order to understand what is influencing the seasonal trends.

**Response:** Thank you for pointing it out, and we have analyzed the seasonal trends of $N_r$ concentrations integrated with changes air mass trajectory (please see added context in Section 4.2). As for $N_r$ emissions, it is well known that $NH_3$ emissions in China typically peaked in summer due to the summertime application of fertilizer for double cropping in together with higher temperature, and the lowest values occurred in winter (Paulot et al., 2014; Kang et al., 2016; Zhang et al., 2018). In contrast, the highest $NO_2$ emissions generally occur in winter because of domestic heating needs, and minimum values generally occur in spring (Zhang et al., 2007). Thus, we directly used previous literature reported to explain corresponding results in the present study.

References:

Paulot, F., Jacob, D.J., Pinder, R.W., Bash, J.O., Travis, K., and Henze, D.K.: Ammonia emissions in the United States, European Union, and China derived by high-resolution inversion of ammonium wet deposition data: Interpretation with a new agricultural emissions inventory (MASAGE_$NH_3$), J. Geophys. Res. Atmos., 119, 4343–4364, https://doi:10.1002/2013JD021130, 2014.

Kang, Y. N., Liu, M. X., Song, Y., Huang, X., Yao, H., Cai, X. H., Zhang, H. S., Kang, L., Liu, X. J., Yan, X. Y., He, H., Zhang, Q., Shao, M., and Zhu, T.: High-resolution ammonia emissions inventories in China from 1980 to 2012, Atmos. Chem. Phys., 16, 2043–2058, 2016.

Zhang, Q., Streets, D. G., He, K., Wang, Y., Richter, A., Burrows, J. P., Uno, I., Jang, C. J., Chen, D., Yao, Z., and Lei, Y.: $NO_x$ emission trends for China, 1995-2004: The view from the ground and the view from space, J. Geophys. Res., 112, D22306, 2007.

Zhang, L., Chen, Y. F., Zhao, Y. H., Henze, D. K., Zhu, L. Y., Song, Y., Paulot, F., Liu, X. J., Pan, Y. P., and Huang, B. X.: Agricultural ammonia emissions in China: reconciling bottom-up and top-down estimates, Atmos. Chem. Phys., 18, 339–355, 2018.

Line 478: Instead of presenting bulk deposition, is it possible to estimate wet deposition fluxes by subtracting the dry deposition fluxes from bulk deposition? This allows a comparison between wet and dry deposition.

**Response:** Our previous work (Liu et al., 2006; Zhang et al., 2008) showed the ratios of wet-only and bulk deposition of inorganic N being 0.68-0.93 in North China Plain. Therefore it seems not possible to estimate wet deposition fluxes by multiplying a coefficient or subtracting the dry deposition fluxes from bulk deposition, since fraction of dry deposited N in bulk deposition is variable and not fixed across monitoring years. Anyway, we mentioned this in the revision.

References:

Liu X.J., Ju X.T., Zhang Y., He C.E., Kopsch J., and Zhang F.S.: Nitrogen deposition in agroecosystems in the Beijing area. Agriculture, Ecosystems & Environment 113,

370-377, 2006.

Zhang Y., Liu X.J., Fangmeier A., Goulding K.T.W., and Zhang F.S.: Nitrogen inputs and isotopes in precipitation in the North China Plain. Atmospheric Environment 42, 1436-1448, 2008.

Lines 462-481: How do these deposition fluxes compare to other parts of the world over this recent time period? I also recommend plotting the spatial distribution of the deposition fluxes on a map because it is difficult to get a sense of the spatial patterns from the text and numbers in this paragraph.

**Response:** On the basis of 2001 ensemble-mean modeling results from 21 global chemical transport models (Vet et al., 2014), three global N deposition hotspots were western Europe (with levels from 20.0 to 28.1 kg N $ha^{-1}$ $yr^{-1}$, South Asia (Pakistan, India, and Bangladesh) from 20.0 to 30.6 kg N $ha^{-1}$ $yr^{-1}$ and East Asia from 20 to 38.6 kg N $ha^{-1}$ $yr^{-1}$ in eastern China (the global maximum). Extensive areas of high deposition from 10 to 20 kg N $ha^{-1}$ $yr^{-1}$ appear in the eastern United States and southeastern Canada as well as most of central Europe. Obviously, our estimated total N deposition fluxes (dry plus wet/bulk deposition, averaging from 34.2 kg N $ha^{-1}$ $yr^{-1}$ at background sites to 59.7 kg N $ha^{-1}$ $yr^{-1}$ at urban sites, Table 1) showed a much higher values. Relevant comparisons have been reported in our previous work (Xu et al., 2015).

As for data presentation, we think that the use of Table is reasonable and useful due to following two reasons. First, our analysis was based on land use types rather than single sampling site, and thus it is impractical to plot the spatial distribution of the deposition fluxes on a map. Second, using Tables can directly provide basic data for scientific communities for carrying out other relevant research. Therefore, we keep the Table as it is.

References:

Xu, W., Luo, X.S., Pan, Y.P., Zhang, L., Tang, A.H., Shen, J.L., Zhang, Y., Li, K.H., Wu, Q.H., Yang, D.W., Zhang, Y.Y., Xue, J., Li, W.Q., Li, Q.Q., Tang, L., Lu, S.H., Liang, T., Tong, Y.A., Liu, P., Zhang, Q., Xiong, Z.Q., Shi, X.J., Wu, L.H., Shi, W.Q., Tian, K., Zhong, X.H., Shi, K., Tang, Q.Y., Zhang, L.J., Huang, J.L., He,

C.E., Kuang, F.H., Zhu, B., Liu, H., Jin, X., Xin, Y.J., Shi, X.K., Du, E.Z., Dore, A.J., Tang, S., Collett, J.L., Goulding, K., Sun, Y.X., Ren, J., Zhang, F.S., and Liu, X.J.: Quantifying atmospheric nitrogen deposition through a nationwide monitoring network across China. Atmos. Chem. Phys. 15 (13), 12345–12360, 2015.

Vet, R., Artz, R. S., Carou, S., Shaw, M., Ro, C.-U., Aas, W., Baker, A., Bowersox, V. C., Dentener, F., Galy-Lacaux, C., Hou, A., Pienaar, J. J., Gillett, R., Forti, M. C., Gromov, S., Hara, H., Khodzher, T., Mahowald, N. M., Nickovic, S., Rao, P. S. P., and Reid, N. W.: A global assessment of precipitation chemistry and deposition of sulfur, nitrogen, sea salt, base cations, organic acids, acidity and pH, and phosphorus, Atmos. Environ., 93, 3–100, 2014.

Line 572: If you sum dry and wet/bulk deposition fluxes, the total deposition will be overestimated because the bulk deposition already includes dry deposition.

**Response:** This concern was answered in our previous response to "Lines 220-221". In fact, our wet/bulk (including wet plus sedimentary deposition) + dry deposition (gases plus fine particles (non-sedimentary) deposition) denote a complete total N deposition. This means the wet/bulk deposition is not pure 'wet' deposition while the dry deposition is not complete 'dry' deposition. According to our previous studies (Liu et al., 2006; Zhang et al., 2008), annual difference between bulk and wet deposition was 1.3-9.6 kg N $ha^{-1}$ in northern Chinese agroecosystems. Therefore, to avoid misunderstanding, we defined the total N deposition as the sum of dry and bulk deposition in this study, although it is in principle defined as the sum of dry and wet deposition.

References:

Liu, X.J., Ju, X.T., Zhang, Y., He, C.E., Kopsch, J., and Zhang, F.S.: Nitrogen deposition in agroecosystems in the Beijing area, Agr. Ecosyst. Environ. 113(1), 370–377, doi:10.1016/j.agee.2005.11.002, 2006.

Zhang, Y., Liu, X. J., Fangmeier, A., Goulding, K. T. W., and Zhang, F. S.: Nitrogen inputs and isotopes in precipitation in the North China Plain, Atmos. Environ., 42, 1436–1448, 2008.

Figure 8: Could you discuss the results in Fig. 8b? All of the previous trends were

urban > rural > background. I find it interesting that the trend for the ratio of reduced to oxidized N is reversed. Also, why is this ratio important?

**Response:** The opposite trend for the ratio of reduced to oxidized N is reasonable, as it depends on proportion of reduced and oxidized N deposition in the total deposition. This ratio can be used to indicate the relative contribution of $N_r$ from agricultural and industrial activities to N deposition (Xu et al., 2015) because the major anthropogenic source of reduced N ($NH_3$ and particulate $NH_4^+$) is mainly affected by $NH_3$ volatilized from animal excrement and the application of nitrogenous fertilizers in agriculture, while anthropogenic sources of oxidized N ($NO_2$, $HNO_3$ and particulate $NO_3^-$) is primarily dominated by $NO_x$ emitted from fossil fuel combustion in transportation, power plant, and factories.

As shown in Fig. 8b, the averaged ratios at three land use types were slightly higher in the 2013-2015 period than in the 2011-2012 period, indicating agricultural $NH_3$ emission played a more and more important role in N deposition. This result, in turn, supports our conclusion from sensitivity tests by the GEOS-Chem model that mitigation of agricultural $NH_3$ emissions should be a priority to tackle serious N deposition in eastern China.

As suggested by the referee, we added the following discussion in the revision (in the Section 4.4):

"This conclusion to some extent is supported by increased ratios of the ratio of reduced to oxidized N in the total deposition at three land use types (Fig. 8b), as the major anthropogenic source of reduced N is mainly affected by $NH_3$ volatilized from animal excrement and the application of nitrogenous fertilizers in agriculture. Absence of $NH_3$ emission controls may be the main reason for a small and non-significant change in the total N deposition between 2011-12 and 2013-15 (Fig. S6, Supplement), despite enforcement of stringent emission controls on $NO_x$ and $SO_2$."

Reference:

Xu, W., Luo, X.S., Pan, Y.P., Zhang, L., Tang, A.H., Shen, J.L., Zhang, Y., Li, K.H., Wu, Q.H., Yang, D.W., Zhang, Y.Y., Xue, J., Li, W.Q., Li, Q.Q., Tang, L., Lu, S.H.,

Liang, T., Tong, Y.A., Liu, P., Zhang, Q., Xiong, Z.Q., Shi, X.J., Wu, L.H., Shi, W.Q., Tian, K., Zhong, X.H., Shi, K., Tang, Q.Y., Zhang, L.J., Huang, J.L., He, C.E., Kuang, F.H., Zhu, B., Liu, H., Jin, X., Xin, Y.J., Shi, X.K., Du, E.Z., Dore, A.J., Tang, S., Collett, J.L., Goulding, K., Sun, Y.X., Ren, J., Zhang, F.S., and Liu, X.J.: Quantifying atmospheric nitrogen deposition through a nationwide monitoring network across China, Atmos. Chem. Phys. 15 (13), 12345–12360, 2015.

Section 4.1 and Figure 9: The correlation results show there is good agreement between satellite and ground-based observations. Can you quantify the differences using metrics? E.g., what are the percent differences for each month and annually? The correlation may be good, but the actual concentrations can still be different. Given the good relationship between satellite and surface measurements, are long term satellite data available for conducting temporal trend analysis?

**Response:** It is difficult to quantify the differences between satellite and ground-based observations using a uniform unit. Since ground and satellite measurements give the mixing ratios of $N_r$ species ($NH_3$ and $NO_2$) in the surface layer and tropospheric integrated column densities of the species, respectively, estimating the satellite-derived ground concentrations of $N_r$ species required their corresponding vertical profiles. Unfortunately, measurements of vertical profiles of concentrations above the surface are rare. On this point, in earlier version we stated in the text “To make a more accurate comparison, the vertical profile is recommended to convert the columns to the ground concentrations in future work”. Alternatively, we analyzed the correlations between satellite and ground-based observations to detect whether there is a consistency in spatial and temporal distributions.

As for temporal analysis, the following paragraph in the Section 4.1 can answer whether long term satellite data are available for conducting temporal trend analysis.

“…the OMI_$NO_2$ retrieval can well capture the temporal variations of surface $NO_2$ concentrations over eastern China, whereas the IASI_$NH_3$ retrievals better capture temporal variability in surface concentrations for the northern region. The weak correlations observed between IASI_$NH_3$ observations and surface measurements at ten of the fourteen sites in the southern region (Fig. S7, Supplement) suggest that the

IASI_$NH_3$ observations need to be improved for investigating temporal variability in $NH_3$ concentration, despite that the satellite observation is at a specific time of day while the surface concentrations integrate across the diurnal cycle of emissions and mixing layer evolution."

Section 4.2: There is too much speculation on the causes of the seasonal trends. Most of the discussion is based on what previous literature reported. I think you need to analyze other datasets to examine the factors affecting the Nr trends.

**Response:** In the revision, we analyzed datasets of air mass trajectory to examine influence of potential atmospheric transport on the resulting seasonal $N_r$ trends. The following paragraphs were added as follows:

"In order to identify potential transport of $NO_2$, $pNH_4^+$ and $pNO_3^-$ from northern region, we calculated three-day backward trajectories arriving at five southern sites (Nanjing, Baiyun, Taojing, Ziyang and Huinong) during January, April, July and October using the TrajStat. The TrajStat analysis generally showed that the high proportions (overall 10-36%) of air masses from the north to the south of eastern China occurred in the autumn/winter, suggesting that the transport of $NO_2$, $pNH_4^+$ and $pNO_3^-$ from northern China would result in increases in their respective concentrations in autumn/winter south of the Qinling Mountains-Huaihe River line, except at Ziyang site (Fig. S14, Supplement).

Line 725: Could you provide the actual emissions amount from x tonnes in 2010 to y tonnes in 2014? Even though the emissions declined by a certain percentage, the actual emissions amount in 2014 might still be very large. If this is the case, then you will likely not observe a significant decrease in Nr concentrations.

**Response:** In the revised paper, we added the actual emission amount for the years 2010 and 2014. We now state that "…total annual emissions of $SO_2$ and $NO_x$ were reduced by 12.9% and 8.6% in 2014 (approximately 9.9 Tg S $yr^{-1}$ and 6.3 Tg N $yr^{-1}$, respectively), respectively, compared with those in 2010 (approximately 11.3 Tg S $yr^{-1}$ and 6.9 Tg N $yr^{-1}$, respectively)".

Yes, since $NO_x$ emissions were still at high level in 2014. We did not find a significant

decrease in $NO_2$ concentrations in the current study. For total $N_r$, persistent high concentrations is likely due to the absence of $NH_3$ regulations, as $NH_3$ emission reduction had a larger influence on $N_r$ concentration (for details, please see our response to next comment to Lines 733-734)

Lines 733-734: How much ammonia is emitted relative to NOx and SO2? I would think NOx and SO2 emissions are higher than those of ammonia. If this is the case, wouldn't NOx and SO2 emissions reductions have larger effects on Nr?

**Response:** Yes, total annual emissions of $NO_x$ and $SO_2$ (average over 2011-2015, approximately 7.0 Tg N $yr^{-1}$ and 9.8 Tg S $yr^{-1}$) were higher than those of $NH_3$ emission (10.0 Tg N $yr^{-1}$) during the period of 2011-2015 in eastern China (details of emission data are given in Section 4.5). In addition, the annual molar ratios of $(2SO_2+NO_x)/NH_3$ were greater than 1 (ranging from 1.3 to 1.8) during the period. These results suggest that $NH_3$ emissions presented the limiting factor to the formation of secondary inorganic ions (e.g., particulate $NH_4^+$ and $NO_3^-$), and its emission reductions have large effects on $N_r$ (e.g., gaseous $NH_3$ and particulate $NH_4^+$ and $NO_3^-$). This is also true at the national scale, as the molar amount of $(2SO_2+NO_x)$ still substantially exceeded that of $NH_3$ at least until 2015 (Zhang et al., 2017).

Reference:

Zhang, X. M., Wu, Y. Y., Liu, X. J., Reis, S., Jin, J. X., Dragosits, U., Damme, Van M., Clarisse, L., Whitburn, S., and Coheur, P. F.: Ammonia emissions may be substantially underestimated in China, Environ. Sci. Techno., 51, 12089-12096, 2017.

Lines 757-773: I don't think you can really say that ammonia emissions reductions are more important than NOx and SO2 emissions reductions. If ammonia emissions have been increasing, why is the Nr concentration in air and precipitation not increasing (many of the trends were not significant in sect. 3.2)? Also, is it possible that the NOx and SO2 emissions reductions are not large enough? See earlier comment about the actual emissions amount for NOx and SO2 could be very large despite 9-13% decrease in emissions. Is it appropriate to make this conclusion given that five years of data were analyzed? You also discussed how ammonia neutralizes

acidic gases and plays a role in limiting Nr. However, it does not mean that this process is more effective than reducing NOx and SO2 emissions which decrease the formation of acidic gases in the first place.

**Response:** Based on the discussions in Lines 757-773, we did not give the viewpoint that $NH_3$ emissions reductions are more important than $NO_x$ and $SO_2$ emissions reductions. We concluded that implementation of $NH_3$ control strategies, relative to current $NO_x$ and $SO_2$ emission controls, should be considered to mitigate atmospheric $N_r$ pollution. Between the periods 2013-2015 and 2011-2012, the mean concentrations of $NH_3$ and $pNH_4^+$ overall showed non-significant increases (10-38%) at all land use types**,** whereas small changes in remaining $N_r$ species occurred. As a result, annual total $N_r$ concentration in air showed increases to varying extent at three land use types. This also highlights the importance of $NH_3$ emission reduction in controlling $N_r$ pollution. Indeed, for individual species small changes in air concentrations of $NO_2$, $HNO_3$ and $pNO_3^-$ may be due to that the $NO_x$ and $SO_2$ emissions reductions are not large enough.

To avoid misunderstanding, we now state that "implementation of $NH_3$ control strategies, together with more stringent $NO_x$ and $SO_2$ emission controls, should be considered to mitigate atmospheric $N_r$ pollution."

Lines 775-783: This paragraph needs to mention the NOx and SO2 emissions in the northern region especially given the increased emissions for winter heating? How does they compare with ammonia emissions over an annual basis? A map of the spatial distribution of the ammonia emissions and agriculture activity levels would easily demonstrate that these are higher in the northern region.

**Response:** Thank you for this suggestion. We added the following discussions in Section 4.4 in the revision.

"In addition, higher $NH_3$ concentration is also likely due to the higher $NH_3$ volatilization in calcareous soils than that in the acidic red soil, as mentioned in Section 2.1. Total annual $NH_3$ emissions in northern region increased from 4.3 Tg N $yr^{-1}$ in 2011 to 4.7 Tg N $yr^{-1}$ at an annual rate of 1.8%. In contrast, the emissions of $NO_x$ and $SO_2$ averaged 2.8 Tg N $yr^{-1}$ and 3.7 Tg S $yr^{-1}$ during 2011-2015, and

decreased at annual rates of 6.8 and 5.7%, respectively (details of the emissions will be illustrated in Section 4.5). Such reductions may enhance free $NH_3$ in the atmosphere. However, according to a modeling study by Han et al. (2017), the influence of removing anthropogenic $SO_2$ emissions on dry N deposition fluxes during 2010-2014 was quite weak, with the change within -0.5~0.5 (kg N $ha^{-1}$ $yr^{-1}$) over most regions in China."

We think that current discussion is sufficient to explain why total dry N deposition fluxes at three land use types were higher in the northern region of eastern China than in the southern region. Given that the article is already relatively lengthy and this part of discussion is not the core, we did not compare the spatial distribution of the ammonia emissions and agriculture activity levels in eastern China in the revision.

Reference:

Han, X., Zhang, M. G., Skorokhod, A., and Kou, X. X.: Modeling dry deposition of reactive nitrogen in China with RAMS-CMAQ, Atmos. Environ., 166, 47–61, 2017.

Line 801: This should be Fig. S12

**Response**: Corrected.

Line 803: This should be Sect. S2

**Response**: Corrected.

Lines 799-811: I think the model simulation and results require further analysis and discussion. The model apportions the contributions of various sources to ammonium and nitrate deposition and suggests agricultural activity is the main contributor. There needs to be more details on the model scenario (e.g. NH3 and NOx emissions estimated from the various sources). Is the larger contribution from agriculture due to larger emissions relative to other sources or is it because area sources have larger impact than point sources in the model? Also, to support the idea that NH3 emissions reductions are important in reducing Nr deposition, you could perform a sensitivity analysis using different scenarios of NH3 emissions reductions for future years.

**Response:** Thank you for this suggestion. The larger contribution from agriculture is due to larger emissions relative to other sources. In the revised paper, we now state

that "The total $NH_3$ and $NO_x$ emissions from each source over eastern China and its contribution to total emissions in China are presented in Table S13 in the Supplement. The $NH_3$ and $NO_x$ emissions over eastern China are 11.6 Tg N $yr^{-1}$ and 8.5 Tg N $yr^{-1}$ in 2010, which, respectively, account for 90% and 89% of their total emissions over China. Agricultural sources, including fertilizer use and livestock, comprise most of the $NH_3$ emissions while fuel combustion activities, including industry, power plant, and transportation contribute most of the $NO_x$ emissions and small amounts of $NH_3$ emissions. Both $NH_3$ and $NO_x$ have natural sources (including lightning, biomass burning and soil emissions), but are negligible compared to anthropogenic emissions over eastern China."

Based on outputs from the model simulation, it is obvious that controlling agricultural $NH_3$ emission can undoubtedly lower N deposition. Thanks for the suggestion on performance of scenarios analysis of $NH_3$ emission reduction, we conducted a separate model simulation which reduce emissions from fertilizer use by 20%.We add the following sentences in the text:

"To test the importance of future ammonia emission control strategies, we conducted separate model simulations which reduced $NH_3$ emissions from fertilizer use by 20%. The results showed that a 20% reduction in fertilizer $NH_3$ emissions can lead to a 7.4% decrease in total N deposition over Eastern China"

In future study, we will attempt to use improved $NH_3$ emission (e.g., Zhang et al., 2018) inventories to detail the relative contribution of emissions sources to N deposition and further scenarios analysis of $NH_3$ emissions.

Reference:

Zhang, L., Chen, Y. F., Zhao, Y. H., Henze, D. K., Zhu, L. Y., Song, Y., Paulot, F., Liu, X. J., Pan, Y. P., and Huang, B. X.: Agricultural ammonia emissions in China: reconciling bottom-up and top-down estimates, Atmos. Chem. Phys., 18, 339–355, 2018.

Line 809: What do you mean by improper fertilizer application? Do you mean too excessive? How much fertilizer is applied annually and is this amount much higher than normal? More background on this issue would be useful.

**Response:** “improper fertilizer application” means N fertilizers were not applied in appropriate fertilization pattern (e.g., fertilizing with a suitable choice of chemical, at the correct application level, selecting the best of the year and location). To make it clear, we now state that “These results indicate that reducing $NH_3$ emissions by use of appropriate fertilization patterns (e.g., 4 R technologies (Right amount, Right time, Right form and Right application technique), Ju et al., 2009) should be a priority in curbing N deposition in eastern China”.

Reference:

Ju, X.T., Xing, G.X., Chen, X.P., Zhang, S.L., Zhang, L.J., Liu, X.J., Cui, Z.L., Yin, B., Christie, P., Zhu, Z.L., and Zhang, F.S.: Reducing environmental risk by improving N management in intensive Chinese agricultural systems, Proc. Natl. Acad. Sci. U. S. A. 106, 3041-3046, 2009.

Line 884: Do you have annual precipitation amounts from weather stations, which can show whether interannual variability in precipitation amounts affect wet deposition?

**Response:** We measured precipitation amounts at 27 study sites during 2011-2015. According to suggestion by the referee, we selected 16 sites with continuous 5-year measurements, and our results demonstrated an obvious interannual variability in precipitation amounts. Thus, wet deposition to some extent can be affected by the change in precipitation amounts.

In the revised paper, we added Figure S14 in the Supplement, and stated in the text that “For example, a large inter-annual variation in precipitation amount was observed at the selected 16 sites during 2011-2015, which partially lead to inter-annual changes in wet/bulk N deposition.

**Anonymous Referee #2**

This paper presents a statistical summary and discussion of measurements of components of reactive nitrogen (Nr) in the air and in bulk deposition from the 27 sites of a national network that are located in the eastern part of China. The measurement dataset spans the 5-year period from 2011-2015 inclusive. Measurements are also converted into estimates of wet and dry deposition. The authors analyse various spatiotemporal aspects of the concentrations and deposition dataset including seasonality, trends over the 5-year period, and a comparison between sites in the northern half and the southern half of eastern China. The authors supplement the analysis of measurement data with some GEOS-Chem model runs to explore source contributions to Nr in this region. Discussion includes implication for policymakers concerning the different trends in emissions of Nr versus concentrations and deposition of Nr and of the need to include emissions of NH3 in emissions reductions planning. The dataset is comprehensive. The presentation of the results is thorough and the text and figures and tables are very clearly presented. There is an extensive discussion. The data are of importance for understanding Nr in eastern China.

**Response**: Thanks for the recognition of our contribution. Below we provide a point-by-point response to the species comments, together with proposed changed in the revised manuscript (in blue).

Specific comments:

Five years is not a long time period to attempt to discern 'true' long-term trends in concentrations of atmospheric species. The authors recognise that their time period is short in respect of this aspect of their analysis but they could phrase relevant parts of their text to be more cautious about conclusions on long-term trends.

**Response:** The suggestion has been implemented in the revision.

L124: Replace "subsequence" with "subsequent"

**Response:** Agree and done.

L207: It is not clear what is meant by the phrase "where field sampling was carried

out after the year 2010". Is this intended to mean that at some sites the measurements did not begin until after 2010?

**Response:** We are sorry for confusing the referee. It means that at eleven sites the measurements begin after the year 2011. We now state that "…where field sampling was carried out after the year 2011 (i.e., the years between 2012 and 2015) and/or interrupted during the period due to instrument failure (details in Table S1, Supplement)".

L271-2: There is a contradiction between a sentence that states that IASI data up until 31 December 2015 was used and the following sentence that states that data only up until 30 September 2014 was used.

**Response:** There was a wrong expression in this sentence. Actually, we used the daily IASI-$NH_3$ data from 1 January 2011 to 31 December 2015 for the spatial analysis, and from January 2011 to 30 September 2014 for temporal analysis.

We now state that "The daily IASI-$NH_3$ data (provided by the Atmospheric Spectroscopy Group at Université Libre De Bruxelles, data available at http://iasi.aeris-data.fr/$NH_3$/) from 1 January 2011 to 31 December 2015 was used for the spatial analysis in the present study. For the temporal analysis, we used the IASI_$NH_3$ from 1 January 2011 to 30 September 2014 because an update of the input meteorological data on 30 September 2014 had caused a substantial increase in the retrieved atmospheric $NH_3$ columns."

Table 1: (1) State in the caption or footnote what the significance test is testing, i.e. that it is testing for significant difference in mean concentration of a pollutant at a given site type between the northern region and the southern region. (2) The footnote should read LUY not LSY to be consistent with column heading.

**Response:** We now state in the footnote that "$^{*}$ and $^{**}$ denote significance at the 0.05 and 0.01 probability levels for difference in annual mean $N_r$ concentrations at a given site type between northern and southern regions, respectively."

Also, we uniformly used "LUT" as an abbreviation of land use types in the footnote and column heading.

Figure 2: The reader is referred to Table S1 in the supplement for the number of sites

for each land use type in each region, but cannot the reader be directed more easily to Table 1 in the main paper for these numbers?

**Response:** The reader cannot be directly referred to Table 1. For comparison between the periods 2011-2012 and 2013-2015, the sampling sites for land use types shown in Figure 2 have continuous 5-year (2011-2015) measurements (in total 21 sites for dry measurements, and 16 sites for wet/bulk measurements). For spatial comparisons in Table 1, the annual mean concentrations of $N_r$ species in air and precipitation for land use types were calculated based on measurements at all 27 sites.

Figure 3: (1) I assume the data shown are the means for the 5-year period, in which case it may be helpful to make this explicit in the opening sentence thus: "Seasonal mean concentrations averaged over 2011-2015 of*: : :*.". (2) As for Figure 2 (should be 3?), can the text "in Table S1 in the supplement" be replaced more directly with "in Table 1". (3) The last part of the caption should refer to significant differences between "seasons" not "sites".

**Response:** In the revised paper, we rephrased the start of caption of Figure 2 to "Seasonal mean concentrations averaged over 2011-2015 of...".

We replaced "Table S1 in the supplement" by "Table 1", as seasonal averages were calculated based on measurements at all 27 sites. Also, we changed "sites" to "seasons".

Figure 4: The same 3 comments as made above in connection with Figure 3.

**Response:** In the revised paper, we have made corresponding corrections on Figure 4 according to the referee's comments on Figure 3.

Table 2: Same comments as for Table 1.

Response: In the revision we made corresponding corrections on Table 2 according to the referee's comments on Table 1.

Figure 5: Can the reader be directed to Table 2, rather than to Table S1 in the supplement, for the number of sites of each type in each region.

**Response:** The reader cannot be referred to Table 2. For details, please see our response to similar comments on Figure 2.

Figure 7: Same comments as for Figure 3 (but with substitution of reference to Table

2 rather than to Table 1).

**Response:** In the revised paper, we made corresponding corrections on the caption of Figure 7 according to the referee's comments on Figure 3.

Figure 8: Same comments as for Figure 7.

**Response:** The reader cannot be directly referred to Table 1. Please see our response to the referee's comment on Figure 2.

L598: Rephrase start of sentence to "Eastern China is a highly industrialized*: : :*"

Response: Agree and done.

L 761: In comparing ion balance, presumably the (molar) concentration of NH4+ was compared against the sum of the molar concentrations of NO3- and TWICE the molar concentration of SO42-? The factor 2 is missing from the text and from the axis title of Figure 10f.

**Response:** Thank you for pointing it out. In the revised paper, we analyzed the correlation of $NH_4^+$ with the sum of $NO_3^-$+$2SO_4^{2-}$. Also, Figure 10f was redrawn and the corresponding sentences were changed, now read as: "At urban and rural sites, monthly mean $pNH_4^+$ concentrations significantly positively correlated with the sum of $p2SO_4^{2-}$ and $pNO_3^-$ concentrations (Fig. 10f). However, the slopes of regression equations between them were both smaller than unity (0.35 and 0.46 at urban and rural sites, respectively)…". In addition, we changed "Table S1" to "Table 1" in the caption of Figure 10.

MS No.: acp-2018-424

# Spatial-temporal patterns of inorganic nitrogen air concentrations and deposition in eastern China

Wen Xu[1,2], Lei Liu[3], Miaomiao Cheng[4], Yuanhong Zhao[5], Lin Zhang[5], Yuepeng Pan[6], Xiuming Zhang[7], Baojing Gu[8], Yi Li[9], Xiuying Zhang[3], Jianlin Shen[10], Li Lu[11], Xiaosheng Luo[12], Yu Zhao[13], Zhaozhong Feng[2*], Jeffrey L. Collett, Jr.[14], Fusuo Zhang[1], Xuejun Liu[1*]

[1]College of Resources and Environmental Sciences, Key Laboratory of Plant-Soil Interactions of MOE, Beijing Key Laboratory of Cropland Pollution Control and Remediation, China Agricultural University, Beijing 100193, China

[2]State Key Laboratory of Urban and Regional Ecology, Research Center for Eco-Environmental Sciences, Chinese Academy of Sciences, Shuangqing Road 18, Haidian District, Beijing, 100085, China

[3]Jiangsu Provincial Key Laboratory of Geographic Information Science and Technology, International Institute for Earth System Science, Nanjing University, Nanjing, 210023, China

[4]State Key Laboratory of Environmental Criteria and Risk Assessment, Chinese Research Academy of Environmental Sciences, Beijing 100012, China

[5]Laboratory for Climate and Ocean-Atmosphere Sciences, Department of Atmospheric and Oceanic Sciences, School of Physics, Peking University, Beijing 100871, China

[6]State Key Laboratory of Atmospheric Boundary Layer Physics and Atmospheric Chemistry (LAPC), Institute of Atmospheric Physics, Chinese Academy of Sciences, Beijing, 100029, China

[7]School of Agriculture and Food, The University of Melbourne, Victoria, 3010, Australia

[8]Department of Land Management, Zhejiang University, Hangzhou 310058, People's Republic of China

[9]Arizona Department of Environmental Quality, Phoenix, AZ 85007, USA

[10]Institute of Subtropical Agriculture, Chinese Academy of Sciences, Changsha 4410125, China

[11]Institute of Surface-Earth System Science, Tianjin University, Tianjin, 300072, China

[12]Institute of Plant Nutrition, Resources and Environmental Sciences, Henan Academy of Agricultural Sciences, Henan Key Laboratory of Agricultural Eco-environment, Zhengzhou, 450002, China

[13]State Key Laboratory of Pollution Control & Resource Reuse, School of the Environment, Nanjing University, 163 Xianlin Ave., Nanjing, Jiangsu 210023, China

[14]Department of Atmospheric Science, Colorado State University, Fort Collins, Colorado, 80523 USA

[*]Correspondence to: X. J. Liu (liu310@cau.edu.cn) and Z.Z. Feng (fzz@rcees.ac.cn)

**Abstract:**

Five-year (2011-2015) measurements of gaseous $NH_3$, $NO_2$ and $HNO_3$ and particulate $NH_4^+$ and $NO_3^-$ in air and/or precipitation were conducted at twenty-seven sites in a Nationwide Nitrogen Deposition Monitoring Network (NNDMN) to better understand spatial and temporal (seasonal and annual) characteristics of reactive nitrogen ($N_r$) concentrations and deposition in eastern China. Our observations reveal annual average concentrations (16.4-32.6 μg N $m^{-3}$), dry deposition fluxes (15.8-31.7 kg N $ha^{-1}$ $yr^{-1}$) and wet/bulk deposition fluxes (18.4-28.0 kg N $ha^{-1}$ $yr^{-1}$) based on land use were ranked as urban > rural > background sites. Annual concentrations and dry deposition fluxes of each $N_r$ species in air were comparable at urban and background sites in northern and southern regions, but were significantly higher at northern rural sites. These results, together with good agreement between spatial distributions of $NH_3$ and $NO_2$ concentrations determined from ground measurements and satellite observations, demonstrate that atmospheric $N_r$ pollution is heavier in the northern region than in the southern region. No significant inter-annual trends were found in the annual $N_r$ dry and wet/bulk N deposition at almost all of the selected sites. A lack of significant changes in annual averages between the 2013-2015 and 2011-2012 periods for all land use types, suggests that any effects of current emission controls are not yet apparent in $N_r$ pollution and deposition in the region. Ambient concentrations of total $N_r$ exhibited a non-significant seasonal variation at all land use types, although significant seasonal variations were found for individual $N_r$ species (e.g., $NH_3$, $NO_2$ and $pNO_3^-$) in most cases. In contrast, dry deposition of total $N_r$ exhibited a consistent and significant seasonal variation at all land use types, with the highest fluxes in summer and the lowest in winter. Based on sensitivity tests by the GEOS-Chem model, we found that $NH_3$ emissions from fertilizer use (including chemical and organic fertilizers) were the largest contributor (36%) to total inorganic $N_r$ deposition over eastern China. Our results not only improve the understanding of spatial-temporal variations of $N_r$ concentrations and deposition in this pollution hotspot, but also provide useful information for policy-makers that mitigation of $NH_3$

emissions should be a priority to tackle serious N deposition in eastern China.

## 1. Introduction

In China, and globally, human activities have dramatically increased emissions of nitrogen oxides ($NO_x$=NO+$NO_2$) and ammonia ($NH_3$) into the atmosphere since the beginning of the industrial revolution (Galloway et al., 2008; Liu et al., 2013). $NO_x$ and $NH_3$ emitted to the atmosphere are transformed to nitrogen-containing particles (e.g., particulate $NH_4^+$ and $NO_3^-$, and organic nitrogen) (Ianniello et al., 2010; Zhang et al., 2015), which are major chemical constituents of airborne $PM_{2.5}$ (particulate matter with a diameter of 2.5 μm or less) and have implications for air quality and climate (Fuzzi et al., 2015). As a result of elevated reactive nitrogen ($N_r$) emissions, nitrogen (N) deposition through dry and wet processes has also substantially increased over China (Liu et al., 2013; Lu et al., 2007, 2014; Jia et al., 2014, 2016), and excessive deposition of N has resulted in detrimental impacts including decreased biological diversity (Bobbink et al., 2010), nutrient imbalance (Li et al., 2016), increased soil acidification (Yang et al., 2015), and eutrophication of water bodies (Fenn et al., 2003)~~, and increased greenhouse gas emissions (Gruber and Galloway, 2008)~~. Furthermore, $N_r$-associated haze pollution episodes, characterized by high concentrations of $PM_{2.5}$, occur frequently in China, as evidenced in particular in 2013 (Guo et al., 2014; Huang et al., 2014; Tian et al., 2014).

In order to control its notorious air pollution, China has reduced national emissions of $SO_2$ and particulate matter by 14% and 30%, respectively, from 2005 to 2010 (MEPC, 2011). Additionally, stringent measures (e.g., using selective catalytic/non-catalytic reduction systems, and implementing tighter vehicle emission standards) were implemented during the 12$^{th}$ Five Year Plan (FYP) period (2011-2015), with aims to reduce 2015 annual emissions of $SO_2$ and $NO_x$ by 8% and 10%, respectively, relative to 2010 levels (Xia et al., 2016). However, there is as yet no regulation or legislation that deals with national $NH_3$ emissions and thus emission reductions of $SO_2$ and $NO_x$ to achieve desired air-quality improvement goals will be compromised (Gu et al., 2014). Significant increases in $PM_{2.5}$ concentrations have been observed in the years 2013 and 2014 as compared to 2012, excluding the

influence of meteorological conditions on inter-annual variations (Liang et al., 2015). Other studies with more conclusive evidence have likewise suggested that $NH_3$ plays a vital role in sulfate formation and exacerbates severe haze pollution development in urban regions of China (Wang et al., 2016), even acting as the key limiting factor for the formation of secondary inorganic aerosol (Wu et al., 2016). In addition, due to higher local and regional concentrations of $NH_3$ in the atmosphere, nitrate-driven haze pollution occurred during summertime in urban environment in the North China Plain (Li et al., 2018). The absolute and relative concentrations of particulate nitrate in urban Beijing increased with haze development (Pan et al., 2016). Also, nitrate contributed to a large fraction of the elevated $PM_{2.5}$ concentrations at a rural site in the North China Plain and high $NH_3$ in the early morning accelerated the formation of fine nitrates (Wen et al., 2015).

High rates of N deposition have also been observed during 2011-2014 across China (Xu et al., 2015). However, to date no study, based on long-term ground-based observations, has provided any information on the effectiveness of $SO_2$ and $NO_x$ emission controls on N deposition in China. Non-linearities have been identified between reductions in emission and deposition in Europe over the last 3 decades (Aguillaume et al., 2016; Fowler et al., 2007). Due to the tightly coupled yet complex relationship between emissions, concentrations and deposition, long-term monitoring networks can provide a test of the effectiveness of emission controls (Erisman et al., 2003). Currently two national N deposition networks are operational in China, i.e. the Nationwide Nitrogen Deposition Monitoring Network (NNDMN, Liu et al., 2011; Xu et al., 2015) and the Chinese Ecosystem Research Network (CERS, Zhu et al., 2015). The NNDMN containing 43 *in situ* monitoring sites has been operational since 2010 to measure wet N deposition and ambient concentrations of five major $N_r$ species (i.e., gaseous $NH_3$, $NO_2$ and $HNO_3$, and particulate $NH_4^+$ and $NO_3^-$), the latter for ~~subsequence~~ subsequent estimation of dry deposition. The CERS was established in 1988 and mainly focused on wet N deposition at 41 field stations. In addition to ground-based measurements, satellite observations enable retrieval of atmospheric $NH_3$ and $NO_2$ with high temporal and spatial resolutions (Dammer et al., 2016;

Russell et al., 2012), providing a means to reveal spatial distributions and long-term trends of ambient $NH_3$ and $NO_2$ levels at regional to global scales, and also to evaluate the effectiveness of emission controls (Krotkov et al., 2016). However, to effectively use the vast satellite data sets for environmental monitoring, it is critical to validate these remote sensing observations using *in situ* surface observations (Pinder et al., 2011; Van Damme et al., 2015).

Eastern China is a developed region with the largest densities of population, economic activity and resource consumption in the country (He et al., 2015). Recent satellite observations indicate that tropospheric $NH_3$ and $NO_2$ levels in eastern China were both much greater than other regions of the world from 2005-2015 (Demmer et al., 2016; Krotkov et al., 2016). Accordingly, this region received the highest levels of dry N deposition in the world (Vet et al., 2014), and was regarded as a primary export region of N deposition for neighboring countries (Ge et al., 2014). Based on meta-analysis of published observations, some studies have provided information on the magnitudes, spatial distributions, and decadal variations of wet/bulk N deposition in China (Liu et al., 2013; Jia et al., 2014), but the analyzed data were limited to time periods between 1980 and 2010. Although a recent study (Jia et al., 2016) has reported a clear increasing trend of dry N deposition in eastern China between 2005 and 2014, considerable uncertainty may exist due to estimates of gaseous $HNO_3$ and particulate $NH_4^+$ and $NO_3^-$ ($pNH_4^+$ and $pNO_3^-$) concentrations using $NO_2$ satellite data, which is in part manifested by Liu et al. (2017a). Furthermore, seasonal patterns of $N_r$ concentrations and deposition have not yet been systematically investigated at a large spatial scale in this region, although spatial patterns of dry $N_r$ deposition for representative months of four seasons (i.e., January for winter, April for spring, July for summer, October for autumn) in 2010 have been mapped with the RAMS-CMAQ model (Han et al., 2017). Thus, the spatial and temporal (annual and seasonal) variations of $N_r$ concentrations, and dry and wet deposition in eastern China require further exploration using ground-based measurements, especially for time periods after 2010. Our previous work (Xu et al., 2015) used multiyear measurements (mainly from Jan. 2010 to Sep. 2014) at the 43 sites in the NNDMN, aiming to provide the

first quantitative information on atmospheric $N_r$ concentrations and pollution status across China, and to analyze overall fluxes and spatial variations of N deposition in relation to anthropogenic $N_r$ emissions from six regions.

The present study aims to examine spatial-temporal (annual and seasonal) characteristics of $N_r$ concentrations in air ($NH_3$, $NO_2$, $HNO_3$, $pNH_4^+$ and $pNO_3^-$) and precipitation ($NH_4^+$-N and $NO_3^-$-N) and their corresponding dry and wet/bulk N deposition, through a 5-year (2011-2015) monitoring period at 27 NNDMN sites in eastern China. In addition, we compare spatial-temporal variability of measured $NH_3$ and $NO_2$ concentrations with variations of the corresponding satellite retrieval columns, as well as inter-annual trends in $N_r$ deposition and emissions. Finally, emission sources contributing to total N deposition over eastern China are examined.

## 2. Materials and methods

### 2.1 Study area and site descriptions

The present study was conducted in eastern China, which is distinguished by the "Hu Line" (She, 1998). This region has spatial heterogeneity in levels of economic development, and ~~resulting in~~ significant spatial differences in $NH_3$ and $NO_x$ emissions (Fig. 1b and c). Thus, to better analyze spatial and temporal variabilities in measured $N_r$ concentrations and deposition, we divided eastern China into northern and southern regions using the Qinling Mountains-Huaihe River line (Fig. 1a), of which the division basin was based on the differences in natural conditions, agricultural production, geographical features and living customs. As for specific differentiations, for example, the northern region adopted a centralized domestic heating policy for late autumn and winter seasons but the south has not; annual average precipitation amounts were generally greater than 800 mm in the south but were less than 800 mm in the north. In addition, the north is dominated by calcareous soils, which could result in higher soil $NH_3$ volatilization (Huang et al., 2015), vs. the acidic red soil in the south.

The NNDMN was operated in line with international standards by China Agricultural University (CAU); 35 NNDMN sites were located in eastern China (Xu et al., 2015). For our analysis, we considered twenty-seven sites in total, with 5-year

continuous data: 13 sites were located in north of the Qinling Mountains-Huaihe River line (China Agricultural University-CAU, Zhengzhou-ZZ, Dalian-DL, Shuangzhuang-SZ, Quzhou-QZ, Yangqu-YQ, Zhumadian-ZMD, Yanglin-YL, Yucheng-YC, Gongzhulin-GZL, Lishu-LS, Lingshandao-LSD, Changdao-CD), and 14 sites were located in south of the line (Nanjing-NJ, Baiyun-BY, Wenjiang-WJ, Wuxue-WX, Taojing-TJ, Fengyang-FY, Zhanjiang-ZJ, Fuzhou-FZ, Fenghua-FH, Ziyang-ZY, Yangting-YT, Jiangjin-JJ, Huinong-HN, Xishan-XS).

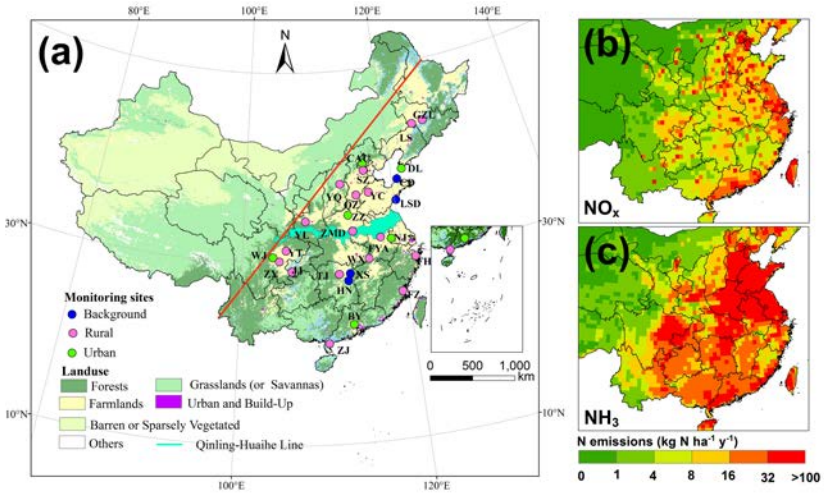


**Figure 1**. Spatial distributions of the 27 monitoring sites (a), $NO_x$ emissions (b) and $NH_3$ emissions (c) in Eastern China ($NH_3$ and $NO_x$ emission data were for the year 2010 and obtained from Liu et al. (2017b)).

All the sites are located as far away as possible and practical from local direct emission sources to increase regional representativeness. They can be divided into three categories according to their geopolitical location and their proximity to the main emission sources: urban sites (abbreviated as U), rural sites (cropland areas, R), and background sites (coastal and forest areas, B). Information on the monitoring sites, such as land use types, coordinates, and measurement periods are listed in Table S1 of the Supplement. Detailed descriptions of all the sites including the surrounding environment and nearby emission sources can be found in Xu et al. (2015).

**2.2 Field sampling and chemical analysis**

Continuous measurements were performed during the period from January 2011 to December 2015 at the 27 study sites, except for eleven sites (ZZ, ZMD, YC, LSD, NJ, WX, FYA, ZJ, YT, JJ, and HN), where field sampling was carried out after the year ~~2010~~ 2011 (i.e., the years between 2012 and 2015) and/or interrupted during the period due to instrument failure (details in Table S1, Supplement). Ambient $N_r$ concentrations of gaseous $NH_3$ and $HNO_3$, and $pNH_4^+$ and $pNO_3^-$ (for which the empirically determined effective size cut-off for aerosol sampling is of the order of 4.5 µm) were measured using an active DELTA (DEnuder for Long-Term Atmospheric sampling; Tang et al., 2009) system; gaseous $NO_2$ was sampled in three replicates with passive diffusion tubes (Gradko International Limited, UK). The air intakes of the DELTA system and the $NO_2$ tubes were mounted 2 m above the ground at most sites and protected from precipitation and direct sunlight with a rigid plastic box and a PVC shelter, respectively. All measurements of $N_r$ concentration were based on monthly sampling (one sample per month for each $N_r$ species). Detailed information on measuring methods and collection are given in Sect. S1 of the Supplement.

To collect precipitation (here termed as wet/bulk deposition, which contains wet and some dry deposition due to the use of an open sampler) samples, a standard precipitation gauge (SDM6, Tianjin Weather Equipment Inc., China) was continuously exposed beside the DELTA system (ca. 2 m). Immediately after each precipitation event (08:00–08:00 next day, Greenwich Mean Time +8), samples (including rain and melted snow) were collected and stored in clean polyethylene bottles (50 mL) at -18 $^oC$ until sent to the CAU laboratory for analysis. Each collector was rinsed three times with high-purity water after each collection.

In the analytical laboratory, acid-coated denuders and aerosol filters were extracted with 6 and 10 mL of high-purity water (18.2 MΩ), respectively, and analyzed for $NH_4^+$-N with an AA3 continuous-flow analyzer (CFA) (BranC Luebbe GmbH, Norderstedt, Germany). Carbonate-coated denuders and filters were both extracted with 10 mL 0.05% $H_2O_2$ solution followed by analysis of $NO_3$-N using the same CFA. $NO_2$ samples, extracted with a solution containing sulfanilamide, $H_3PO_4$,

and N-1-naphthylethylene-diamine, were determined using a colorimetric method by absorption at a wavelength of 542 nm (Xu et al., 2016). Precipitation samples were filtered through a syringe filter (0.45 mm, Tengda Inc., Tianjin, China) and analyzed for $NH_4^+$-N and $NO_3^-$-N using the CFA as mentioned above. Quality assurance and quality control procedures adopted in the analytical laboratory are described by Xu et al. (2017). Further details of precipitation measurement, samples handling, and chemical analysis are reported in Xu et al. (2015).

**2.3 Deposition estimate**

Wet/bulk deposition of $NH_4^+$-N and $NO_3^-$-N were calculated per month and year by multiplying the precipitation amount by their respective volume-weighted mean (VWM) concentrations. The dry deposition flux of gaseous and particulate $N_r$ species was calculated as the product of measured concentrations by modeled deposition velocities ($V_d$). The dry deposition velocities of five $N_r$ species were calculated by the GEOS (Goddard Earth Observing System)-Chem chemical transport model (CTM) (Bey et al., 2001; http://geos-chem.org), and have been reported in a companion paper (Xu et al., 2015). In brief, the model calculation of dry deposition of $N_r$ species follows a standard big-leaf resistance-in-series model as described by Wesely (1989) for gases and Zhang et al. (2001) for aerosol. We used archived hourly $V_d$ from January 2011 to May 2013 and filled the gap for the period (from June 2013 to December 2015) when GEOS meteorological data are unavailable using the mean values calculated from all the available simulations. The monthly $V_d$ at each site was averaged from the hourly dataset.

**2.4 Satellite retrievals of $NH_3$ and $NO_2$**

Comparisons between satellite observations and ground-based measurements were evaluated at the twenty-seven sites in order to accurately examine the spatial-temporal pattern of $NH_3$ and $NO_2$ concentrations. For $NH_3$, we used the products retrieved from the Infrared Atmospheric Sounding Interferometer (IASI) instrument (aboard the MetOp-A platform), which crosses the equator at a mean local solar time of 9:30 a.m. and 9:30 p.m. The IASI-$NH_3$ product is based on the calculation of a spectral hyperspectral range index and subsequent conversion to $NH_3$

total columns via a neural network. The details of the IASI-$NH_3$ retrieval method are described in Whitburn et al. (2016). We only considered the observations from the morning overpass as they are generally more sensitive to $NH_3$ because of higher thermal contrast at this time of day (Van Damme et al., 2015; Dammers et al., 2016). The daily IASI-$NH_3$ data (provided by the Atmospheric Spectroscopy Group at Université Libre De Bruxelles, data available at http://iasi.aeris-data.fr/$NH_3$/) from 1 January 2011 to 31 December 2015 was used for the spatial analysis in the present study. For the temporal analysis, ~~We~~ we ~~did not~~ used the IASI_$NH_3$ ~~after 30 September 2014 for the temporal analysis~~from 1 January 2011 to 30 September 2014 because an update of the input meteorological data on 30 September 2014 had caused a substantial increase in the retrieved atmospheric $NH_3$ columns. Only observations with a cloud coverage lower than 25%, and relative error lower than 100% or absolute error smaller than $5\times10^{15}$ molecules $cm^{-2}$ were processed. The methodology is provided in detail in Liu et al. (2017b). In brief, all observations were gridded to a 0.5° latitude × 0.5° longitude grid, and then we calculated the monthly arithmetic mean by averaging the daily values with observations points within each grid cell. Similarly, we calculated the annual arithmetic mean by averaging the daily values with observations points within the grid cell over the whole year.

For $NO_2$ we used the products from the Ozone Monitoring Instrument (OMI) resided on NASA's EOS-Aura satellite, which was launched in July 2004 into a sun-synchronous orbit with a local equator crossing time at approximately 1:45 p.m. OMI detects the backscattered solar radiation from the Earth's atmosphere within the UV-vis spectral window between 270-500 nm, to achieve nearly global coverage daily, with a spatial resolution ranging from 13 km × 24 km at nadir to 24 km × 128 km at the edge of the swath (Russell et al., 2012). We used tropospheric $NO_2$ retrievals from the DOMINO (Dutch Finnish Ozone Monitoring Instrument) algorithm version 2. The retrieval algorithm is described in detail in Boersma et al. (2007). The tropospheric $NO_2$ columns used in this study are monthly means from 1 January 2011 to 30 December 2015 with a spatial resolution of 0.125° latitude × 0.125° longitude (data available at http://www.temis.nl/airpollution/no2.html).

## 2.5 Statistical analysis

One-way analysis of variance (ANOVA) and two-independent-samples *t* tests were applied to detect significant differences in seasonal mean concentrations and deposition fluxes of measured $N_r$ species as well as their annual mean deposition fluxes for three land use types (rural, urban and background). As there was large site-to-site variability in annual $N_r$ concentrations and deposition fluxes at monitoring sites within the same land use types, averaging data into annual values for land use types is unlikely to be truly representative of actual trends. Thus, annual trends of the variables were evaluated at a single site scale rather than by land use type. Trend analysis was conducted using Theil regression (Theil, 1992) and the Mann-Kendall test (Gilbert, 1987; Marchetto et al., 2013). We defined an increasing (decreasing) trend as a positive (negative) slope of the Theil regression, while a statistical significance level ($p$<0.01) of a trend was evaluated by the non-parametric Mann-Kendall test ($p$ value). Non-parametric methods usually have the advantage of being insensitive to outliers, and allow missing data and non-normal distribution of data (Gilbert, 1987; Salmi et al., 2002), appropriate for the analyzed data set. The Mann-Kendall method is appropriate for detection of monotonic trends in data series that have no seasonal variation or autocorrelation. Atmospheric concentrations and deposition fluxes of $N_r$ species, however, generally have distinct seasonal variability (Pan et al., 2012) and the Mann-Kendall test is thus applied to annual values.

Satellite observations during 2005-2015 indicate that tropospheric $NO_2$ levels peaked in 2011 over China (Krotkov et al., 2016; Duncan et al., 2016) and $NO_x$ emissions peaked in 2011/2012 (Miyazaki et al., 2017; van der A et al., 2017; Souri et al., 2017). To assess the impact of emission control measures on measured $N_r$ concentrations and deposition fluxes at different land use types, we compared arithmetic mean values averaged from the last 3-year period (2013-2015) with those averaged from the first 2-year period (2011-2012) for monitoring sites with continuous 5-year measurements (twenty-one sites for dry, and seventeen sites for wet/bulk). Seasonal concentrations and deposition fluxes of measured $N_r$ species were calculated using the arithmetic average of matched seasons during the sampling

periods; spring refers to March-May, summer covers June-August, autumn refers to September-November, and winter covers December-February.

## 3. Results

### 3.1 Spatial variability in concentrations of $N_r$ species in air and precipitation

Summary statistics of monthly mean concentrations of $NH_3$, $NO_2$, $HNO_3$, $pNH_4^+$, and $pNO_3^-$ at the twenty-seven monitoring sites during 2011-2015 are listed in Table S2 of the Supplement. Monthly mean concentrations of $NH_3$, $NO_2$, $HNO_3$, $pNH_4^+$, and $pNO_3^-$ ranged from 0.16 (TJ)-39.57 (WJ), 0.55 (LS)-29.06 (WJ), 0.04 (YQ)-4.93 (CAU), 0.11 (ZY)-57.20 (QZ), and 0.01 (DL)-32.06 (ZZ) μg N $m^{-3}$, respectively. On the basis of geographical location and classification of each site, the annual mean concentrations of each $N_r$ species were calculated for three land use types in eastern China and its northern and southern regions (Table 1**)**.

**Table 1.** Annual average (standard error) concentrations of various $N_r$ compounds in air and precipitation at different land use types in eastern China and its northern and southern regions for the 5-year period 2011-2015.

| Region[a] | LUTY[b] | Ambient conc. μg N $m^{-3}$ | | | | | | Rainwater conc. mg N $L^{-1}$ | | |
|---|---|---|---|---|---|---|---|---|---|---|
| | | $NH_3$ | $NO_2$ | $HNO_3$ | $pNH_4^+$ | $pNO_3^-$ | Total $N_r$ | $NH_4^+$ | $NO_3^-$ | TIN |
| EC | Urban | 8.5 | 10.2 | 1.6 | 8.2 | 4.0 | 32.6 | 1.6 | 1.9 | 3.5 |
| | (n=6) | (1.4) | (1.0) | (0.2) | (1.8) | (0.8) | (4.1) | (0.3) | (0.2) | (0.5) |
| | Rural | 7.2 | 6.0 | 1.2 | 6.7 | 2.8 | 23.9 | 1.7 | 1.4 | 3.1 |
| | (n=17) | (0.9) | (0.5) | (0.1) | (1.1) | (0.3) | (2.7) | (0.2) | (0.2) | (0.4) |
| | BKD[c] | 3.9 | 5.2 | 0.9 | 4.5 | 1.9 | 16.4 | 1.4 | 1.2 | 2.6 |
| | (n=4) | (0.6) | (0.3) | (0.1) | (0.4) | (0.3) | (1.4) | (0.3) | (0.4) | (0.6) |
| NREC | Urban | 8.1 | 11.7 | 1.6 | 8.6 | 5.1 | 35.1 | 2.2 | 2.4 | 4.6 |
| | (n=3) | (2.4) | (1.6) | (0.3) | (2.3) | (1.4) | (7.7) | (0.4) | (0.2) | (0.4) |
| | Rural | 9.9 | 7.4 | 1.4 | 9.2 | 3.7 | 31.6 | 2.4 | 2.0 | 4.4 |
| | (n=8) | (1.2)** | (0.7)* | (0.1)* | (1.9)* | (0.5)* | (3.8)** | (0.3)** | (0.2)** | (0.4)** |
| | BKD | 4.7 | 5.7 | 1.0 | 5.1 | 2.4 | 18.8 | 1.8 | 1.5 | 3.3 |
| | (n=2) | (0.6) | (0.3) | (0.1) | (0.2) | (0.3) | (0.1) | (0.2) | (0.3) | (0.1) |
| SREC | Urban | 8.9 | 8.7 | 1.6 | 7.9 | 2.9 | 30.1 | 1.1 | 1.5 | 2.6 |
| | (n=3) | (1.8) | (0.6) | (0.1) | (3.1) | (0.2) | (4.5) | (0.3) | (0.3) | (0.6) |
| | Rural | 4.9 | 4.6 | 1.0 | 4.5 | 1.9 | 17.0 | 1.1 | 0.9 | 2.0 |

| | | | | | | | | | |
|---|---|---|---|---|---|---|---|---|---|
| (n=9) | (0.6) | (0.6) | (0.1) | (0.6) | (0.2) | (1.7) | (0.2) | (0.1) | (0.3) |
| BKD | 3.1 | 4.7 | 0.8 | 4.0 | 1.4 | 14.0 | 1.0 | 0.6 | 1.6 |
| (n=2) | (0.7) | (0.4) | (0.1) | (0.2) | (0.2) | (0.6) | (0.0) | (0.0) | (0.0) |

[a] EC: eastern China; NREC: northern region of eastern China; SREC: southern region of eastern China. [b] LUT~~LSY~~: land use type; n denotes number of monitoring sites. [c] BKD: Background. * and ** denote significance at the 0.05 and 0.01 probability levels for difference in annual mean $N_r$ concentrations at a given site type between northern and southern regions, respectively. ~~* Significant at the 0.05 probability level. ** Significant at the 0.01 probability level.~~

In eastern China, annual mean concentrations of $NH_3$, $NO_2$, $HNO_3$, $pNH_4^+$, and $pNO_3^-$ at the urban sites (averages for the 5-year, 1.6 ± 0.2 (for $HNO_3$) to 10.2 ± 1.0 (for $NO_2$) μg N $m^{-3}$) ~~were~~ increased by 18, 70, 33, 23, and 43%, respectively, compared with their corresponding concentrations at the rural sites (1.2 ± 1.0 (for $HNO_3$) to 7.2 ± 0.9 (for $NH_3$) μg N $m^{-3}$); they also increased by 78-118% compared with the concentrations at the background sites (0.9 ± 0.1 (for $HNO_3$) to 5.2 ± 0.3 (for $NO_2$) μg N $m^{-3}$)~~18-44% and 78-120% higher than their corresponding concentrations at the rural (1.2 ± 1.0 to 7.2 ± 0.9 μg N $m^{-3}$) and background (0.9 ± 0.1 to 5.2 ± 0.3 μg N $m^{-3}$) sites, respectively~~ (Table 1). Analogous patterns also occurred for all measured $N_r$ in each region, except for $NH_3$ and $pNH_4^+$ in the northern region, for which the mean concentrations were 18% and 7% lower at the urban sites than at the rural sites, respectively.

Comparing northern vs. southern regions (Table 1), at urban sites the annual mean concentrations of $NH_3$, $HNO_3$, and $pNH_4^+$ showed smaller non-significant differences (-1~9%), whereas $NO_2$ and $pNO_3^-$ showed larger non-significant increases (34 and 76%, respectively) in the north. By contrast, the mean concentrations of all measured $N_r$ species were significantly ($p$<0.05) higher (by 40-104%) at rural sites in northern region. Similarly, individual concentrations at background sites were 21-71% higher in the northern than southern region. Averaged across three land use types, the annual mean $N_r$ concentrations of five $N_r$ species in the north increased to varying extent (by 84% for $pNO_3^-$, 63% for $pNH_4^+$, 57% for $NH_3$, 47% for $NO_2$, and 28% for

$HNO_3$) compared with those in the south. The annual concentrations of total $N_r$ (i.e., the sum of five $N_r$ species) decreased in the order urban > rural > background in eastern China as a whole and in the north and south regions; further, the annual total $N_r$ concentrations at urban and background sites were 17 and 34% higher ($p$>0.05) in the north than in the south, respectively, whereas those at northern rural sites (31.6 ± 3.8 μg N $m^{-3}$) were significantly ($p$<0.05) higher than the means at southern rural sites (17.0 ± 1.7 μg N $m^{-3}$).

The monthly VWM concentrations of $NH_4^+$-N, $NO_3^-$-N, and TIN (the sum of $NH_4^+$-N and $NO_3^-$-N) were in the ranges 0.01 (BY)-26.77 (YC), 0.06 (XS)-28.92 (WJ), and 0.09 (XS)-50.29 (YC) mg N $L^{-1}$, respectively (Table S3, Supplement). In eastern China and in each region, the annual VWM concentrations of $NO_3^-$-N and TIN showed a declining trend of urban > rural > background, whereas those of $NH_4^+$-N followed the order rural ≥ urban > background (Table 1). Comparing northern and southern regions, the annual concentrations of $NH_4^+$-N, $NO_3^-$-N, and TIN were comparable at urban and background sites, and were significantly ($p$<0.05) higher at northern rural sites.

### 3.2 Annual variability in concentrations of $N_r$ species in air and precipitation

During the 2011-2015 period the annual mean concentrations of measured $N_r$ species in air exhibited no significant trends at the twenty-two selected sites except for $NH_3$ at four sites (ZZ, DL, ZMD, YL), $HNO_3$ at three sites (DL, LSD, BY), $pNH_4^+$ at one site (XS), and total $N_r$ at three sites (ZMD, YL, WJ) (Fig. S1a-f, Supplement). Similarly, no significant trends were found for the annual VWM concentrations of $NH_4^+$-N, $NO_3^-$-N, and TIN in precipitation at the seventeen selected sites, with the exception of $NO_3^-$-N at one site (SZ) (Fig. S2a-c, Supplement).

Fig. 2 compares annual average concentrations of all measured $N_r$ species between the periods 2013-2015 and 2011-2012 for three land use types. In eastern China the mean concentrations of $NH_3$ and $pNH_4^+$ showed non-significant increases (10-38%) at all land use types except $pNH_4^+$ at background sites, which showed a small reduction (8%) (Fig. 2a, d). By contrast, the mean concentrations of remaining $N_r$ species at three land use types showed smaller and non-significant changes: -8~3%

for $NO_2$ (Fig. 2b), -13~5% for $HNO_3$ (Fig. 2c), and -1~5% for $pNO_3^-$ (Fig. 2e). The relative changes in the annual total $N_r$ concentration were also not significant, with the largest increase at rural sites (16%) and smaller increases at urban (4%) and background (1%) sites (Fig. 2f). Separated by regions, annual mean concentrations of five $N_r$ species at three land use types mostly showed increases (4-57%) in the north, and reductions (0.3-21%) in the south (Fig. 2a-f). The relative changes in individual concentrations at northern rural sites (9% reduction for $HNO_3$, and 9-52% increases for the other species) and southern rural sites (4% increase for $pNH_4^+$, and 0.3-21% reductions for other species) were not significant. The annual total $N_r$ concentrations showed small relative changes (from -1% to 5%) across all land use types in the two regions, except at northern rural sites, which exhibited a larger but non-significant increase (25%) (Fig. 2f). Due to significant interannual variability, longer records are needed to better assess the significance of any concentration changes.

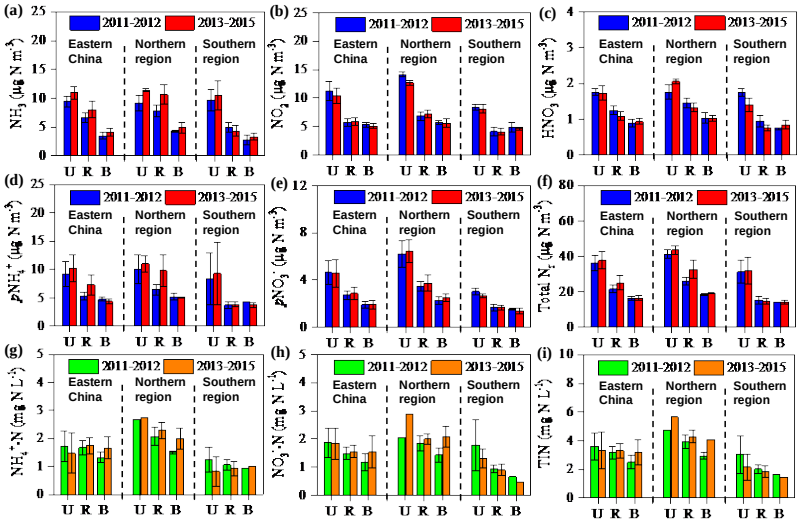


**Figure 2**. Comparison of annual mean concentrations of **(a)** $NH_3$; **(b)** $NO_2$; **(c)** $HNO_3$; **(d)** $pNH_4^+$; **(e)** $pNO_3^-$; and **(f)** total $N_r$: sum of all measured $N_r$ in air and volume-weighted concentrations of $NH_4^+$ **(g)**; $NO_3^-$ **(h)** and total inorganic N (TIN): sum of $NH_4^+$ and $NO_3^-$ **(i)** in precipitation between the 2011-2012 period and the 2013-2015 period for different land use types in eastern China and its northern and southern regions. U, R, and B denote urban, rural, and background sites, respectively.

The number of sites for each land use type in each region can be found in Table S1 in the Supplement. The error bars are the standard errors of means.

In eastern China, the annual VWM concentrations of $NH_4^+$-N, $NO_3^-$-N and TIN showed the largest increase of 26-31% at background sites, a smaller increase of 4-5% at rural sites, and a decrease of 2-14% at urban sites; however, those changes were not significant (Fig. 2g-i). Regionally, their respective concentrations showed increases (3-45%) in the north and reductions (5-33%) in the south, except for a small increase (4%) in $NH_4^+$-N at background sites.

### 3.3 Seasonal variability in concentrations of $N_r$ species in air and precipitation

Fig. 3 shows seasonal patterns of $NH_3$, $NO_2$, $HNO_3$, $pNH_4^+$, $pNO_3^-$ and total $N_r$ concentrations for three land use types in eastern China and its northern and southern regions, averaged from corresponding measurements at the twenty-seven study sites (details for each site are given in Tables S4-S9 of the Supplement). Average $NH_3$ concentrations at all land use types decreased in the order summer > spring > autumn > winter, and significant seasonal differences generally occurred between summer and winter (Fig. 3a). Conversely, the average $NO_2$ concentration generally showed the highest value in winter and the lowest in summer; differences between seasonal concentrations were sometimes significant at rural sites in the south and background sites, but not at urban sites (Fig. 3b). The seasonal changes in the $HNO_3$ concentration were generally small and not significant for all land use types (Fig. 3c).

The average $pNH_4^+$ concentration exhibited a non-significant seasonal variation across all land use types, except for southern rural sites which showed significantly higher values in winter than in summer (Fig. 3d). The highest $pNH_4^+$ concentrations mostly occurred in winter. The average $pNO_3^-$ concentrations at all land use types followed the order winter > spring, ~ autumn > summer; the seasonal changes are sometimes significant, except for urban sites in eastern China and its northern region (Fig. 3e). The average concentration of total $N_r$ usually showed small and non-significant seasonal differences for all land use types (Fig. 3f).

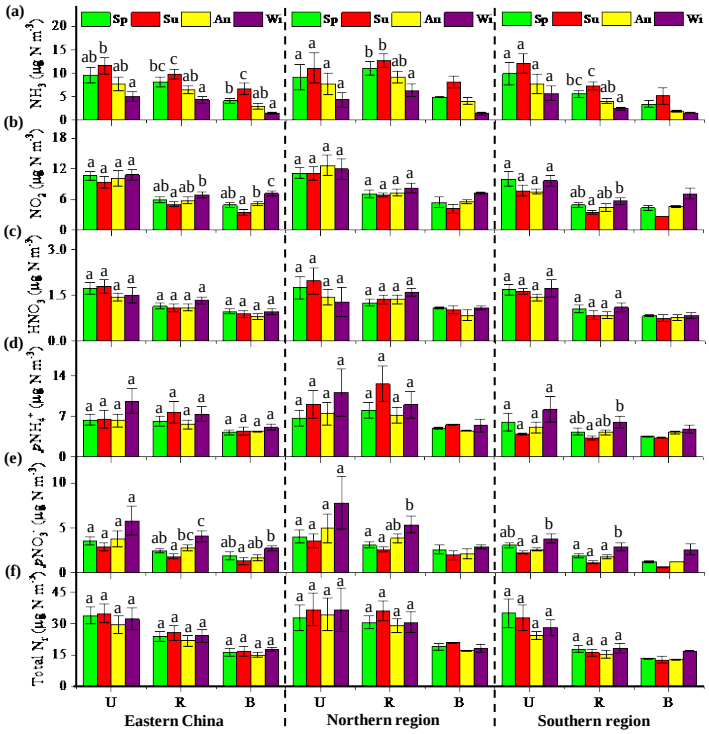


**Figure 3**. Seasonal mean concentrations averaged over 2011-2015 of **(a)** $NH_3$; **(b)** $NO_2$; **(c)** $HNO_3$; **(d)** $pNH_4^+$; **(e)** $pNO_3^-$; and **(f)** total $N_r$: sum of all measured $N_r$ in air at different land use types in eastern China and its northern and southern regions. Sp, Su, Au, and Wi represent spring, summer, autumn, and winter, respectively. U, R, and B denote urban, rural, and background sites, respectively. The number of sites for each land use type in each region can be found in ~~Table S1 in the Supplement~~Table 1. The error bars are the standard errors of means, and values without same letters on the bars denote significant differences between the ~~sites~~ seasons ($p$<0.05).

In eastern China and its two regions, the seasonal VWM concentrations of $NH_4^+$-N, $NO_3^-$-N and TIN in precipitation at three land use types (averaged from the twenty-seven sites, details in Tables S10-S12 of the Supplement) showed a similar seasonal pattern, with the highest values in winter and the lowest in summer or autumn (Fig. 4a-c). Significant seasonal differences usually occurred between winter and the other three seasons at all land use types, except background sites and southern

urban sites.

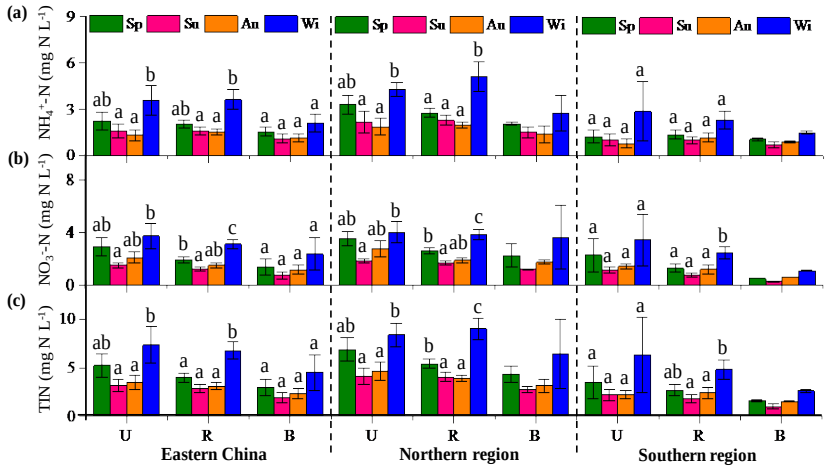


**Figure 4**. Seasonal mean concentrations averaged over 2011-2015 of $NH_4^+$ **(a)**; $NO_3^-$ **(b)** and total inorganic N (TIN): sum of $NH_4^+$ and $NO_3^-$ **(c)** in precipitation at different land use types in eastern China and its northern and southern regions. Sp, Su, Au, and Wi represent spring, summer, autumn, and winter, respectively. U, R, and B denote urban, rural, and background sites, respectively. The number of sites for each land use type in each region can be found in ~~Table S1 in the Supplement~~Table 1. The error bars are the standard errors of means, and values without same letters on the bars denote significant differences between the ~~sites~~ seasons ($p$<0.05).

### 3.4 Spatial variability in dry and wet/bulk N deposition of $N_r$ species

Dry deposition fluxes of $NH_3$, $HNO_3$, $NO_2$, $pNH_4^+$, and $pNO_3^-$ ranked in the order urban > rural > background in eastern China and in both southern and northern regions (except for $pNH_4^+$ in the north) (Table 2). Comparing northern and southern regions, at urban sites the mean dry $pNH_4^+$ deposition was slightly higher (2%) in the north, whereas larger enhancements (24-69%) in the mean fluxes were found in the north for the remaining $N_r$ species. By contrast, individual fluxes were significantly higher (by 64-138%) at northern rural sites, except for $HNO_3$ which showed a large non-significant increase (58%). At northern background sites, the mean dry deposition fluxes of $NH_3$ and $NO_2$ were much higher (159%) and lower (68%), respectively; however, only small differences in the means were found for $HNO_3$ (6% lower in the

north), $pNH_4^+$ (5% lower), and $pNO_3^-$ (14% higher). The spatial pattern of total N dry deposition flux (the sum of the fluxes of the five $N_r$ species) by land use types ranked in the same order as individual $N_r$ species in eastern China. Compared with the southern region, mean total N fluxes in the north region were significantly higher (by 85%) at rural sites, but showed non-significant increases at urban and background sites (33 and 38%, respectively).

The wet/bulk deposition fluxes of $NH_4^+$-N, $NO_3^-$-N, and TIN ranked in the order urban > rural > background in eastern China and in each region (except for $NH_4^+$-N in the south) (Table 2). In addition, their respective fluxes were generally comparable in northern and southern regions.

**Table 2.** Annual average (standard error) dry and wet/bulk deposition fluxes (kg N $ha^{-1}$ $yr^{-1}$) of various $N_r$ compounds at different land use types in eastern China and its northern and southern regions for the 5-year period 2011-2015.

| Region[a] ~~LUY~~[b] LUT[b] | | Dry deposition | | | | | | Wet/bulk deposition | | |
|---|---|---|---|---|---|---|---|---|---|---|
| | | $NH_3$ | $NO_2$ | $HNO_3$ | $pNH_4^+$ | $pNO_3^-$ | Total $N_r$ | $NH_4^+$ | $NO_3^-$ | TIN |
| EC | Urban | 12.6 | 4.4 | 7.7 | 4.8 | 2.1 | 31.7 | 12.6 | 15.4 | 28.0 |
| | (n=6) | (1.4) | (1.2) | (1.6) | (1.4) | (0.5) | (4.6) | (1.9) | (0.7) | (2.2) |
| | Rural | 9.1 | 2.9 | 4.6 | 4.0 | 1.5 | 22.1 | 11.9 | 10.2 | 22.1 |
| | (n=17) | (0.9) | (0.3) | (0.6) | (0.7) | (0.2) | (2.3) | (1.0) | (0.5) | (1.4) |
| | BKD[c] | 7.9 | 1.8 | 3.5 | 1.9 | 0.8 | 15.8 | 10.7 | 7.7 | 18.4 |
| | (n=4) | (2.1) | (0.6) | (0.2) | (0.3) | (0.1) | (1.5) | (1.8) | (0.3) | (1.8) |
| NREC | Urban | 13.9 | 5.2 | 9.4 | 4.9 | 2.7 | 36.2 | 13.9 | 14.1 | 28.0 |
| | (n=3) | (1.9) | (2.5) | (3.0) | (1.9) | (1.0) | (8.2) | (3.5) | (1.0) | (4.4) |
| | Rural | 12.1** | 3.6* | 5.7 | 5.7* | 2.1** | 29.3** | 12.3 | 10.3 | 22.6 |
| | (n=8) | (1.3) | (0.4) | (1.0) | (1.2) | (0.3) | (3.2) | (1.3) | (0.7) | (1.8) |
| | BKD | 11.4 | 0.9 | 3.4 | 1.9 | 0.8 | 18.4 | 7.8 | 7.6 | 15.4 |
| | (n=2) | (0.6) | (0.7) | (0.3) | (0.7) | (0.2) | (0.7) | (1.4) | (0.8) | (0.6) |
| SREC | Urban | 11.2 | 3.6 | 5.9 | 4.8 | 1.6 | 27.2 | 11.4 | 16.6 | 28.0 |
| | (n=3) | (2.0) | (0.3) | (0.6) | (2.6) | (0.2) | (4.0) | (2.0) | (0.4) | (2.1) |
| | Rural | 6.5 | 2.2 | 3.6 | 2.4 | 1.0 | 15.8 | 11.6 | 10.2 | 21.8 |
| | (n=9) | (0.5) | (0.4) | (0.6) | (0.4) | (0.2) | (1.4) | (1.5) | (0.9) | (2.2) |

| | | | | | | | | | |
|---|---|---|---|---|---|---|---|---|---|
| BKD (n=2) | 4.4 (1.0) | 2.7 (0.2) | 3.6 (0.3) | 2.0 (0.1) | 0.7 (0.1) | 13.3 (0.7) | 13.6 (0.1) | 7.9 (0.1) | 21.5 (0.1) |

[a] EC: eastern China; NREC: northern region of eastern China; SREC: southern region of eastern China. [b] LUT~~LSY~~: land use type; n denotes number of monitoring sites. [c] BKD: Background. * and ** denote significance at the 0.05 and 0.01 probability levels for difference in annual mean $N_r$ concentrations at a given site type between northern and southern regions, respectively. ~~*Significant at the 0.05 probability level. **Significant at the 0.01 probability level.~~

### 3.5 Annual variability in dry and wet/bulk N deposition

The annual trends of dry deposition fluxes of individual $N_r$ species at the twenty-one selected sites are consistent with trends in their respective ambient concentrations, except for $HNO_3$ at three sites (SZ, LSD, and ZY) (Figs. S3a-e and S1a-e, Supplement). A consistent picture is also seen for the total dry N deposition fluxes at all but two sites (DL and WJ) (Figs. S3f and S1f, Supplement). Similarly, the annual trends of wet/bulk deposition fluxes of $NH_4^+$-N, $NO_3^-$-N and TIN at seventeen selected sites are similar to their respective concentrations in precipitation (Fig. S4a-c, Supplement).

In eastern China the annual average dry deposition fluxes of $NH_3$, $NO_2$, $HNO_3$, $pNH_4^+$ and $pNO_3^-$ showed non-significant increases (2-39%) or reductions (1-19%) between the periods 2011-2012 and 2013-2015 at the three land use types (Fig. 5a-e), similar in sign and magnitude to their respective concentrations described earlier. The annual average total N dry deposition fluxes showed small and non-significant increases across the study periods: 2% at urban sites, 9% at rural sites, and 7% at background sites (Fig. 5f). The sign and magnitude of period-to-period changes in dry deposition and ambient concentrations of all measured $N_r$ species were generally similar between the southern and northern regions.

Wet/bulk deposition fluxes of $NH_4^+$-N, $NO_3^-$-N, and TIN generally decreased (4-29%) between 2011-2012 and 2013-2015 periods at all land use types in eastern China; one exception was $NO_3^-$-N, which exhibited a small increase (3%) at urban sites (Fig. 5g-i). Similar tendencies were also observed in both northern and southern

regions.

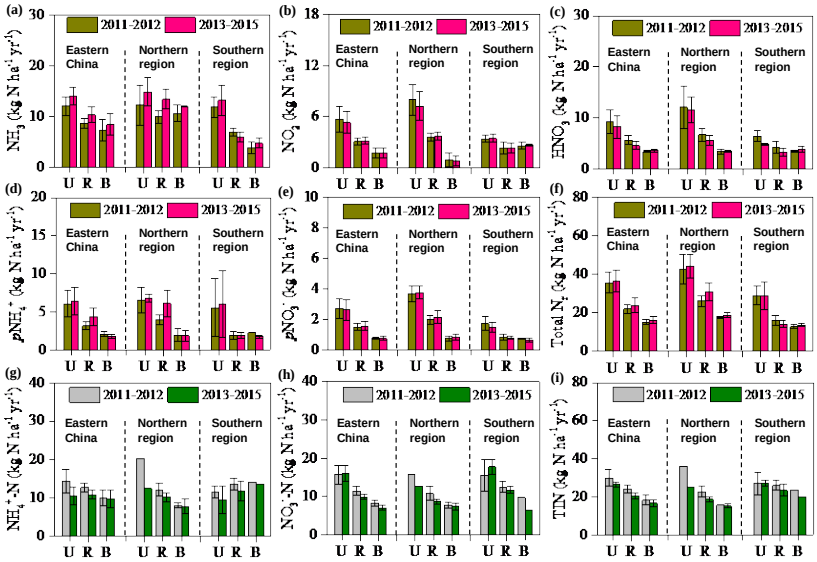


**Figure 5**. Comparison of dry deposition of **(a)** $NH_3$; **(b)** $NO_2$; **(c)** $HNO_3$; **(d)** $pNH_4^+$; **(e)** $pNO_3^-$; and **(f)** total $N_r$: sum of all measured $N_r$ in air and wet/bulk deposition of $NH_4^+$ **(g)**; $NO_3^-$ **(h)** and total inorganic N (TIN): sum of $NH_4^+$ and $NO_3^-$ **(i)** in precipitation between the 2011-2012 period and the 2013-2015 period for different land use types in eastern China and its northern and southern regions. U, R, and B denote urban, rural, and background sites, respectively. The number of sites for each land use type in each region can be found in Table S1 in the Supplement. The error bars are the standard errors of means.

### 3.6 Seasonal variability in dry and wet/bulk deposition of $N_r$ species

Seasonal variations of dry deposition of individual $N_r$ species at each site are shown in Tables S4-S9 in the Supplement. In eastern China and in each region, dry $NH_3$ deposition fluxes at all land use types followed the order summer > spring > autumn > winter, with the seasonal changes usually significantly different (Fig. 6a). Similarly, dry the $NO_2$ deposition flux was also at its minimum in winter, but its maximum was found in summer at urban and rural sites and in autumn at background site; seasonal differences in most cases were not significant (Fig. 6b). Seasonal

patterns of dry $HNO_3$ deposition flux at all land use types were similar to those for dry $NH_3$ deposition fluxes, and the resulting seasonal changes were sometimes significant, except at northern urban sites (Fig. 6c).

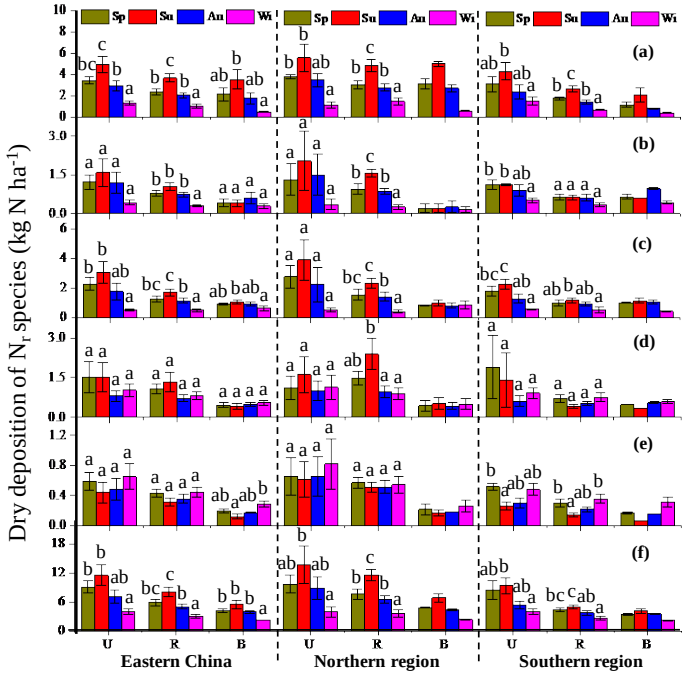


**Figure 6**. Seasonal mean dry deposition averaged over 2011-2015 of **(a)** $NH_3$; **(b)** $NO_2$; **(c)** $HNO_3$; **(d)** $pNH_4^+$; **(e)** $pNO_3^-$; and **(f)** total $N_r$: sum of all measured $N_r$ in air at different land use types in eastern China and its northern and southern regions. Sp, Su, Au, and Wi represent spring, summer, autumn, and winter, respectively. U, R, and B denote urban, rural, and background sites, respectively. The number of sites for each land use type in each region can be found in ~~Table S1 in the Supplement~~Table 2. The error bars are the standard errors of means, and values without same letters on the bars denote significant differences between the ~~sites~~ seasons ($p$<0.05).

Dry $pNH_4^+$ deposition fluxes peaked in spring or summer at urban and rural sites, but remained at similar levels across the four seasons at background sites; however, no significant seasonal variations were found at any land use types except for rural sites in the north (Fig. 6d). Dry $pNO_3^-$ deposition fluxes were higher in spring and

winter than in summer and autumn at all land use types, and the seasonal changes were sometimes significant at background sites and at southern urban and rural sites (Fig. 6e). Total dry N deposition fluxes at all land use types showed similar seasonal variations to dry $NH_3$ deposition, with the highest values in summer and the lowest in winter; significant seasonal differences generally were observed between winter and the other three seasons (Fig. 6f).

Wet/bulk deposition fluxes of $NH_4^+$-N, $NO_3^-$-N, and TIN all showed significant seasonal variation at urban and rural sites, but not at background sites, with the highest values in summer and the lowest in winter (Fig. 7a-c).

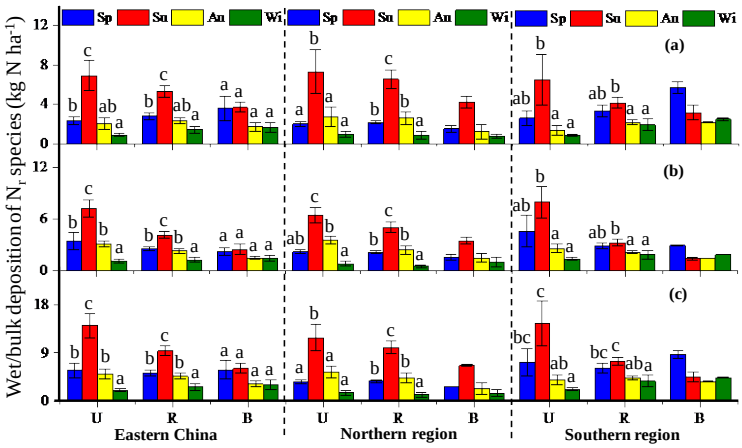


**Figure 7**. Seasonal mean wet/bulk deposition averaged over 2011-2015 of $NH_4^+$ **(a)**; $NO_3^-$ **(b)** and total inorganic N (TIN): the sum of $NH_4^+$ and $NO_3^-$ **(c)** in precipitation at different land use types in eastern China and its northern and southern regions. Sp, Su, Au, and Wi represent spring, summer, autumn, and winter, respectively. U, R, and B denote urban, rural, and background sites, respectively. The number of sites for each land use type in each region can be found in Table ~~S1 in the Supplement~~2. The error bars are the standard errors of means, and values without same letters on the bars denote significant differences between the ~~sites~~ seasons ($p$<0.05).

### 3.7 Spatial-temporal variability in total annual dry and wet/bulk deposition of $N_r$ species

In eastern China total annual mean N deposition (dry plus wet/bulk) fluxes at rural and background sites were comparable (on average, 44.3 ± 3.0 and 34.3 ± 0.7 kg N $ha^{-1}$ $yr^{-1}$, respectively), but significantly lower than those at urban sites (59.7 ± 6.1 kg N $ha^{-1}$ $yr^{-1}$) (Tables 1 and 2, and Fig. S5, Supplement). Similar tendencies for total N deposition fluxes were observed in the southern region, while in the north a significant difference was only found between urban and background sites (Fig. S5, Supplement). From 2011 to 2015, no significant annual trend was found in the total N deposition at sixteen selected sites (Fig. S6a, Supplement). The total annual mean N deposition fluxes at three land use types showed small and non-significant reductions (1-5%) between 2011-12 and 2013-15 (Fig. S6b, Supplement). Regionally, the total fluxes at each land use type were of similar magnitude in the two periods. Also, the $NH_x$ (wet/bulk $NH_4^+$-N deposition plus dry deposition of $NH_3$ and particulate $NH_4^+$)/$NO_y$ (wet/bulk $NO_3^-$-N deposition plus dry deposition of $NO_2$, $HNO_3$ and particulate $NO_3^-$) ratio showed a non-significant annual trend across all sites (Fig. 8a). At all land use types, the averaged ratios were slightly higher in the 2013-2015 period than in the 2011-2012 period (Fig. 8b).

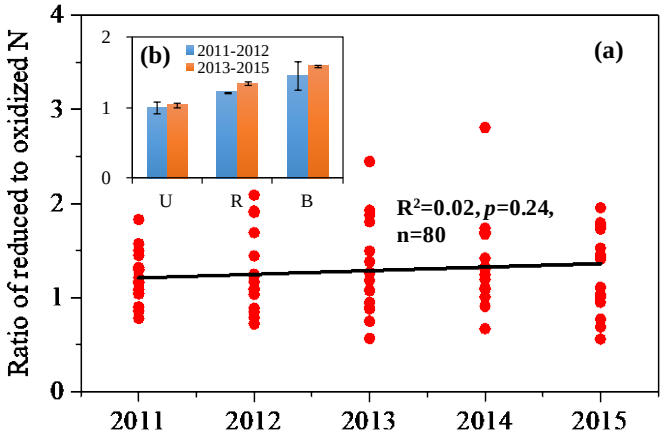


**Figure 8**. Annual trend of the ratio of $NH_x$ (wet/bulk $NH_4^+$-N deposition plus dry deposition of $NH_3$ and particulate $NH_4^+$) to $NO_y$ (wet/bulk $NO_3^-$-N deposition plus dry deposition of $NO_2$, $HNO_3$ and particulate $NO_3^-$) across sixteen selected sites **(a)**, with a comparison between the 2011-2012 period and the 2013-2015 period for

different land use types in eastern China **(b)**. U, R, and B denote urban, rural, and background sites, respectively. The number of sites with the same land use type can be found in Fig. S6 in the Supplement.

## 4. Discussion

### 4.1 Comparisons of $NH_3$ and $NO_2$ measurements with satellite data

Eastern China, as is a highly industrialized and polluted region, and has been proven to be a hot-spot of $N_r$ ($NH_3$ and $NO_x$) emission and deposition globally (Vet et al., 2014; Kanakidou et al., 2016). The results presented above showed that, in eastern China, annual mean concentrations of measured $N_r$ species in air and precipitation were generally higher in the north than in the south (Table 1). This is likely due to higher consumption of energy and application of N-fertilizers, along with lower precipitation amounts in the north, previously identified as key factors affecting spatial patterns of N deposition in China (Liu et al., 2013; Jia et al., 2014; Zhu et al., 2015). Because only 27 sites covering a range of land use types were included in the present study, additional information would be valuable in determining whether the observed spatial patterns adequately represent conditions in eastern China. To address this issue, we use measured $NH_3$ and $NO_2$ concentrations to evaluate remote sensing techniques for retrieving $NH_3$ and $NO_2$ concentrations. If accurate, those remote sensing techniques are well suited to ascertain regional species distributions. $NH_3$ and $NO_x$ are primary emissions with important anthropogenic emissions (Fowler et al., 2013). NO, the main component of emitted $NO_x$, is oxidized in the atmosphere to $NO_2$. $NO_2$ is further oxidized via daytime or nighttime chemistry to $HNO_3$ (Khoder, 2002). $NH_3$ and $HNO_3$ can react to form fine particle ammonium nitrate (Seinfeld and Pandis, 2006). Thus, spatial patterns of $NH_3$ and $NO_2$ observed from space can be useful indicators of reduced and oxidized $N_r$ pollution over eastern China.

From satellite observations (Fig. 9a, b), it can be seen that both IASI_$NH_3$ and OMI_$NO_2$ columns show clearly higher values over the northern region of eastern China. Overall, satellite observations and surface measurements for $NH_3$ and $NO_2$ (plotted on the maps of Fig. 9a, b) show a similar spatial pattern. Significant positive

correlations were found between IASI_$NH_3$ column observations and NNDMN_$NH_3$ measurements (r=0.72, $p$<0.001) (Fig. 9c) and between OMI_$NO_2$ observations and NNDMN_$NO_2$ measurements (r=0.86, $p$<0.001) (Fig. 9d) at the 27 surface measurement locations, suggesting that satellite measurements of $NH_3$ and $NO_2$ can be used to capture regional differences in $NH_3$ and $NO_2$ pollution. Looking beyond the surface measurement location, the satellite observations further confirm the existence of greater $N_r$ pollution in the northern region of eastern China than in the southern region.

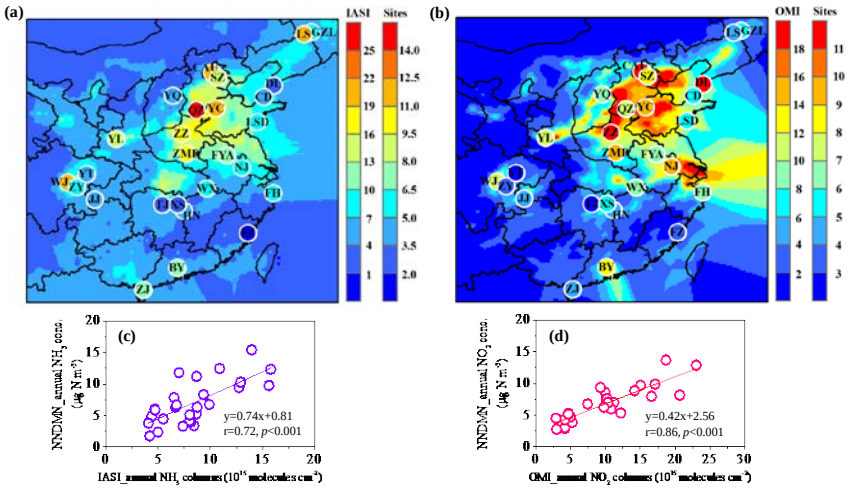


**Figure 9**. Spatial variation of atmospheric $N_r$ in eastern China: **(a)** NNDMN_$NH_3$ concentrations vs. IASI_$NH_3$ columns; **(b)** NNDMN_$NO_2$ concentrations vs. OMI_$NO_2$ columns; **(c)** relationship of NNDMN_$NH_3$ concentrations vs. IASI_$NH_3$ columns; **(d)** relationship of NNDMN_$NO_2$ concentrations vs. OMI_$NO_2$ columns.

To further explore temporal concentration variability, monthly mean satellite $NH_3$ and $NO_2$ columns are compared with monthly mean ground concentrations of $NH_3$ and $NO_2$ (Figs. S7 and S8, Supplement). The linear correlation between satellite columns and surface $NH_3$ concentrations is significant ($p$<0.05) at the ten sites (r=0.32-0.87) in the northern region and at four sites (r=0.46-0.84) in the southern region (Fig. S7, Supplement), while the linear correlation between satellite columns and surface $NO_2$ concentrations is significant at the ten sites (r=0.28-0.68) in the

northern region and nine sites (r=0.36-0.66) in the southern region (Fig. S8, Supplement). These results indicate that the OMI_$NO_2$ retrieval can well capture the temporal variations of surface $NO_2$ concentrations over eastern China, whereas the IASI_$NH_3$ retrievals better capture temporal variability in surface concentrations for the northern region. The weak correlations observed between IASI_$NH_3$ observations and surface measurements at ten of the fourteen sites in the southern region (Fig. S7, Supplement) suggest that the IASI_$NH_3$ observations need to be improved for investigating temporal variability in $NH_3$ concentration, despite that the satellite observation is at a specific time of day while the surface concentrations integrate across the diurnal cycle of emissions and mixing layer evolution. It should be noted that a direct comparison between surface concentration and satellite column measurements is inevitably affected by many factors, such as changes in boundary layer height, vertical profiles of species, and interferences from cloud and aerosol (Van Damme et al., 2015). Nevertheless, the ratio of satellite column to surface concentration measurements is meaningful as it can provide insight into sensitivity of a satellite retrieval to variation in the concentration of a gas in the surface layer (Meng et al., 2008). To make a more accurate comparison, the vertical profile is recommended to convert the columns to the ground concentrations in future work.

### 4.2 Seasonal variations of $N_r$ concentration and deposition

The seasonal concentrations of $N_r$ species in air and precipitation are dependent on their sources and meteorological conditions. The highest concentrations of $NH_3$ in summer at all land use types (Fig. 3a) are most likely due to enhanced $NH_3$ emission from natural and fertilized soils, and biological sources such as humans, sewage systems and organic waste in garbage containers (Chang et al., 2016). Zhang et al. (2018) showed that $NH_3$ emissions in China show a strong summer peak, with emissions about 50% higher in summer than spring and autumn. The lowest concentrations of $NH_3$ in winter (Fig. 3a) can be ascribed to low ~~the reduced~~ $NH_3$ volatilization under cold condition ~~at low air temperature~~, high snow coverage, and ~~low~~less agricultural activities (Cao et al., 2009) with large ~~as well as~~ consumption of $NH_3$ to form $NH_4NO_3$ ~~(Fig. 3a, d and e)~~ and~~/or~~ $(NH_4)_2SO_4$. The lower $NO_2$

concentration in summer (Fig. 3b) might result from ~~greater~~higher atmospheric mixing in a deeper boundary layer and a higher rate of oxidation of $NO_2$ to $HNO_3$ by reaction with OH (Atkins and Lee, 1995), which is more abundant in summer due to greater photochemical activity. Increased $NO_2$ emissions from greater coal combustion for domestic heating (from middle November to middle March) in ~~Northern~~ northern China may also enhance $NO_x$ emissions and subsequent $NO_2$ concentrations in autumn/winter (Zhao et al., 2011).

Particulate $NH_4^+$ and $NO_3^-$ are mainly generated via chemical reactions between $NH_3$ and inorganic acids (e.g., $HNO_3$, $H_2SO_4$). We found that concentrations of $pNH_4^+$ and $pNO_3^-$ at all land use types usually peaked in winter because low temperature and high emissions of $NO_x$ and $SO_2$ are favorable for formation of $NH_4NO_3$ and $(NH_4)_2SO_4$ aerosols (Xu et al., 2016), consistent with higher concentrations of $pNH_4^+$ and $pNO_3^-$. In addition, in winter temperature inversions in combination with stable meteorological conditions (e.g., low wind speed) limit horizontal and vertical exchange of pollutants, and further elevated atmospheric $pNH_4^+$ and $pNO_3^-$ levels (Liu et al., 2017). In order to identify potential transport of $NO_2$, $pNH_4^+$ and $pNO_3^-$ from northern region, we calculated three-day backward trajectories arriving at five southern sites (Nanjing, Baiyun, Taojing, Ziyang and Huinong) during January, April, July and October using the TrajStat. The TrajStat analysis generally showed that the high proportions (overall 10-36%) of air masses from the north to the south of eastern China occurred in the autumn/winter, suggesting that the transport of $NO_2$, $pNH_4^+$ and $pNO_3^-$ from northern China would result in increases in their respective concentrations in autumn/winter south of the Qinling Mountains-Huaihe River line, except at Ziyang site (Fig. S13, Supplement).

Nitric acid is a secondary pollutant, formed through gas phase reaction of $NO_2$ with the OH radical, reaction of $NO_3$ with aldehydes or hydrocarbons or hydrolysis of $N_2O_5$ (Khoder, 2002). Nitric acid concentrations are expected to be further influenced by air temperature, relative humidity and ambient $NH_3$ concentrations (Allen et al., 1989); fine particle $NH_4NO_3$ formation is favored at low temperatures and high relative humidities. Due to a lack of information regarding primary formation

pathways and influencing factors at our study sites, we cannot offer a definitive explanation for small and differing seasonal patterns of $HNO_3$ concentrations observed at the three land use types (Fig. 3c).

Ammonium-N and nitrate-N in precipitation mainly originate from corresponding reduced (e.g., $NH_3$, $pNH_4^+$) and oxidized (e.g., $HNO_3$, $NO_2$, $pNO_3^-$) N in air, scavenged respectively, by rain and/or snow events (Seinfeld and Pandis, 2006). At all land use types, the seasonal variation of $NH_4^+$-N concentration in precipitation was opposite to that of reduced N (the sum of $NH_3$ and $pNH_4^+$) concentrations (Figs. 4a and S9a in the Supplement), whereas a similar seasonal pattern was found between $NO_3^-$-N and oxidized N (the sum of $HNO_3$, $NO_2$ and $pNO_3^-$) concentrations (Figs. 4b and S9b in the Supplement). Higher precipitation amounts in summer could account for lower $NH_4^+$-N concentrations in summer (Figs. 4a and S10 in the Supplement) due to a dilution effect (Xu et al., 2015). In contrast, seasonal variations of rainwater $NO_3^-$-N concentrations were more likely dominated by seasonal changes in oxidized N concentrations rather than precipitation amount.

The seasonal variation of $NH_3$ dry deposition is generally similar to that of $NH_3$ concentration (Figs. 3a and 6a). Given comparable seasonal mean $V_d$ for $NH_3$ across the four seasons in most cases (Fig. S11a-c, Supplement), the seasonality of $NH_3$ deposition is mainly dominated by changes in ambient $NH_3$ concentrations. Seasonal deposition fluxes of $NO_2$ and $HNO_3$ both differ appreciably (Fig. 6b, c), showing similar variation to seasonality of their respective $V_d$ values (Fig. S11d-i, Supplement). Given weaker seasonal fluctuations of $NO_2$ and $HNO_3$ concentrations, the seasonality of $NO_2$ and $HNO_3$ dry deposition are primarily functions of changes in $V_d$. Similar analyses suggest that seasonal variation of $pNO_3^-$ dry deposition was mainly caused by differences in seasonal $pNO_3^-$ concentrations (Figs. 3e and 6e), whereas that of $pNH_4^+$ dry deposition was primarily driven by seasonal changes in $V_d$ (Figs. 6c and S11j-l, Supplement).

### 4.3 The role of $NH_3$ in mitigation of $N_r$ air pollution

The latest pollutant emissions statistics from the Chinese Ministry of Environmental Protection

(http://www.zhb.gov.cn/gkml/hbb/qt/201507/t20150722_307020.htm) showed that total annual emissions of $SO_2$ and $NO_x$ were reduced by 12.9% and 8.6% in 2014 (approximately 9.9 Tg S $yr^{-1}$ and 6.3 Tg N $yr^{-1}$, respectively), respectively, compared with those in 2010 (approximately 11.3 Tg S $yr^{-1}$ and 6.9 Tg N $yr^{-1}$, respectively). This suggests that the goal set for the 12th FYP period was fulfilled ahead of time. Our field measurements demonstrate that annual mean concentrations of each $N_r$ species and total $N_r$ did not show significant decreasing trends at most sites during the 2011-2015 period (Fig. S1a-f, Supplement). Furthermore, annual mean total $N_r$ concentrations showed non-significant increases (1-16%) at three land use types during the 2013-2015 period compared with 2011-2012 (Fig. 2f). These results together suggest that $N_r$ pollution may be not effectively mitigated in eastern China during the 12th FYP, likely due to the absence of $NH_3$ regulations, despite enforcement of a "Zero Increase Action Plan" by the Ministry of Agriculture for national fertilizer use (X. J. Liu et al., 2016).

Ammonia is the primary alkaline gas in the atmosphere. It plays an important role in formation of $(NH_4)_2SO_4$ and $NH_4NO_3$ aerosols (Seinfeld and Pandis, 2006). These secondary inorganic aerosols account for 40–57 % of the $PM_{2.5}$ concentrations in eastern China (Yang et al., 2011; Huang et al., 2014). Based on monthly mean molar concentrations, there were significant positive linear correlations between $NH_3$ and $pNH_4^+$, $NO_2$ and $pNO_3^-$, $SO_2$ and $pSO_4^{2-}$, $pNH_4^+$ and $pNO_3^-$, and $pNH_4^+$ and $pSO_4^{2-}$ at all land use land types except for a non-significant relationship of $NH_3$ with $pNH_4^+$ at background sites (Fig. 10a-e). These results suggest that the precursor gases are responsible for the formation of secondary inorganic ions (i.e., $pNH_4^+$, $pNO_3^-$, and $pSO_4^{2-}$) locally at urban and rural sites, while secondary inorganic ions at background sites likely originated from long-distance transport. The ratio of $NH_3$ to $NH_x$ ($NH_3$ plus $pNH_4^+$) concentrations at urban (0.53 ± 0.15) and rural (0.52 ± 0.16) sites exceeded values at background (0.43 ± 0.16) sites. According to Walker et al. (2004), a value greater than 0.5 indicates that $NH_x$ is more likely to be from local sources as opposed to long-range transport.

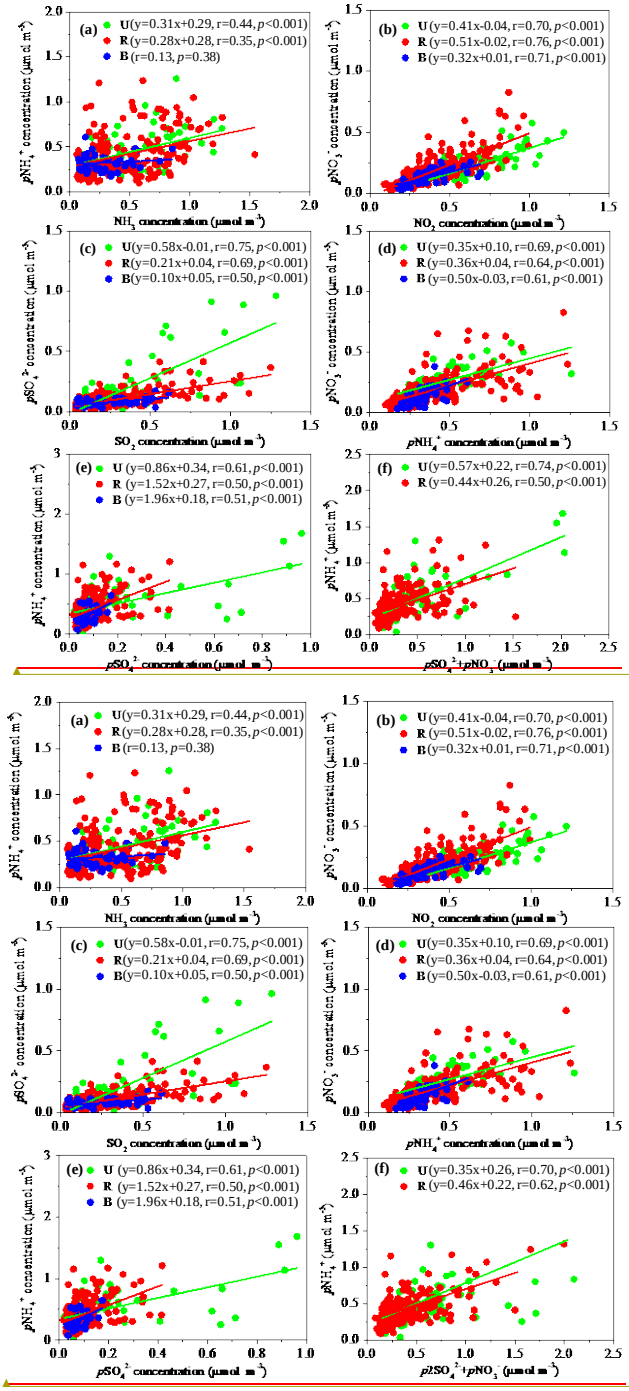





**Figure 10**. Correlations of monthly mean molar concentrations of (a) $pNH_4^+$ vs. $NH_3$; (b) $pNO_3^-$ vs. $NO_2$; (c) $pSO_4^{2-}$ vs. $SO_2$; (d) $pNO_3^-$ vs. $pNH_4^+$; (e) $pNH_4^+$ vs. $pSO_4^{2-}$;

带格式的：字体：（默认）Times New Roman，小四，字体颜色：自动设置

带格式的：缩进：首行缩进： 2 字符

带格式的：字体：+西文正文，五号，字体颜色：自动设置

带格式的：缩进：首行缩进： 2 字符

(f) $pNH_4^+$ vs. ($p2SO_4^{2-}$ + $pNO_3^-$) at three land use types in eastern China. The number of sites with the same land use type in each region can be found in Table 1~~S1 in the Supplement~~.

It is known that $NH_3$ in the atmosphere is preferentially neutralized by $H_2SO_4$ to form $(NH_4)_2SO_4$ and/or $NH_4HSO_4$, with any remainder available for potential reaction with $HNO_3$ to form $NH_4NO_3$. At urban and rural sites, monthly mean $pNH_4^+$ concentrations significantly positively correlated with the sum of $p2SO_4^{2-}$ and $pNO_3^-$ concentrations (Fig. 10f). However, the slopes of regression equations between them were both smaller than unity (0.~~57~~35 and 0.~~44~~46 at urban and rural sites, respectively), indicating an incomplete neutralization of acidic species ($HNO_3$ and $H_2SO_4$) by $NH_3$ at urban and rural sites. In other words, $NH_3$ is a factor limiting the formation of secondary inorganic ions. A model simulation by Wang et al. (2011) found that, without $NH_3$ emission controls, $NO_3^-$ in $PM_{2.5}$ will be enhanced by 10% in 2030 compared with 2005 in China, despite improved $NO_x$ emissions controls. As reported by Zhang et al. (2017), total $NH_3$ emissions in China increased from 12.1 Tg N $yr^{-1}$ in 2000 to 15.6 Tg N $yr^{-1}$ in 2015 at an annual rate of 1.9%. In contrast, total emissions of $NO_x$ and $SO_2$ have decreased or stabilized in recent years, and were estimated to be 8.4 Tg N $yr^{-1}$ and 12.5 Tg S $yr^{-1}$ in 2014, respectively (Xia et al., 2016). Based on these factors, implementation of $NH_3$ control strategies, ~~relative to~~together with more stringent~~current~~ $NO_x$ and $SO_2$ emission controls, should be considered to mitigate atmospheric $N_r$ pollution.

### 4.4 The role of $NH_3$ emission in control of N deposition

The present results showed that total dry N deposition fluxes at three land use types were higher in the northern region of eastern China than in the southern region (Table 1), mainly due to higher $NH_3$ dry deposition resulting from higher $NH_3$ concentrations in the north. This is especially true for northern rural sites (Table 1), mostly located in the North China Plain (NCP) (see details in Xu et al. (2015)). The NCP (that is, the plain areas in Beijing, Tianjin, Hebei, Henan, and Shandong provinces), a highly populated region with intensive agricultural production, contributes 30-40% of the total annual $NH_3$ emissions in China (Huang et al., 2012).

In addition, higher $NH_3$ concentration is also likely due to the higher $NH_3$ volatilization in calcareous soils than that in the acidic red soil, as mentioned in Section 2.1. Total annual $NH_3$ emissions in northern region increased from 4.3 Tg N $yr^{-1}$ in 2011 to 4.7 Tg N $yr^{-1}$ at an annual rate of 1.8%. In contrast, the emissions of $NO_x$ and $SO_2$ averaged 2.8 Tg N $yr^{-1}$ and 3.7 Tg S $yr^{-1}$ during 2011-2015, and decreased at annual rates of 6.8 and 5.7%, respectively (details of the emissions will be illustrated in Section 4.5). Such reductions may enhance free $NH_3$ in the atmosphere. However, according to a modeling study by Han et al. (2017), the influence of removing anthropogenic $SO_2$ emissions on dry N deposition fluxes during 2010-2014 was quite weak, with the change within -0.5~0.5 (kg N $ha^{-1}$ $yr^{-1}$) over most regions in China. Thus, we anticipate that reducing $NH_3$ emissions can effectively control N deposition.

To further examine contributions of $NH_3$ emissions to total (wet plus dry) N deposition at each site and over eastern China, we conducted model sensitivity tests using the nested GEOS-Chem atmospheric chemistry model driven by the GEOS-5 assimilated meteorological fields at a horizontal resolution of $1/2^o \times 2/3^o$. The model used anthropogenic emissions from the Multi-Resolution Emission Inventory of China (MEIC, http://meicmodel.org) for the year 2010, except for $NH_3$ emissions that are taken from the Regional Emission in Asia (REAS-v2) inventory (Kurokawa et al., 2013), with an improved seasonality derived by Zhao et al. (2015). The total $NH_3$ and $NO_x$ emissions from each source over eastern China and its contribution to total emissions in China are presented in Table S13 in the Supplement. The $NH_3$ and $NO_x$ emissions over eastern China are 11.6 Tg N $yr^{-1}$ and 8.5 Tg N $yr^{-1}$ in 2010, which, respectively, account for 90% and 89% of their total emissions over China. Agricultural sources including fertilizer use and livestock, comprise most of the $NH_3$ emissions while fuel combustion activities, including industry, power plant, and transportation contribute most of the $NO_x$ emissions and small amounts of $NH_3$ emissions. Both $NH_3$ and $NO_x$ have natural sources (including lightning, biomass burning and soil emissions), but are negligible compared to anthropogenic emissions over eastern China. Details of the model emissions and mechanisms have been

described elsewhere (Zhao et al., 2017, Xu et al., 2018).

~~In brief, anthropogenic sources of $NH_3$ emissions include fertilizer use, livestock, human waste, and fuel combustion (that in power plant, industry, transportation and residential), whereas $NO_x$ emission sources include industry, power, transportation, and residential. Both $NH_3$ and $NO_x$ have natural sources (including lighting, biomass burning and soil emissions). It should be pointed out that fertilizer $NH_3$ emissions include both chemical fertilizer and manure fertilizer.~~

We evaluate the model simulations by comparing with measured bulk (both $NH_4^+$-N and $NO_3^-$-N) fluxes. The model biases for bulk $NH_4^+$-N and $NO_3^-$-N deposition were 23 and -23%, respectively (Fig. ~~S8~~S12, Supplement). These biases are reasonable, given uncertainties in $N_r$ emissions and predictions of meteorology. Given that model evaluation is not central to this work, we presented the details in Sect. ~~S1~~ S2 in the Supplement. As shown in Fig. 11, fertilizer use is the dominant source of total N deposition at all sites, with contributions between 16-50%. Also, over eastern China the largest contribution was from fertilizer use (36%) relative to livestock (10%), industry (14%), power plant (11%), transportation (9%), and other sources (20%, the sum of contributions from human waste, residential activities, soil, lighting and biomass burning). These results indicate that reducing $NH_3$ emissions ~~from improper~~by use of appropriate fertilization patterns (e.g., 4 R technologies (Right amount, Right time, Right form and Right application technique), Ju et al., 2009) ~~fertilizer (including chemical and organic fertilizer) application~~ should be a priority in curbing N deposition in eastern China~~.~~. This conclusion to some extent is supported by increased ratios of reduced to oxidized N in the total deposition at three land use types (Fig. 8b), as the major anthropogenic source of reduced N is mainly affected by $NH_3$ volatilized from animal excrement and the application of nitrogenous fertilizers in agriculture. Absence of $NH_3$ emission controls may be the main reason for a small and non-significant change in the total N deposition between 2011-12 and 2013-15 (Fig. S6, Supplement), despite enforcement of stringent emission controls on $NO_x$ and $SO_2$. To test the importance of future $NH_3$ emission control strategies, we conducted separate model simulations which reduced $NH_3$ emissions from fertilizer

use by 20%. The results show that a 20% reduction in fertilizer $NH_3$ emissions can lead to 7.4% decrease in total N deposition over Eastern China.

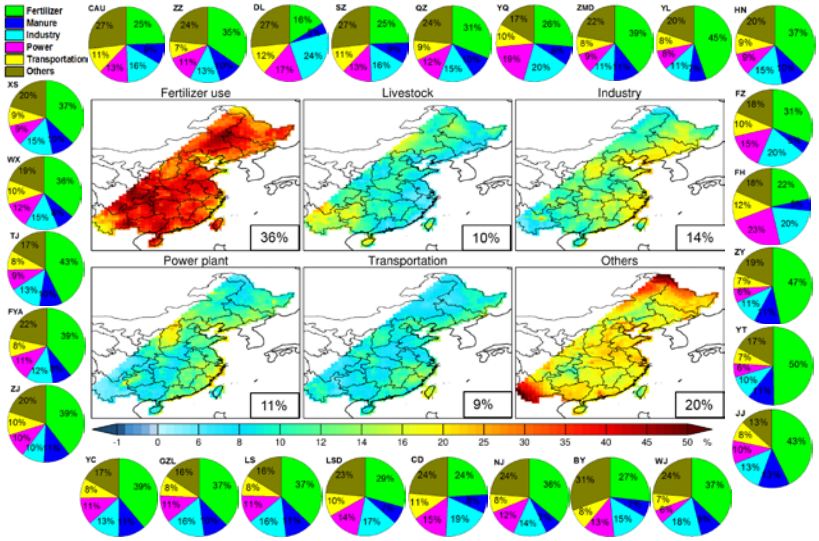


**Figure 11**. Fractional contributions to total N deposition from emission sectors (i.e. fertilizer use, livestock, industry, power plant, transportation, and others including emissions from human waste, residential activities, soil, lighting and biomass burning) at the twenty-seven sites and over eastern China.

### 4.5 Deposition response to emission change

Similar to $N_r$ concentrations, there were no significant decreasing trends in dry and bulk deposition of total N or of individual $N_r$ species at almost all study sites (Figs. S3 and S4, Supplement). In addition, we found that changes in annual mean deposition fluxes of various $N_r$ species are fairly small between the 2013-2015 and 2011-2012 periods (Fig. 5). These results suggest that current emission controls did not effectively reduce N deposition in eastern China.

To further assess the relationship between emission and deposition change, we considered the emissions of $SO_2$, $NO_x$ and $NH_3$ affecting the sixteen study sites with continuous and simultaneous dry and bulk deposition measurements (Fig. S6 and Table S1, Supplement). The regional $NH_3$ emission data for 2011-2015 were derived from Zhang et al. (2017), while $SO_2$ and $NO_x$ emission data for 2011-2014 were

derived from Xia et al. (2016) (emission data for the year 2015 were provided by Prof. Yu Zhao, and were unpublished). We compared these annual data with annual mean deposition values from the 16 sites. It should be noted that such assessment is subject to some uncertainty, as emission data was estimated based on the areas belonging to eastern China.

A clear decreasing trend in $SO_2$ and $NO_x$ emissions was observed, with reductions of 32% and 25% in 2015 compared to 2011, respectively (Fig. 12a, b). This reduction is directly related to the widespread use of selective catalytic reduction and flue gas de-sulfurization on power plants and industries (Van der A et al., 2017), and to a lesser extent to the introduction of new emission standards for cars (F. Liu et al., 2016). In contrast, $NH_3$ emissions generally showed a gradual increasing trend between 2011 and 2015 (Fig. 12c**)**, as control strategies have not yet been enacted and implemented for $NH_3$ emissions in China.

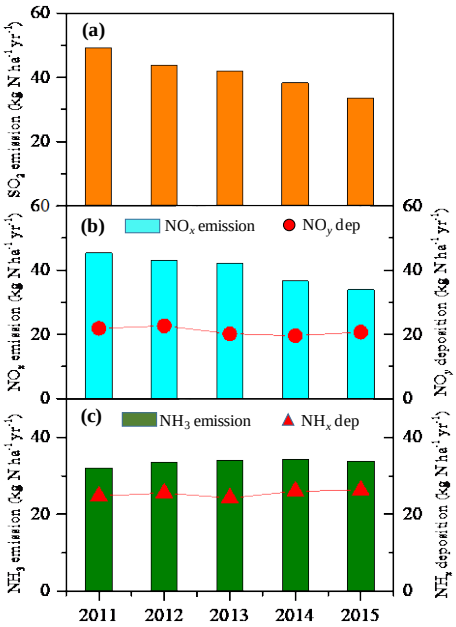


**Figure 12**. Emissions of $SO_2$ (a), $NO_x$ (b) and $NH_3$ (c) obtained as average data from the areas belonging to eastern China, compared with deposition values in the same periods (mean values from the sixteen sites showing in Fig. S6 and Table S1 in the

911 Supplement , 5-year averages).

912 Regarding N deposition, a non-significant increasing trend was found for $NH_x$
913 (slope=0.36 kg N $ha^{-1}$ $yr^{-1}$) between the 2011 and 2015 period, whereas $NO_y$
914 deposition exhibited a non-significant decreasing trend (slope=0.54 kg N $ha^{-1}$ $yr^{-1}$).
915 Also, there were non-significant linear correlations between $NH_x$ deposition and $NH_3$
916 emission and between $NO_y$ deposition and $NO_x$ emission. This is not surprising given
917 that atmospheric chemistry is complex and often behaves non-linearly (Fowler et al.,
918 2007; Fagerli and Aas, 2008). Interactions between the different pollutants,
919 precipitation variability, changes in the relative amounts and lifetimes of the chemical
920 species and in gas-particle partitioning all may contribute to the lack of correlation
921 between emission and deposition trends. Non-linearities between emission and
922 deposition change have been described also elsewhere (Aguillaume et al., 2016;
923 Karlsson et al., 2011). Deposition in eastern China is also influenced by emissions
924 from outside the region, further degrading any expected correlation with local
925 emissions.

926 **4.6 Uncertainties and limitations**

927 The present study examined annual trends of concentrations of $N_r$ species in air
928 and precipitation as well as dry and bulk N deposition based on Kendall tests and only
929 five annual data values (2011-2015). Although the test can use as few as 4 data points,
930 indications of statistically significant trends for datasets are unlikely to be truly
931 representative of the trends that are actually occurring due to in the short duration of
932 the measurement dataset. Longer time series (e.g., more than 10-year) will likely
933 allow detection of more significant time trends in future work. Another uncertainty
934 may arise from the fact that we used fixed monthly mean dry deposition velocities of
935 gaseous and particulate $N_r$ species for the same months from June 2013 to December
936 2015. Nevertheless, the uncertainty in the $V_d$ value did not largely affect the
937 deposition trend, as the annual trend in dry deposition of $N_r$ species is more likely
938 driven by changes in ambient $N_r$ concentrations than to changing deposition velocities,
939 as evident from fairly low standard deviations of annual mean $V_d$ of $N_r$ species at our
940 selected 27 sites between 2008 and 2012 (~0.029 for $NH_3$, ~0.005 for $NO_2$, ~0.054

for $HNO_3$, and ~0.019 for both $pNH_4^+$ and $pNO_3^-$, data were extracted from Zhao et al. (2017)).

In addition, we did not account for inter-annual changes in meteorology, which also strongly influences atmospheric $N_r$ levels and N deposition (Xu et al., 2015, 2017). For example, air concentrations of $NO_2$, $NH_3$, and $pNH_4^+$ and $pNO_3^-$ trend to increase under the relatively stagnant conditions prior to a cold front's arrival and decrease substantially after the cold front brings precipitation and strong winds into the region (Xu et al., 2017). On the inter-annual time scale, the frequency of cold front passages may be affected by large-scale circulation patterns such as the position of the Siberian high for eastern China (Jia et al., 2015). For example, a large inter-annual variation in precipitation amount was observed at the selected 16 sites during 2011-2015 (Fig. S14, Supplement), which partially lead to inter-annual changes in wet/bulk N deposition. However, ~~Given~~ given that *in-situ* measurements of other meteorological variables (e.g., air temperature, relative humidity, air pressure, wind speed and direction) are not available, and that GEOS-5 assimilated meteorological fields were updated after May 2013, an evaluation of the effect of meteorology on $N_r$ concentration and deposition is recommended for future work.

Uncertainties also exist in the source attribution calculated with the GEOS-Chem simulations, since results largely depend on the emission inventories fed to the model. Zhao et al. (2017) pointed out that uncertainties in current $NH_3$ emissions inventories (e.g. large range of the emission value in current studies and absence of inclusion of bi-directional $NH_3$ exchange between the land and atmosphere) may influence nitrogen deposition simulation in China. Future work based on improved $NH_3$ emission inventories (e.g., Zhang et al., 2018) and including bidirectional ammonia exchange with the surface is essential to better examine source attribution of N deposition in China.

## 5. Conclusion

We have characterized spatial and temporal (annual and seasonal) variations in concentrations and deposition of major $N_r$ species in air ($NH_3$, $NO_2$, $HNO_3$, $pNH_4^+$, and $pNO_3^-$) and precipitation ($NH_4^+$-N and $NO_3^-$-N) for three land use types (e.g.,

971 urban, rural and background) in eastern China by examining five-year (2011-2015) *in*
972 *situ* measurements at twenty-seven sites. We further examined regional features of $N_r$
973 pollution by comparison of satellite and surface measurements of $NH_3$ and $NO_2$ and
974 examined the sources of total N deposition over the whole region for the year 2010
975 using the GEOS-Chem model at horizontal resolution of $1/2^o \times 2/3^o$. Our major
976 results and conclusions are as follows:

977 In eastern China, annual mean concentrations and dry and bulk deposition fluxes
978 of measured $N_r$ species in air and precipitation generally ranked in the order urban >
979 rural > background. The air concentrations and dry deposition were usually higher at
980 all land use types in the northern region of eastern China than in the southern region,
981 especially (except $HNO_3$) at rural sites, for which the differences reached statistically
982 significant levels. This is also true for the annual VWM concentrations of $NH_4^+$-N,
983 $NO_3^-$-N, and TIN in precipitation, whereas bulk deposition fluxes of these species
984 were comparable for matched land use types between the northern and southern
985 regions.

986 No significant trends in the annual mean concentrations and dry and bulk
987 deposition fluxes of measured $N_r$ species in air and precipitation were observed at
988 almost all sites during the 2011-2015 period. Also, annual averages of these values
989 showed non-significant changes between the 2011-2012 and 2013-2015 periods for all
990 land use types. Ambient total concentrations of measured $N_r$ species showed a
991 non-significant seasonal variation at all land use types, whereas individual $N_r$ species
992 exhibited a significant seasonal variation in most cases, except for $NO_2$ and $pNH_4^+$ at
993 urban sites, and $HNO_3$ at all land use types. Unlike air concentrations, dry deposition
994 of total $N_r$ showed a consistent and significant seasonal variation for each land use
995 type, with the highest values in summer and the lowest values in winter. The $V_d$ was a
996 dominant factor influencing seasonal variations of $NO_2$, $HNO_3$, and $pNH_4^+$
997 concentrations, while seasonal variations of $NH_3$ and $pNO_3^-$ are mainly influenced by
998 their respective air concentrations. The concentrations of $NH_4^+$-N, $NO_3^-$-N, and TIN
999 in precipitation showed significant seasonal variations, ranking in a consistent order
1000 of winter > spring > autumn ~ summer. Also, significant seasonal variations in bulk

deposition were also found, following in a consistent order of summer > spring ~ autumn > winter.

Both IASI satellite-retrieved $NH_3$ columns and OMI satellite-retrieved $NO_2$ columns over eastern China showed higher values in the north than in the south. In addition, significant positive correlations were found between measured $NH_3$ concentrations and retrieved $NH_3$ columns, and between measured $NO_2$ concentrations and columns. These results together reveal that atmospheric $N_r$ pollution is more serious in the northern region, and also suggest that satellite retrievals of $NH_3$ and $NO_2$ columns can provide useful information on spatial concentration variability of these two key $N_r$ species at a regional or national scale. Weak correlations between IASI_$NH_3$ observations and surface $NH_3$ measurements were found at most selected sites, suggesting that IASI_$NH_3$ observations in their current state are not as readily used to accurately track temporal variability in surface $NH_3$ concentrations.

Ammonia is currently not included in China's emission control policies of air pollution precursors, although the necessity of mitigation has been the subject of discussion during recent years. Across all urban and rural sites, the slopes of the regression relation between $pNH_4^+$ and the sum of $pSO_4^{2-}$ and $pNO_3^-$ were both smaller than unity, indicating control of $NH_3$ emission not only can directly reduce ambient $NH_3$ concentrations, but also lower the formation of $pNH_4^+$ and $pNO_3^-$. Fertilizer use contributed 36% of the total N deposition over eastern China, suggesting reducing $NH_3$ emissions from fertilizer application would be an effective strategy for reducing N deposition. Overall, our findings reveal persistent serious $N_r$ pollution during the 12$^{th}$ FYP period despite implementation of current emission controls, and highlight the importance of $NH_3$ emission control on mitigating future atmospheric $N_r$ concentrations and deposition in eastern China.

**Acknowledgments**

This study was supported by the National Key R&D Program of China (2017YFC0210101 & 2017YFC0210106, 2014BC954202), the National Natural

Science Foundation of China (41705130, 41425007, 31421092) as well as the National Ten-thousand Talents Program of China (X.J. Liu).

## References

Aguillaume, L., Rodrigo, A., and Avila, A.: Long-term effects of changing atmospheric pollution on throughfall, bulk deposition and streamwaters in a Mediterranean forest, Sci. Total Environ. 544, 919–928, https://doi.org/10.1016/j.scitotenv.2015.12.017, 2016.

Allen, A. G., Harrison, R. M., and Erisman, J. W.: Field measurements of the dissociation of ammonium nitrate and ammonium chloride aerosols, Atmos. Environ., 23, 1591–1599, 1989.

Atkins, D. H. F., and Lee, D. S.: Spatial and temporal variation of rural nitrogen dioxide concentrations across the United Kingdom, Atmos. Environ., 29, 223–239, 1995.

Bobbink, R., Hicks, K., Galloway, J., Spranger, T., Alkemade, R., Ashmore, M., Bustamante, M., Cinderby, S., Davidson, E., and Dentener, F.: Global assessment of nitrogen deposition effects on terrestrial plant diversity: a synthesis, Ecol. Appl. 20, 30–59, 2010.

Boersma, K. F., Eskes, H. J., Veefkind, J. P., Brinksma, E. J., van der A, R. J., Sneep, M., van den Oord, G. H. J., Levelt, P. F., Stammes, P., Gleason, J. F., and Bucsela, E. J.: Near-real time retrieval of tropospheric $NO_2$ from OMI, Atmos. Chem. Phys.,7, 2103–2118, https://doi.org/10.5194/acp-7-2103-2007, 2007.

Cao, J. J., Zhang, T., Chow, J. C., Watson, J. G., Wu, F., and Li, H.: Characterization of atmospheric ammonia over Xi'an, China, Aerosol Air Qual. Res., 9, 277–289, 2009.

Chang, Y. H., Liu, X. J., Deng, C. R., Dore, A. J., and Zhuang, G. S.: Source apportionment of atmospheric ammonia before, during, and after the 2014 APEC

summit in Beijing using stable nitrogen isotope signatures, Atmos. Chem. Phys., 16, 11635–11647, https://doi.org/10.5194/acp-16-11635-2016, 2016.

Dammers, E., Palm, M., Van Damme, M., Vigouroux, C., Smale, D., Conway, S., Toon, G. C., Jones, N., Nussbaumer, E., Warneke, T., Petri, C., Clarisse, L., Clerbaux, C., Hermans, C., Lutsch, E., Strong, K., Hannigan, J. W., Nakajima, H., Morino, I., Herrera, B., Stremme, W., Grutter, M., Schaap, M., Wichink Kruit, R. J., Notholt, J., Coheur, P. F., and Erisman, J. W.: An evaluation of IASI-NH3 with ground-based Fourier transform infrared spectroscopy measurements, Atmos. Chem. Phys., 16, 10351–10368, https://doi.org/10.5194/acp-16-10351-2016, 2016.

Erisman, J.W., Grennfelt, P., and Sutton, M.: The European perspective on nitrogen emission and deposition. Environ. Int., 29, 311–325, https://doi.org/10.1016/S0160-4120(02)00162-9, 2003.

Fagerli, H., and Aas, W.: Trends of nitrogen in air and precipitation: model results and observations at EMEP sites in Europe, 1980-2003, Environ. Pollut. 154, 448–461, https://doi.org/10.1016/j.envpol.2008.01.024, 2008.

Fenn, M. E., Baron, J. S., Allen, E. B., Rueth, H. M., Nydick, K. R., Geiser, L., Bowman, W. D., Sickman, J. O., Meixner, T., Johnson, D. W., and Neitlich, P.: Ecological Effects of Nitrogen Deposition in the Western United States, BioScience, 53, 404–420, https://doi.org/10.1641/0006-3568(2003)053[0404:EEONDI]2.0.CO;2, 2003.

Fowler, D., Smith, R., Muller, J., Cape, J. N., Sutton, M., Erisman, J. W., and Fagerli, H.: 2007. Long term trends in sulphur and nitrogen deposition in Europe and the cause of non-linearities, Water Air Soil Pollut., 7, 41–47, https://doi.org/10.1007/s11267-006-9102-x, 2007.

Fowler, D., Coyle, M., Skiba, U., Sutton, M. A., Cape, J. N., Reis, S., Sheppard, L. J., Jenkins, A., Grizzetti, B., Galloway, J. N., Vitousek, P., Leach, A., Bouwman, A. F., Butterbach-Bahl, K., Dentener, F., Stevenson, D., Amann, M., and Voss, M.: The global nitrogen cycle in the twenty-first century, Philos. T. R. Soc. B, 368, 20130164, https://doi.org/10.1098/rstb.2013.0164, 2013.

1091 Fuzzi, S., Baltensperger, U., Carslaw, K., Decesari, S., van Der Gon, H. D., Facchini,
1092 M. C., Fowler, D., Koren, I., Langford, B., Lohmann, U., Nemitz, E., Pandis, S.,
1093 Riipinen, I., Rudich, Y., Schaap, M., Slowik, J. G., Spracklen, D. V., Vignati, E.,
1094 Wild, M., Williams, M., and Gilardoni, S.: Particulate matter, air quality and
1095 climate: lessons learned and future needs, Atmos. Chem. Phys., 15,
1096 8217–8299, https://doi.org/10.5194/acp-15-8217-2015, 2015.
1097 Galloway, J. N., Townsend, A. R., Erisman, J. W., Bekunda, M., Cai, Z., Freney, J. R.,
1098 Martinelli, L. A., Seitzinger, S. P., and Sutton, M. A.: Transformation of the
1099 Nitrogen Cycle: Recent trends, questions, and potential solutions, Science, 320,
1100 889–892, https://doi.org/10.1126/science.1136674, 2008.
1101 Ge, B. Z., Wang, Z. F., Xu, X. B., Wu, J. B., Yu, X. L., and Li, J.: Wet deposition of
1102 acidifying substances in different regions of China and the rest of East Asia:
1103 modeling with updated NAQPMS, Environ. Pollut., 187,
1104 10–21, https://doi.org/10.1016/j.envpol.2013.12.014, 2014.
1105 Gilbert, R. O.: Statistical methods for environmental pollution monitoring, John
1106 Wiley & Sons, 1987.
1107 Gruber, N. and Galloway, J. N.: An Earth-system perspective of the global nitrogen
1108 cycle, Nature, 451, 293–296, https://doi.org/10.1038/nature06592, 2008.
1109 Gu, B. J., Sutton, M. A., Chang, S. X., Ge, Y., and Jie, C.: Agricultural ammonia
1110 emissions contribute to China's urban air pollution, Front. Ecol. Environ., 12,
1111 265–266, https://doi.org/10.1890/14.WB.007, 2014.
1112 Guo, S., Hu, M., Zamora, M. L., Peng, J. F., Shang, D. J., Zheng, J., Du, Z. F., Wu, Z.
1113 J., Shao, M., and Zeng, L. M.: Elucidating severe urban haze formation in China,
1114 Proc. Natl. Acad. Sci. U.S.A., 111,
1115 17373, https://doi.org/10.1073/pnas.1419604111, 2014.
1116 Han, X., Zhang, M. G., Skorokhod, A., and Kou, X. X.: Modeling dry deposition of
1117 reactive nitrogen in China with RAMS-CMAQ, Atmos. Environ., 166,
1118 47–61, https://doi.org/10.1016/j.atmosenv.2017.07.015, 2017.
1119 He, N. P., Zhu, J. X., and Wang, Q. F.: Uncertainty and perspectives in studies of
1120 atmospheric nitrogen deposition in China: A response to Liu et al. (2015), Sci.

Total Environ., 520, 302–304, https://doi.org/10.1016/j.scitotenv.2015.03.063, 2015.

Huang, P., Zhang, J. B., Xin, X. L., Zhu, A. N., Zhang, C. Z., Ma, D. H., Zhu, Q. G., Yang, S., and Wu, S. J.: Proton accumulation accelerated by heavy chemical nitrogen fertilization and its long-term impact on acidifying rate in a typical arable soil in the Huang-Huai-Hai Plain, J. Integr. Agric. 14, 148–157, 2015.

Huang, R. J., Zhang, Y., Bozzetti, C., Ho, K. F., Cao, J. J., Han, Y., Daellenbach, K. R., Slowik, J. G., Platt, S. M., Canonaco, F., Zotter, P., Wolf, R., Pieber, S. M., Bruns, E. A., Crippa, M., Ciarelli, G., Piazzalunga, A., Schwikowski, M., Abbaszade, G., Schnelle-Kreis, J., Zimmermann, R., An, Z., Szidat, S., Baltensperger, U., El Haddad, I., and Prevot, A. S.: High secondary aerosol contribution to particulate pollution during haze events in China, Nature, 514, 218–222, https://doi.org/10.1038/nature13774, 2014.

Huang, X., Song, Y., Li, M. M., Li, J. F., Huo, Q., Cai, X. H., Zhu, T., Hu, M., and Zhang, H. S: A high-resolution ammonia emission inventory in China, Global Biogeochem. Cycles 26, GB1030, https://doi.org/10.1029/2011GB004161, 2012.

Ianniello, A., Spataro, F., Esposito, G., Allegrini, I., Rantica, E., Ancora, M. P., Hu, M., and Zhu, T.: Occurrence of gas phase ammonia in the area of Beijing (China), Atmos. Chem. Phys., 10, 9487–9503, https://doi.org/10.5194/acp-10-9487-2010, 2010.

Jia, B., Wang, Y., Yao, Y., and Xie, Y.: A new indicator on the impact of large-scale circulation on wintertime particulate matter pollution over China, Atmos. Chem. Phys., 15, 11919–11929, https://doi.org/10.5194/acp-15-11919-2015, 2015.

Jia, Y. L., Yu, G. R., He, N. P., Zhan, X. Y., Fang, H. J., Sheng, W. P., Zuo, Y., Zhang, D. Y., and Wang, Q. F.: Spatial and decadal variations in inorganic nitrogen wet deposition in China induced by human activity, Sci. Rep., 4, 3763, https://doi.org/10.1038/srep03763, 2014.

Jia, Y. L.; Yu, G. R.; Gao, Y. N.; He, N. P.; Wang, Q. F.; Jiao, C. C.; and Zuo, Y.: Global inorganic nitrogen dry deposition inferred from ground and space-based measurements, Sci. Rep., 6, 19810, https://doi.org/10.1038/srep19810, 2016.

Ju, X. T., Xing, G. X., Chen, X. P., Zhang, S. L., Zhang, L. J., Liu, X. J., Cui, Z. L., Yin, B., Christie, P., Zhu, Z. L., and Zhang, F. S.: Reducing environmental risk by improving N management in intensive Chinese agricultural systems, Proc. Natl. Acad. Sci. U. S. A. 106, 3041-3046, https://doi/10.1073/pnas.0902655106, 2009.

Kanakidou, M., Myriokefalitakis, S., Daskalakis, N., and Fanourgakis, G.: Past, present, and future atmospheric nitrogen deposition, J. Atmos. Sci., 73, 160303130433005, https://doi.org/10.1175/JAS-D-15-0278.s1, 2016.

Karlsson, G. P., Akselsson, C., Hellsten, S., and Karlsson, P. E.: Reduced European emissions of S and N effects on air concentrations, deposition and soil water chemistry in Swedish forests, Environ. Pollut. 159, 3571–3582. https://doi.org/10.1016/j.envpol.2011.08.007, 2011.

Khoder, M. I.: Atmospheric conversion of sulfur dioxide to particulate sulfate and nitrogen dioxide to particulate nitrate and gaseous nitric acid in an urban area, Chemosphere, 49, 675–684, 2002.

Krotkov, N. A., Mclinden, C. A., Li, C., Lamsal, L. N., Celarier, E. A., Marchenko, S. V., Swartz, W. H., Bucsela, E. J., Joiner, J., Duncan, B. N., Boersma, K. F., Veefkind, J. P., Levelt, P. F., Fioletov, V. E., Dickerson, R. R., He, H., Lu, Z. F., and Streets, D. G.: Aura OMI observations of regional $SO_2$ and $NO_2$ pollution changes from 2005 to 2015, Atmos. Chem. Phys., 16, 4605–4629, https://doi.org/10.5194/acp-16-4605-2016, 2016.

Kurokawa, J., Ohara, T., Morikawa, T., Hanayama, S., JanssensMaenhout, G., Fukui, T., Kawashima, K., and Akimoto, H.: Emissions of air pollutants and greenhouse gases over Asian regions during 2000–2008: Regional Emission inventory in Asia (REAS) version 2, Atmos. Chem. Phys., 13, 11019–11058, https://doi.org/10.5194/acp-13-11019-2013, 2013.

Li, H., Zhang, Q., Zheng, B., Chen, C., Wu, N., Guo, H., Zhang, Y., Zheng, Y., Li, X., and He, K.: Nitrate-driven urban haze pollution during summertime over the North China Plain, Atmos. Chem. Phys., 18, 5293-5306, https://doi.org/10.5194/acp-18-5293-2018, 2018.

Li, Y., Niu, S., and Yu, G.: Aggravated phosphorus limitation on biomass production

under increasing nitrogen loading: a meta-analysis, Global Change Biol., 22, 934–943, https://doi.org/10.1111/gcb.13125, 2016.

Liang, X., Zou, T., Guo, B., Li, S., Zhang, H. Z., Zhang, S. Y., Huang, H., and Chen, S. X.: Assessing Beijing's $PM_{2.5}$ pollution: severity, weather impact, APEC and winter heating, Proc. R. Soc. A., 471, 20150257, https://doi.org/10.1098/rspa.2015.0257, 2015.

Liu, F., Beirle, S., Zhang, Q., van der A, R. J., Zheng, B., Tong, D., and He, K.: $NO_x$ emission trends over Chinese cities estimated from OMI observations during 2005 to 2015, Atmos. Chem. Phys., 17, 9261–9275, https://doi.org/10.5194/acp-17-9261-2017, 2017.

Liu, L., Zhang, X. Y., Zhang, Y., Xu, W., Liu, X. J., Zhang, X. M., Feng, J. L., Chen, X. R., Zhang, Y. H., Lu, X. H., Wang, S. Q., Zhang, W. T., and Zhao, L. M.: Dry particulate nitrate deposition in China, Environ. Sci. Techno., 51, 5572, https://doi.org/10.1021/acs.est.7b00898, 2017a.

Liu, L., Zhang, X., Xu, W., Liu, X., Li, Y., Lu, X., Zhang, Y., and Zhang, W.: Temporal characteristics of atmospheric ammonia and nitrogen dioxide over China based on emission data, satellite observations and atmospheric transport modeling since 1980, Atmos. Chem. Phys., 17, 9365–9378, https://doi.org/10.5194/acp-17-9365-2017, 2017b.

Liu, X. J., Duan, L., Mo, J. M., Du, E. Z., Shen, J. L., Lu, X. K., Zhang, Y., Zhou, X. B., He, C. E., and Zhang, F. S.: Nitrogen deposition and its ecological impact in China: An overview, Environ. Pollut., 159, 2251-2264, https://doi.org/ 10.1016/j.envpol.2010.08.002, 2011.

Liu, X. J., Zhang, Y., Han, W. X., Tang, A., Shen, J. L., Cui, Z. L., Vitousek, P., Erisman, J. W., Goulding, K., Christie, P., Fangmeier, A., and Zhang, F. S.: Enhanced nitrogen deposition over China, Nature, 494, 459–462, https://doi.org/10.1038/nature11917, 2013.

Liu, X. J., Vitousek, P., Chang, Y. H., Zhang, W. F., Matson, P., and Zhang, F. S.: Evidence for a historic change occurring in China, Environ. Sci. Technol., 50, 505–506, https://doi.org/10.1021/acs.est.5b05972, 2016.

Lu, C. Q. and Tian, H. Q.: Spatial and temporal patterns of nitrogen deposition in China: Synthesis of observational data, J. Geophys. Res., 112, D22S05, https://doi.org/10.1029/2006JD007990, 2007.

Lu, C. Q. and Tian, H. Q.: Half-century nitrogen deposition increase across China: A gridded time-series data set for regional environmental assessments, Atmos. Environ., 97, 68–74, https://doi.org/10.1016/j.atmosenv.2014.07.061, 2014.

Marchetto, A., Rogora, M., and Arisci, S.: Trend analysis of atmospheric deposition data: A comparison of statistical approaches, Atmos. Environ., 64, 95–102, 2013.

Meng, Z. Y., Xu, X. B., Wang, T., Zhang, X. Y., Yu, X. L., Wang, S. F., Lin, W. L., Chen, Y. Z., Jiang, Y. A., and An, X. Q.: Ambient sulfur dioxide, nitrogen dioxide, and ammonia at ten background and rural sites in China during 2007-2008, Atmos. Environ., 44, 2625–2631.

Meng, Z. Y., Xu, X. B., Lin, W. L., Ge, B. Z., Xie, Y. L., Song, B., Jia, S. H., Zhang, R., Peng, W., Wang, Y., Cheng, H. B., Yang, W., and Zhao, H.: Role of ambient ammonia in particulate ammonium formation at a rural site in the North China Plain, Atmos. Chem. Phys., 18, 167–184, https://doi.org/10.5194/acp-18-167-2018, 2018.

MEPC (Ministry of Environmental Protection of the People's Republic of China): Report on Environmental Quality in China, 2010. Available online at: http://jcs.mep.gov.cn/hjzl/zkgb/ 2010zkgb/201106/t20110602_211579.htm., 2011.

Miyazaki, K., Eskes, H., Sudo, K., Boersma, K. F., Bowman, K., and Kanaya, Y.: Decadal changes in global surface $NO_x$ emissions from multi-constituent satellite data assimilation, Atmos. Chem. Phys., 17, 807–837, https://doi.org/10.5194/acp-17-807-2017, 2017.

Pan, Y. P., Wang, Y. S., Tang, G. Q., and Wu, D.: Wet and dry deposition of atmospheric nitrogen at ten sites in Northern China, Atmos. Chem. Phys., 12, 6515–6535, https://doi.org/10.5194/acp-12-6515-2012, 2012.

Pan, Y. P., Wang, Y. S., Zhang, J. K., Liu, Z. R., Wang, L. L., Tian, S. L., Tang, G. Q., Gao, W. K., Ji, D. S., and Song, T.: Redefining the importance of nitrate during

haze pollution to help optimize an emission control strategy, Atmos. Environ., 141, 197–202, http://dx.doi.org/10.1016/j.atmosenv.2016.06.035, 2016.

Pinder, R. W., Walker, J. T., Bash, J. O., Cady-Pereira, K. E., Henze, D. K., Luo, M. Z., Osterman, G. B., and Shephard, M. W.: Quantifying spatial and seasonal variability in atmospheric ammonia with in situ and space-based observations, Geophys. Res. Lett., 38, L04802, https://doi.org/10.1029/2010GL046146, 2011.

Russell, A. R., Valin, L. C., and Cohen, R. C.: Trends in OMI $NO_2$ observations over the United States: effects of emission control technology and the economic recession, Atmos. Chem. Phys., 12, 12197–12209, https://doi.org/10.5194/acp-12-12197-2012, 2012.

Salmi, T., Maatta, A., Anttila, P., Ruoho-Airola, T., and Amnell, T.: Detecting trends of annual values of atmospheric pollutants by the Mann–Kendall test and Sen's slope estimates—the Excel template application MAKESENS. Publications on Air Quality No. 31, Finnish Meteorological Institute, Helsinki, Finland, 2002.

Seinfeld, J. H. and Pandis, S. N.: Atmospheric chemistry and physics: from air pollution to climate change, 2nd Edn., Wiley Interscience, New Jersey, 2006.

She, W.: Hu Huanyong: father of China's population geography, China Popul. Today 15, 1–20, 1998.

Souri, A. H., Choi, Y., Jeon, W., Woo, J.-H., Zhang, Q., and Kurokawa, J.-i.: Remote sensing evidence of decadal changes in major tropospheric ozone precursors over East Asia, J. Geophys. Res., 122, 2474–2492, https://doi.org/10.1002/2016JD025663, 2017.

Tang, Y. S., Simmons, I., van Dijk, N., Di Marco, C., Nemitz, E., Dammgen, U., Gilke, K., Djuricic, V., Vidic, S., and Gliha, Z.: European scale application of atmospheric reactive nitrogen measurements in a low-cost approach to infer dry deposition fluxes, Agr. Ecosyst. Environ., 133, 183–195, https://doi.org/10.1016/j.agee.2009.04.027, 2009.

Theil, H.: A Rank-Invariant Method of Linear and Polynomial Regression Analysis, in: Henri Theil's Contributions to Economics and Econometrics, edited by: Raj, B. and Koerts, J., Advanced Studies in Theoretical and Applied Econometrics,

Springer Netherlands, 345–381, 1992.

Tian, S. L., Pan, Y. P., Liu, Z. R., Wen, T. X., and Wang, Y. S.: Size-resolved aerosol chemical analysis of extreme haze pollution events during early 2013 in urban Beijing, China, J. Hazard. Mater., 279, 452–460, https://doi.org/10.1016/j.jhazmat.2014.07.023, 2014.

Van Damme, M., Clarisse, L., Dammers, E., Liu, X., Nowak, J. B., Clerbaux, C., Flechard, C. R., Galylacaux, C., Xu, W., and Neuman, J. A.: Towards validation of ammonia (NH3) measurements from the IASI satellite, Atmos. Meas. Tech., 8, 1575–1591, https://doi. org/10.5194/amt-8-1575-2015, 2015.

van der A, R. J., Mijling, B., Ding, J., Koukouli, M. E., Liu, F., Li, Q., Mao, H., and Theys, N.: Cleaning up the air: effectiveness of air quality policy for $SO_2$ and $NO_x$ emissions in China, Atmos. Chem. Phys., 17, 1775–1789, https://doi.org/10.5194/acp-17-1775-2017, 2017.

Vet, R., Artz, R. S., Carou, S., Shaw, M., Ro, C.-U., Aas, W., Baker, A., Bowersox, V. C., Dentener, F., Galy-Lacaux, C., Hou, A., Pienaar, J. J., Gillett, R., Forti, M. C., Gromov, S., Hara, H., Khodzher, T., Mahowald, N. M., Nickovic, S., Rao, P. S. P., and Reid, N. W.: A global assessment of precipitation chemistry and deposition of sulfur, nitrogen, sea salt, base cations, organic acids, acidity and pH, and phosphorus, Atmos. Environ., 93, 3–100, https://doi.org/10.1016/j.atmosenv.2013.10.060, 2014.

Walker, J. T., Whitall, D. R., Robarge, W., and Paerl, H. W.: Ambient ammonia and ammonium aerosol across a region of variable ammonia emission density, Atmos. Environ., 38, 1235–1246, 2004.

Wang, G. H., Zhang, R. Y., Gomez, M. E., Yang, L. X., Zamora, M. L., Hu, M., Lin, Y., Peng J. F., Guo, S., Meng, J. J., Li, J. J., Cheng, C .L., Hu, T. F., Ren, Y. Q., Wang, Y. S., Gao, J., Cao, J. J., An, Z. S., Zhou, W. J., Li, G. H., Wang, J. Y., Tian, P. F., Marrero-Ortiz, W., Secrest J., Du, Z. F., Zheng, J., Shang, D. J., Zeng, L. M., Shao, M., Wang, W. G., Huang, Y., Wang, Y., Zhu, Y. J., Li, Y. X., Hu, J. X., Pan, B. W., Cai, L., Cheng, Y. T., Ji, Y. M., Zhang, F., Rosenfeld, D., Liss, P. S., Duce, R. A., Kolb, C. E., and Molina, M. J.: Persistent sulfate formation from London

Fog to Chinese haze, Proc. Natl. Acad. Sci. U.S.A., 113, 13630, https://doi.org/10.1073/pnas.1616540113, 2016.

Wang, S. X., Xing, J., Jang, C. R., Zhu, Y., Fu, J. S., and Hao, J. M.: Impact assessment of ammonia emissions on inorganic aerosols in East China using response surface modeling technique, Environ. Sci. Techno., 45, 9293–9300, https://doi. org//10.1021/es2022347, 2011.

Wen, L., Chen, J. M., Yang, L. X., Wang, X. F., Xu, C. H., Sui, X., Yao, L., Zhu, Y. H., Zhang, J. M., Zhu, T., and Wang, W. X.: Enhanced formation of fine particulate nitrate at a rural site on the North China Plain in summer: The important roles of ammonia and ozone, Atmos. Environ., 101, 294–302, http://dx.doi.org/10.1016/j.atmosenv.2014.11.037, 2015.

Wesely, M. L.: Parameterization of surface resistances to gaseous dry deposition in regional-scale numerical-models, Atmos. Environ., 23, 1293–1304, 1989.

Whitburn, S., Van Damme, M., Clarisse, L., Bauduin, S., Heald, C. L., Hadji-Lazaro, J., Hurtmans, D., Zondlo, M. A., Clerbaux, C., and Coheur, P. F.: A flexible and robust neural network IASINH3 retrieval algorithm, J. Geophys. Res.-Atmos., 121, 6581–6599, https://doi.org/10.1002/2016JD024828, 2016.

Xia, Y. M., Zhao, Y., and Nielsen, C. P.: Benefits of China's efforts in gaseous pollutant control indicated by the bottom-up emissions and satellite observations 2000–2014, Atmos. Environ., 136, 43–53, https://doi.org/10.1016/j.atmosenv.2016.04.013, 2016.

Xu, W., Luo, X.S., Pan, Y.P., Zhang, L., Tang, A.H., Shen, J.L., Zhang, Y., Li, K.H., Wu, Q.H., Yang, D.W., Zhang, Y.Y., Xue, J., Li, W.Q., Li, Q.Q., Tang, L., Lu, S.H., Liang, T., Tong, Y.A., Liu, P., Zhang, Q., Xiong, Z.Q., Shi, X.J., Wu, L.H., Shi, W.Q., Tian, K., Zhong, X.H., Shi, K., Tang, Q.Y., Zhang, L.J., Huang, J.L., He, C.E., Kuang, F.H., Zhu, B., Liu, H., Jin, X., Xin, Y.J., Shi, X.K., Du, E.Z., Dore, A.J., Tang, S., Collett, J.L., Goulding, K., Sun, Y.X., Ren, J., Zhang, F.S., and Liu, X.J.: Quantifying atmospheric nitrogen deposition through a nationwide monitoring network across China. Atmos. Chem. Phys., 15, 12345–12360, https://doi.org/10.5194/acp-15-12345-2015, 2015.

Xu, W., Wu, Q. H., Liu, X. J., Tang, A. H., Dore, A. J., and Heal, M. R.: Characteristics of ammonia, acid gases, and $PM_{2.5}$ for three typical land-use types in the North China Plain, Environ. Sci. Pollut. Res., 23, 1158–1172, https://doi.org/10.1007/s11356-015-5648-3, 2016.

Xu, W., Song, W., Zhang, Y., Liu, X., Zhang, L., Zhao, Y., Liu, D., Tang, A., Yang, D., Wang, D., Wen, Z., Pan, Y., Fowler, D., Collett Jr., J. L., Erisman, J. W., Goulding, K., Li, Y., and Zhang, F.: Air quality improvement in a megacity: implications from 2015 Beijing Parade Blue pollution control actions, Atmos. Chem. Phys., 17, 31–46, https://doi.org/10.5194/acp-17-31-2017, 2017.

Xu, W., Zhao, Y. H., Liu, X. J., Dore, A. J., Zhang, L., Liu, L., and Cheng, M.: Atmospheric nitrogen deposition in the Yangtze River basin: Spatial pattern and source attribution, Environ. Pollut., 232, 546–555, https://doi.org/10.1016/j.envpol.2017.09.086, 2018.

Yang, F., Tan, J., Zhao, Q., Du, Z., He, K., Ma, Y., Duan, F., Chen, G., and Zhao, Q.: Characteristics of $PM_{2.5}$ speciation in representative megacities and across China, Atmos. Chem. Phys., 11, 5207–5219, https://doi.org/10.5194/acp-11-5207-2011, 2011.

Yang, Y. H., Li, P., He, H. L., Zhao, X., Datta, A., Ma, W. H., Zhang, Y., Liu, X. J., Han, W. X., Wilson, M. C., and Fang, J. Y.: Long-term changes in soil pH across major forest ecosystems in China, Geophys. Res. Lett., 42, https://doi.org/10.1002/2014GL062575, 2015.

Zhao, Y., Nielsen, C. P., Lei, Y., McElroy, M. B., and Hao, J.: Quantifying the uncertainties of a bottom-up emission inventory of anthropogenic atmospheric pollutants in China, Atmos. Chem. Phys., 11, 2295–2308, https://doi.org/10.5194/acp-11-2295-2011, 2011.

Zhang, L., Chen, Y. F., Zhao, Y. H., Henze, D. K., Zhu, L. Y., Song, Y., Paulot, F., Liu, X. J., Pan, Y. P., and Huang, B. X.: Agricultural ammonia emissions in China: reconciling bottom-up and top-down estimates, Atmos. Chem. Phys., 18, 339–355, https://doi.org/10.5194/acp-18-339-2018, 2018.

Zhang, L. M., Gong, S. L., Padro, J., and Barrie, L.: A size-segregated particle dry

deposition scheme for an atmospheric aerosol module, Atmos. Environ., 35, 549–560, https://doi.org/10.1016/s1352-2310(00)00326-5, 2001.

Zhang, Q., Duan, F. K., He, K. B., Ma, Y. L., Li, H. Y., Kimoto, T., and Zheng, A. H.: Organic nitrogen in $PM_{2.5}$ in Beijing, Front. Env. Sci. Eng., 9, 1004–1014, https://doi.org/10.1007/s11783-015-0799-5, 2015.

Zhang, X. M., Wu, Y. Y., Liu, X. J., Reis, S., Jin, J. X., Dragosits, U., Damme, Van M., Clarisse, L., Whitburn, S., and Coheur, P. F.: Ammonia emissions may be substantially underestimated in China, Environ. Sci. Techno., 51, 12089-12096, https://doi.org/10.1021/acs.est.7b02171, 2017.

Zhao, Y., Zhang, L., Pan, Y., Wang, Y., Paulot, F., and Henze, D. K.: Atmospheric nitrogen deposition to the northwestern Pacific: seasonal variation and source attribution, Atmos. Chem. Phys., 15, 10905–10924, https://doi.org/10.5194/acp-15-10905-2015, 2015.

Zhao, Y., Zhang, L., Chen, Y. F., Liu, X. J., Xu, W., Pan, Y. P., and Duan, L.: Atmospheric nitrogen deposition to China: a model analysis on nitrogen budget and critical load exceedance, Atmos. Environ., 153, 32–40, https://doi.org/10.1016/j.atmosenv.2017.01.018, 2017.

Zhu, J. X., He, N. P., Wang, Q. F., Yan, G. F., Wen, D., Yu, G. R., and Jia, Y. L.: The composition, spatial patterns, and influencing factors of atmospheric wet nitrogen deposition in Chinese terrestrial ecosystems, Sci. Total Environ., 511, 777–785, https://doi.org/10.1016/j.scitotenv.2014.12.038, 2015.

**Sect. S1. Information on measuring methods, sample replications and collection**

The DELTA system comprises contains a sampling train consisted of two potassium carbonate/glycerol-coated denuders in series for trapping acidic trace gases ($HNO_3$ $SO_2$ and HCl), followed by two citric acid-coated borosilicate glass denudes for $NH_3$ and finally by two sets of cellulose filter papers in a 2-stage filter pack at the end of the sampling train. These filters were impregnated with the same alkaline solution as the denuders to capture $NH_4^+$, and with the same acid solution for the collection of $NO_3^-$, $SO_4^{2-}$ and $Cl^-$. The empirically determined effective size cut-off for particle sampling is of the order of 4.5 μm (E. Nemitz, personal communication). The air was drawn through the sampling train at a rate of 0.2-0.4 L $min^{-1}$ and directly into the first denuder with no inlet line to avoid sampling losses. The total sampled air volume of the DELTA system was recorded by the gas meter which was checked every month for data reading, performance and maintenance.

The Gradko passive sampler consists of a 71.0 mm long × 11.0 mm internal diameter acrylic tube with coloured and white thermoplastic rubber caps. Gaseous $NO_2$ is absorbed into a 20% triethanolamine/deionised-water solution coated onto two stainless steel wire meshes within the coloured cap. A constant gas diffusion coefficient based on an assumption of 25 °C was used for the calculation of $NO_2$ concentration, in accordance with the Gradko introduction manual and previous studies (Luo et al., 2013; Shen et al., 2013).

The sampling trains and tubes for field measurements were prepared and measured in the analytical laboratory at China Agricultural University (CAU), Beijing. Each batch of new trains and field (travel) blanks was sealed in individual airtight storage bags and sent monthly to monitoring sites to replace the old ones. After sampling, the blank and exposed trains and tubes were sealed in individual airtight storage bags and sent back to the laboratory, being stored at 4 $^oC$ prior to analysis.

**Sect. S2. The information on the evaluation of GEOS-Chem model**

To evaluate the model simulations, we compared modeled annual wet deposition fluxes of $NH_4^+$-N and $NO_3^-$-N for the year 2010 with their respective observed fluxes (5-year averages). The comparison results are shown in Fig. S12 in the Supplement. The model can partly capture the spatial variations of measured bulk deposition fluxes of $NH_4^+$ and $NO_3^-$ with correlation coefficients of 0.6 and 0.4, respectively. Compared with measurements, model results were 23% higher for bulk $NH_4^+$ deposition, and 23%

lower for bulk $NO_3^-$-N deposition. The model biases were reasonable since simulated N deposition fluxes were for 2010 whereas the observations cover a period from 2000 to 2015. Both $NH_3$ and $NO_x$ emissions change over the time periods, resulting in difference in subsequence N deposition. Besides emissions, inter-annual variations of meteorological conditions especially precipitation can also affect wet deposition fluxes. So model simulated wet deposition fluxes show larger biases. In addition, the model biases also reflect the incapability of the coarse model resolution (about 50 km) to distinguish different land use types (e.g., the forest, rural and urban sites) at such regional scale. Future work is needed to conduct high resolution simulation using regional models combined with improved $N_r$ emission inventories.

**References**

Luo, X. S., Liu, P., Tang, A. H., Liu, J. Y., Zong, X. Y., Zhang, Q., Kou, C. L., Zhang, L. J., Fowler, D., Fangmeier, A., Christie, P., Zhang, F. S., and Liu, X. J.: An evaluation of atmospheric Nr pollution and deposition in North China after the Beijing Olympics, Atmos. Environ., 74, 209–216, https://doi.org/10.1016/j.atmosenv.2013.03.054, 2013.

Shen, J. L., Li, Y., Liu, X.J., Luo, X. S., Tang, A. H., Zhang, Y. Z., and Wu, J. S.: Atmospheric dry and wet nitrogen deposition on three contrasting land use types of an agricultural catchment in subtropical central China, Atmos. Environ., 67, 415–424, https://doi.org/10.1016/j.atmosenv.2012.10.068, 2013.

**Figure captions**

**Figure S1.** Annual mean concentrations of **(a)** $NH_3$; **(b)** $NO_2$; **(c)** $HNO_3$; **(d)** $pNH_4^+$; **(e)** $pNO_3^-$; and **(f)** total $N_r$: sum of all measured $N_r$ in air at twenty-seven sites. Trend analysis (annual concentration vs. time) was conducted at each site. The slope of the Theil regression and *p* value for each site are labeled in black and yellow. U, R, and B denote urban, rural, and background sites, respectively.

**Figure S2**. Annual volume-weighted mean concentrations of $NH_4^+$ **(a)**; $NO_3^-$ **(b)** and total inorganic N (TIN): sum of $NH_4^+$ and $NO_3^-$ **(c)** in precipitation at twenty-seven sites. Trend analysis (annual concentration vs. time) was conducted at each site. The slope of the Theil regression and *p* value for each site are labeled in black and red. U, R, and B denote urban, rural, and background sites, respectively.

**Figure S3**. Annual dry deposition fluxes of **(a)** $NH_3$; **(b)** $NO_2$; **(c)** $HNO_3$; **(d)** $pNH_4^+$; **(e)** $pNO_3^-$; and **(f)** total $N_r$: sum of all measured $N_r$ in air at twenty-seven sites. Trend analysis (annual concentration vs. time) was conducted at each site. The slope of the Theil regression and *p* value for each site are labeled in black and green. U, R, and B denote urban, rural, and background sites, respectively.

**Figure S4**. Annual wet/bulk deposition of $NH_4^+$ **(a)**; $NO_3^-$ **(b)** and total inorganic N (TIN): sum of $NH_4^+$ and $NO_3^-$ **(c)** in precipitation at twenty-seven sites. Trend analysis (annual concentration vs. time) was conducted at each site. The slope of the Theil regression and *p* value for each site are labeled in black and red. U, R, and B denote urban, rural, and background sites, respectively.

**Figure S5**. Total (dry plus wet/bulk) deposition fluxes at the three land use types in eastern China and its northern and southern regions. The number of sixteen selected sites with the same land use type in each region can be found in Figure S6 and Table S1. The error bars are the standard errors of means, and values without same lettersdifferent letters on the bars denote significantly difference between the sites land use types at $p<0.05$.

**Figure S6**. Annual total (dry plus wet/bulk) deposition fluxes during 2011-2105 period at different observation scales: the annual deposition fluxes at sixteen sites (a), and averaged deposition fluxes during the 2011-2012 and 2013-2015 periods for three land use types (b). The number of sixteen selected sites with the same land use type in each region can be found in Table S1. The error bars are the standard errors of means.

Trend analysis (annual concentration vs. time) was conducted at each site. The slope of the Theil regression and *p* value for each site are labeled in black and blue. U, R, and B denote urban, rural, and background sites, respectively.

**Figure S7**. Correlations between NNDMN_$NH_3$ concentration and IASI_$NH_3$ columns at twenty-seven sites. Sites with non-significant correlation were marked in red.

**Figure S8**. Correlations between NNDMN_$NO_2$ measurements and OMI_$NO_2$ columns at twenty-seven sites. Sites with non-significant correlation were marked in green.

**Figure S9**. Seasonal mean concentrations of reduced (the sum of $NH_3$ and $pNH_4^+$) and oxidized (the sum of $HNO_3$, $NO_2$ and $pNO_3^-$) N in air at different land use types in eastern China and its northern and southern regions. The number of sites with the same land use type in each region can be found in Table S1. The error bars are the standard errors of means, and values without same lettersdifferent letters on the bars denote significantly difference between the sites seasons at $p<0.05$. U, R, and B denote urban, rural, and background sites, respectively.

**Figure S10**. Seasonal mean precipitation amount at different land use types in eastern China and its northern and southern regions. The number of sites with the same land use type in each region can be found in Table S1. The error bars are the standard errors of means, and values without same lettersdifferent letters on the bars denote significantly difference between the sites seasons at $p<0.05$. U, R, and B denote urban, rural, and background sites, respectively.

**Figure S11**. Seasonal mean concentrationsdry deposition velocities of $NH_3$, $NO_2$, $HNO_3$, $pNH_4^+$ and/or $pNO_3^-$ at different land use types in eastern China and its northern and southern regions. The number of sites with the same land use type in each region can be found in Table S1. The error bars are the standard errors of means, and values without same lettersdifferent letters on the bars denote significantly difference between the sites seasons at $p<0.05$. U, R, and B denote urban, rural, and background sites, respectively.

**Figure S12**. Comparison of model simulated $NH_4^+$ wet deposition, $NO_3^-$ wet deposition for 2010 with surface observations (5-year averages) at twenty-seven sites. The background colors show the model results and the overplotted dots show the observations. The correlation coefficients (r) and normalized mean bias

(NMB=$\sum_{i=1}^{N}(M_i - O_i) / \sum_{i=1}^{N} O_i$) between N observed and corresponding modeled values are shown inset.

Figure S13. HYSPLIT back-trajectories analysis on the path of air parcels ($NO_2$, particulate $NH_4^+$ and particulate $NO_3^-$) prior to arrival at five selected sites (Nanjing, Baiyun, Taojing, Ziyang and Huinong) in southern region of eastern China during different seasons (January-Winter, April-Spring, July-Summer, October-Autumn).

Figure S14. Annual variations in precipitation amounts at sixteen selected sites.

**Figure S1**

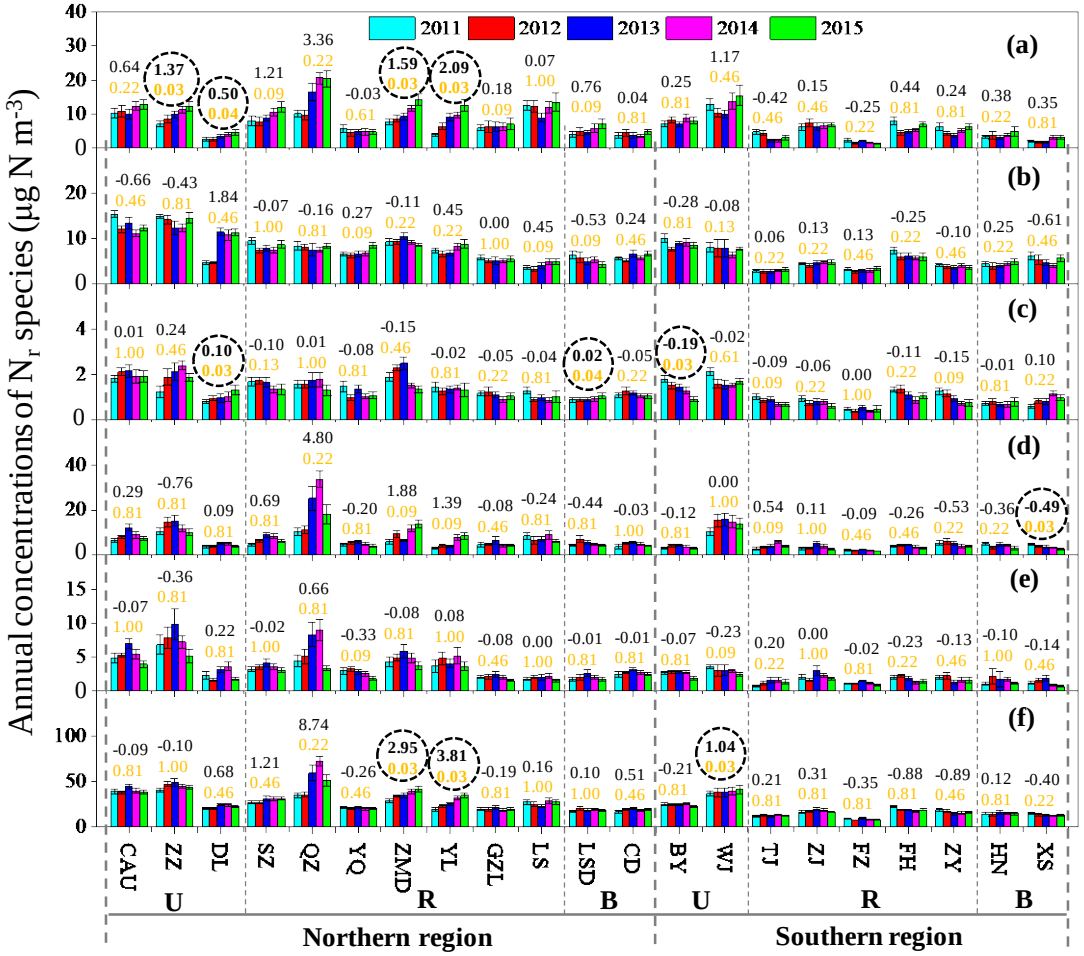
2011
2012
2013
2014
2015
(a)
(b)
(c)
(d)
(e)
(f)
Annual concentrations of $N_r$ species (μg N m$^{-3}$)
CAU
ZZ
DL
SZ
QZ
YQ
ZMD
YL
GZL
LS
LSD
CD
BY
WJ
TJ
ZJ
FZ
FH
ZY
HN
XS
U
R
B
U
R
B
Northern region
Southern region

**Figure S2**

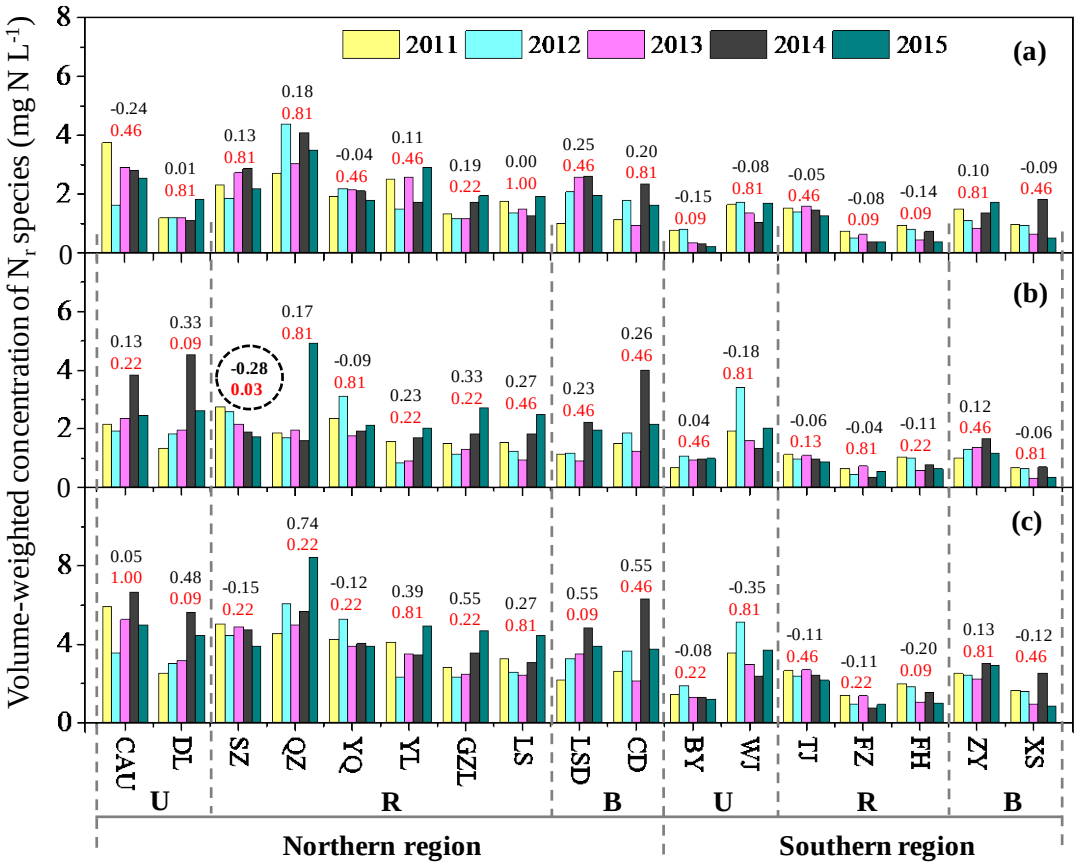
2011
2012
2013
2014
2015
(a)
(b)
(c)
Volume-weighted concentration of $N_r$ species (mg N $L^{-1}$)
CAU
DL
SZ
QZ
YQ
YL
GZL
LS
LSD
CD
BY
WJ
TJ
FZ
FH
ZY
XS
U
R
B
U
R
B
Northern region
Southern region

**Figure S3**

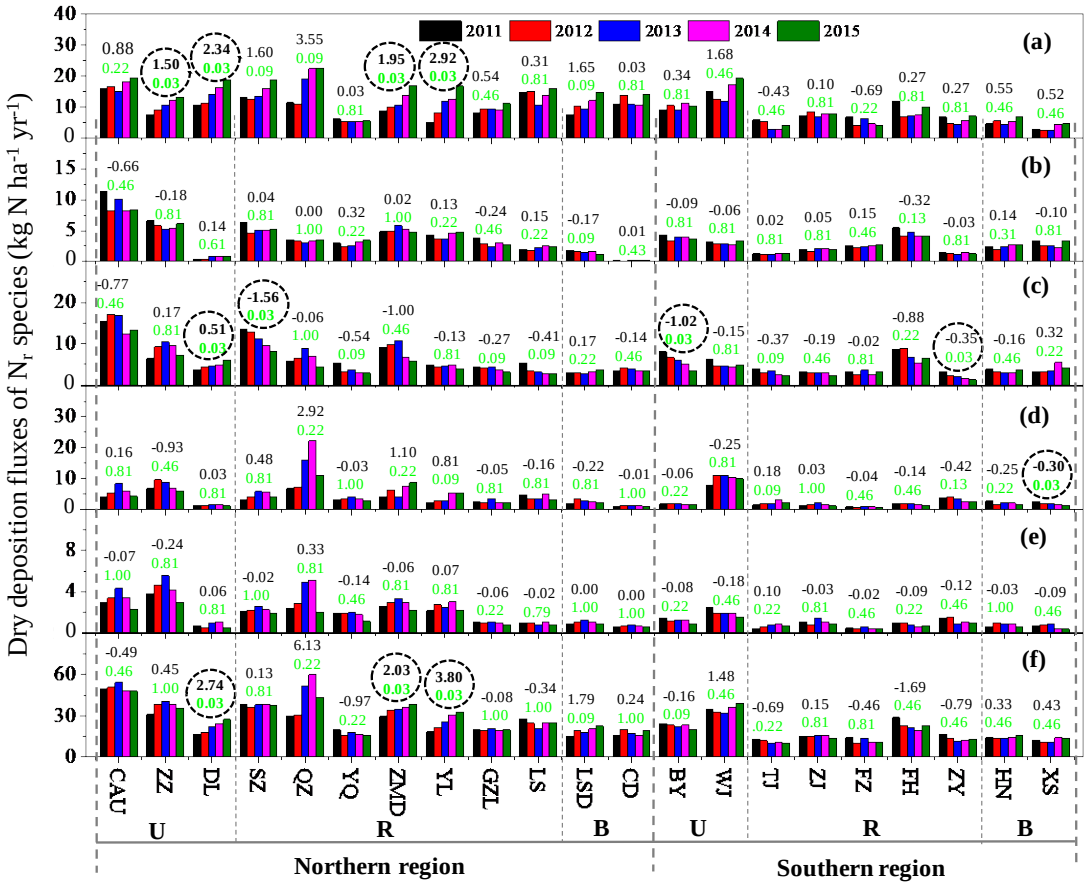
2011
2012
2013
2014
2015
(a)
(b)
(c)
(d)
(e)
(f)
Dry deposition fluxes of $N_r$ species (kg N ha$^{-1}$ yr$^{-1}$)
CAU
ZZ
DL
SZ
QZ
YQ
ZMD
YL
GZL
LS
LSD
CD
BY
WJ
TJ
ZJ
FZ
FH
ZY
HN
XS
U
R
B
U
R
B
Northern region
Southern region

**Figure S4**

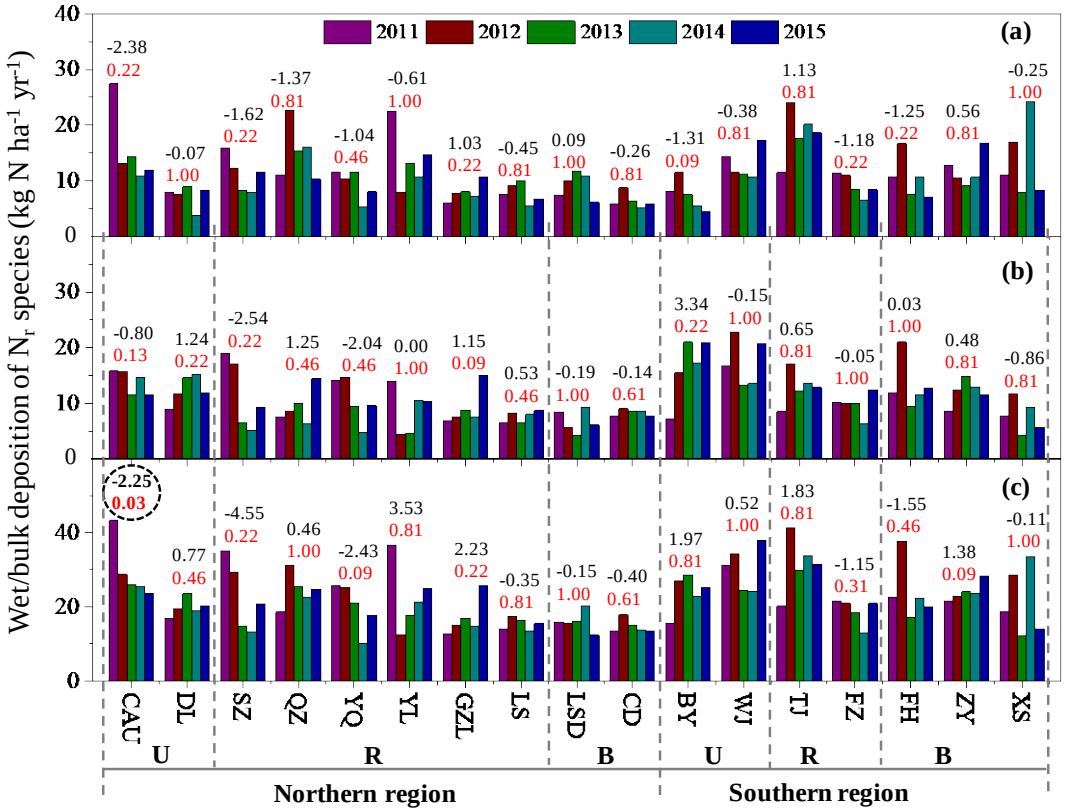
2011
2012
2013
2014
2015
(a)
(b)
(c)
Wet/bulk deposition of $N_r$ species (kg N ha$^{-1}$ yr$^{-1}$)
CAU
DL
SZ
QZ
YQ
YL
GZL
LS
LSD
CD
BY
WJ
TJ
FZ
FH
ZY
XS
U
R
B
U
R
B
Northern region
Southern region

**Figure S5**

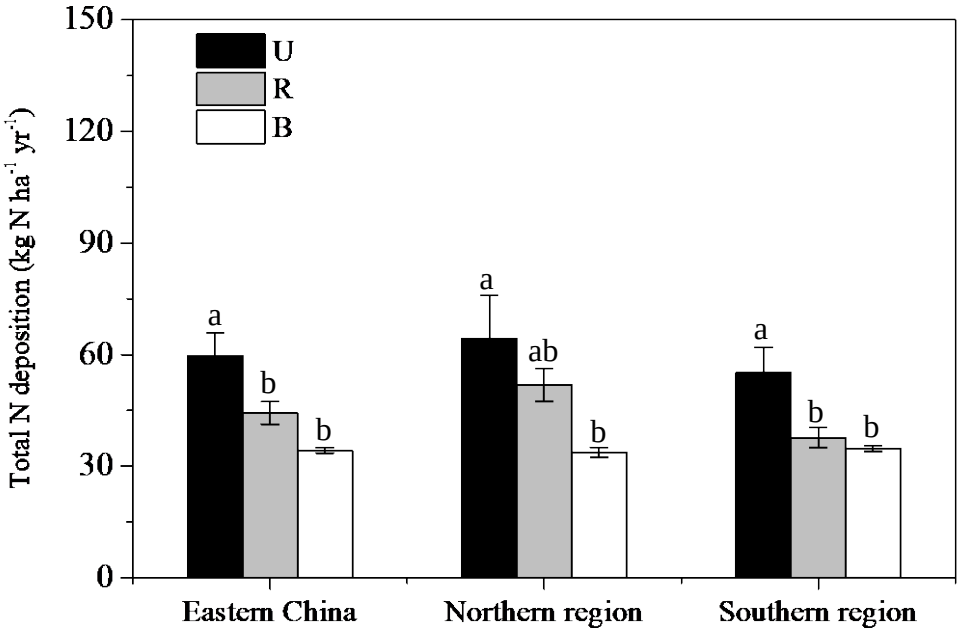
150
120
90
60
30
0
Total N deposition (kg N ha-1 yr-1)
U
R
B
a
b
b
a
ab
b
a
b
b
Eastern China
Northern region
Southern region

**Figure S6**

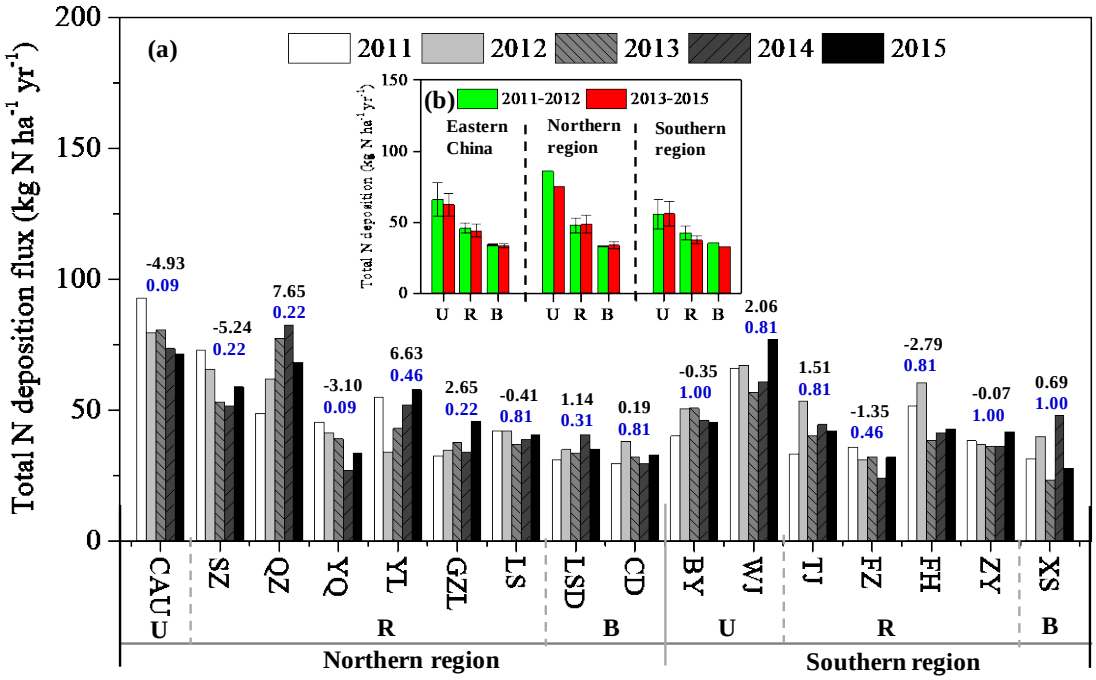
(a)
2011
2012
2013
2014
2015
Total N deposition flux (kg N ha-1 yr-1)
200
150
100
50
0
-4.93
0.09
-5.24
0.22
7.65
0.22
-3.10
0.09
6.63
0.46
2.65
0.22
-0.41
0.81
1.14
0.31
0.19
0.81
-0.35
1.00
2.06
0.81
1.51
0.81
-1.35
0.46
-2.79
0.81
-0.07
1.00
0.69
1.00
CAU
SZ
QZ
YQ
YL
GZL
LS
LSD
CD
BY
WJ
TJ
FZ
FH
ZY
XS
U
R
B
U
R
B
Northern region
Southern region
(b)
2011-2012
2013-2015
Eastern China
Northern region
Southern region
Total N deposition (kg N ha-1 yr-1)
150
100
50
0
U R B
U R B
U R B

**Figure S7**

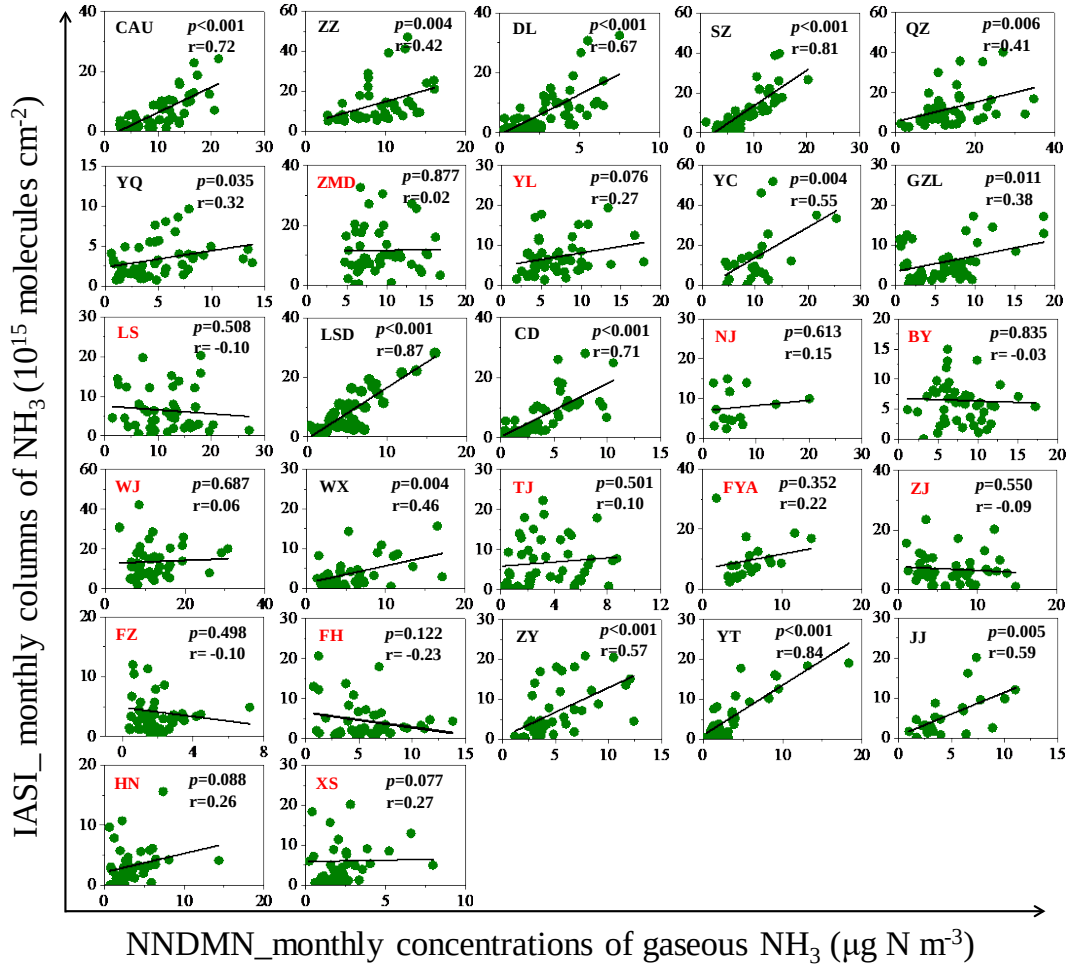
CAU p<0.001 r=0.72
ZZ p=0.004 r=0.42
DL p<0.001 r=0.67
SZ p<0.001 r=0.81
QZ p=0.006 r=0.41
YQ p=0.035 r=0.32
ZMD p=0.877 r=0.02
YL p=0.076 r=0.27
YC p=0.004 r=0.55
GZL p=0.011 r=0.38
LS p=0.508 r= -0.10
LSD p<0.001 r=0.87
CD p<0.001 r=0.71
NJ p=0.613 r=0.15
BY p=0.835 r= -0.03
WJ p=0.687 r=0.06
WX p=0.004 r=0.46
TJ p=0.501 r=0.10
FYA p=0.352 r=0.22
ZJ p=0.550 r= -0.09
FZ p=0.498 r= -0.10
FH p=0.122 r= -0.23
ZY p<0.001 r=0.57
YT p<0.001 r=0.84
JJ p=0.005 r=0.59
HN p=0.088 r=0.26
XS p=0.077 r=0.27
IASI_ monthly columns of NH3 (10^15 molecules cm^-2)
NNDMN_monthly concentrations of gaseous NH3 (μg N m^-3)

**Figure S8**

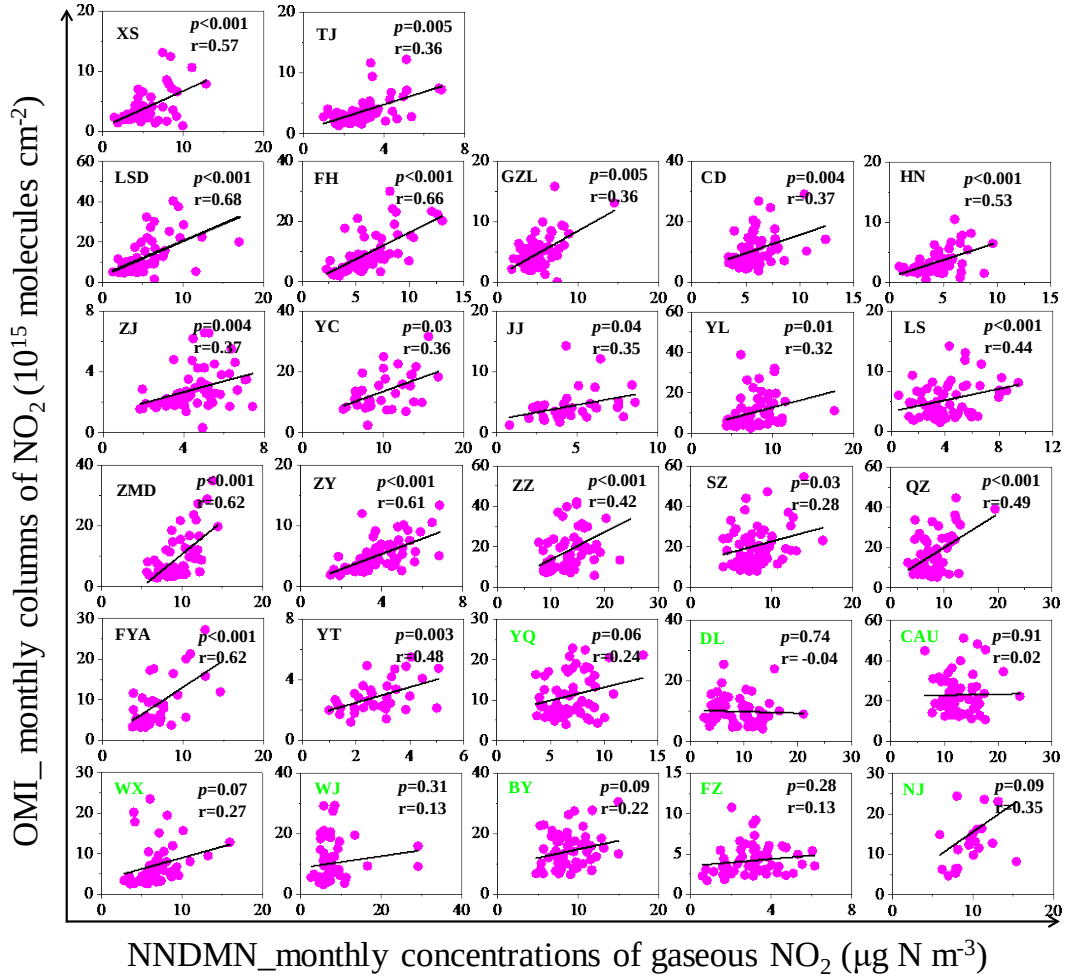
XS p<0.001 r=0.57
TJ p=0.005 r=0.36
LSD p<0.001 r=0.68
FH p<0.001 r=0.66
GZL p=0.005 r=0.36
CD p=0.004 r=0.37
HN p<0.001 r=0.53
ZJ p=0.004 r=0.37
YC p=0.03 r=0.36
JJ p=0.04 r=0.35
YL p=0.01 r=0.32
LS p<0.001 r=0.44
ZMD p<0.001 r=0.62
ZY p<0.001 r=0.61
ZZ p<0.001 r=0.42
SZ p=0.03 r=0.28
QZ p<0.001 r=0.49
FYA p<0.001 r=0.62
YT p=0.003 r=0.48
YQ p=0.06 r=0.24
DL p=0.74 r= -0.04
CAU p=0.91 r=0.02
WX p=0.07 r=0.27
WJ p=0.31 r=0.13
BY p=0.09 r=0.22
FZ p=0.28 r=0.13
NJ p=0.09 r=0.35
OMI_ monthly columns of NO2 (10^15 molecules cm^-2)
NNDMN_monthly concentrations of gaseous NO2 (μg N m^-3)

**Figure S9**

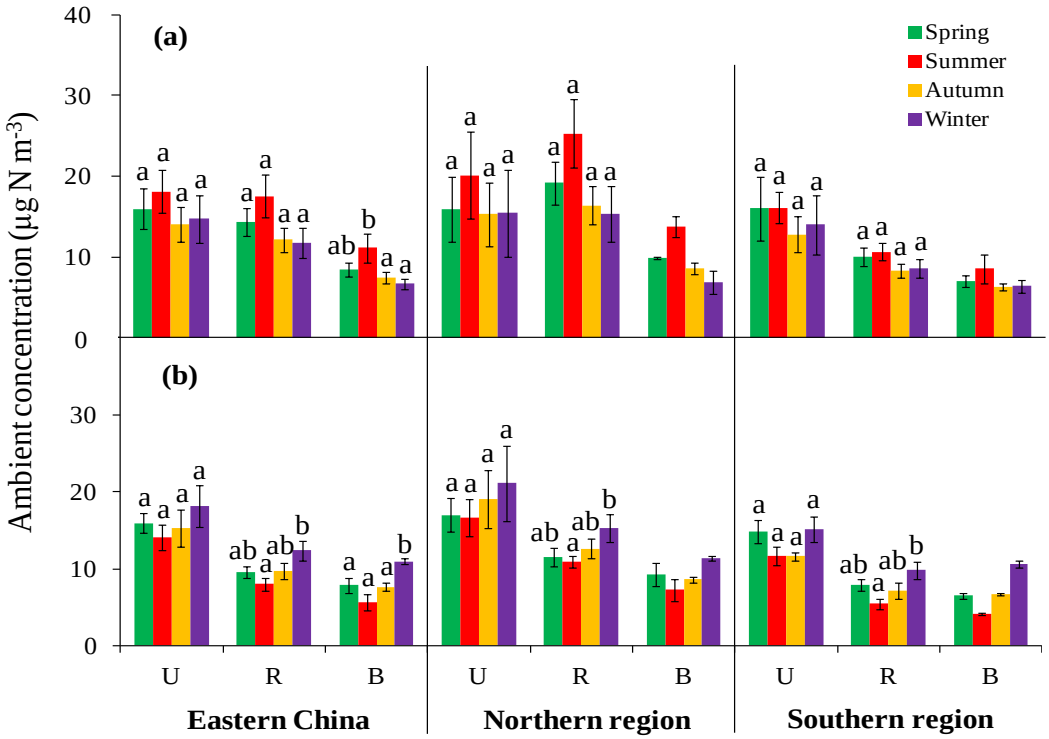
(a)
(b)
Spring
Summer
Autumn
Winter
Ambient concentration (μg N m-3)
40
30
20
10
0
U
R
B
Eastern China
Northern region
Southern region

**Figure S10**

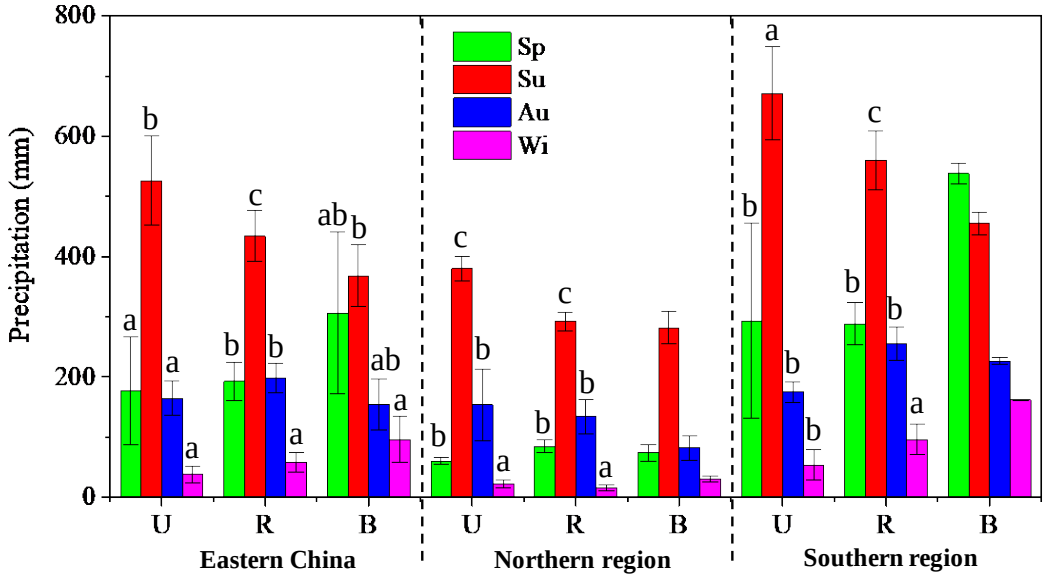
Precipitation (mm)
800
600
400
200
0
Sp
Su
Au
Wi
U
R
B
Eastern China
Northern region
Southern region

## Figure S11

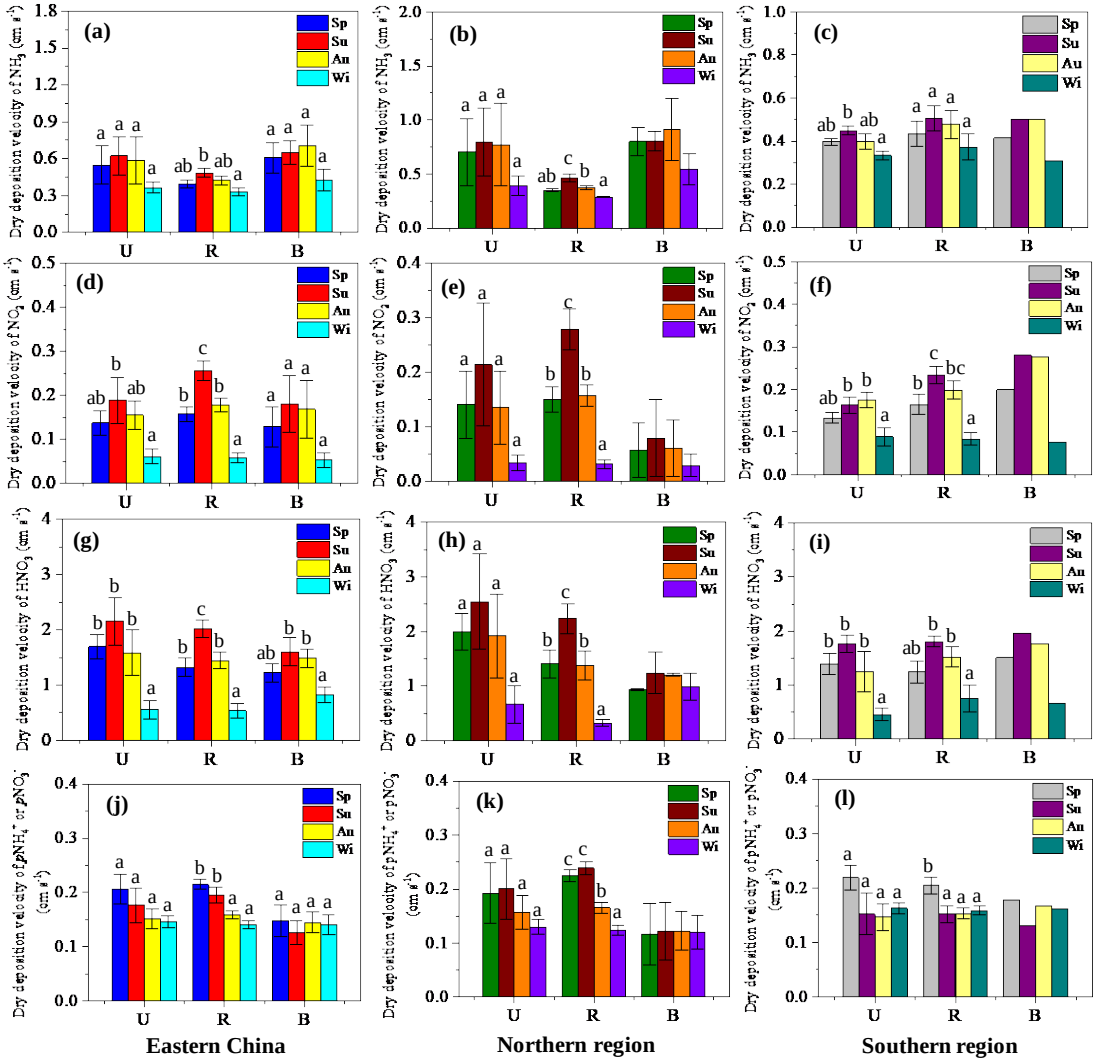
(a)
(b)
(c)
(d)
(e)
(f)
(g)
(h)
(i)
(j)
(k)
(l)
Sp
Su
An
Wi
U
R
B
Eastern China
Northern region
Southern region

**Figure S12**

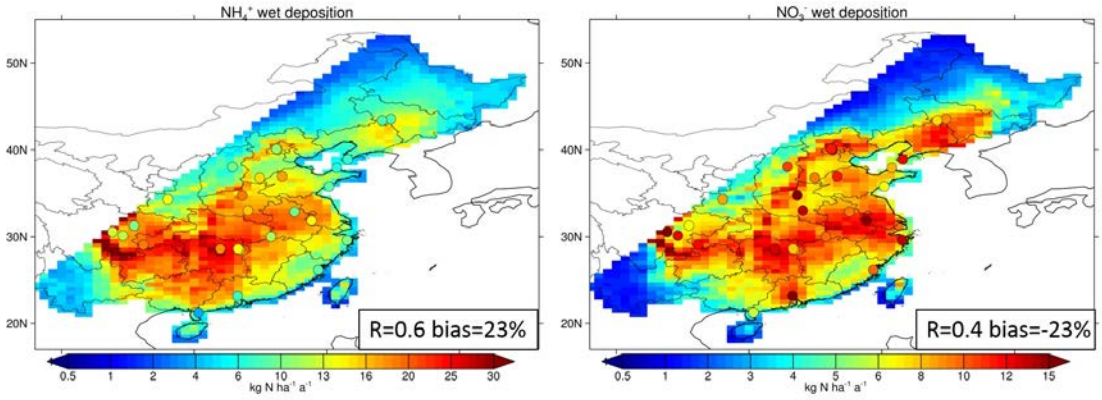
NH4+ wet deposition
50N
40N
30N
20N
R=0.6 bias=23%
0.5 1 2 4 6 10 13 16 20 25 30
kg N ha-1 a-1
NO3- wet deposition
50N
40N
30N
20N
R=0.4 bias=-23%
0.5 1 2 3 4 5 6 8 10 12 15
kg N ha-1 a-1

## Figure S13

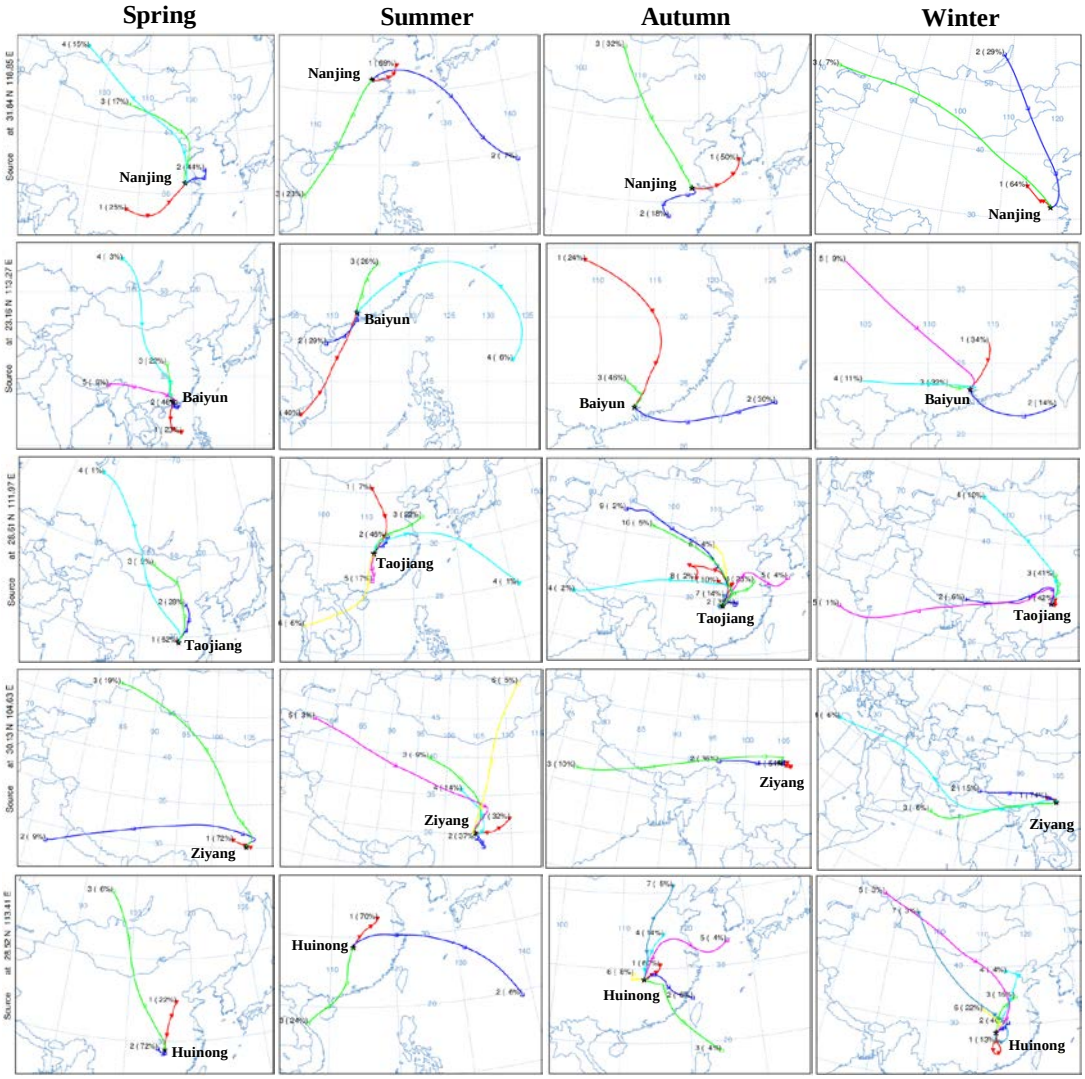
Spring
Summer
Autumn
Winter
Nanjing
Baiyun
Taojiang
Ziyang
Huinong

**Figure S14**

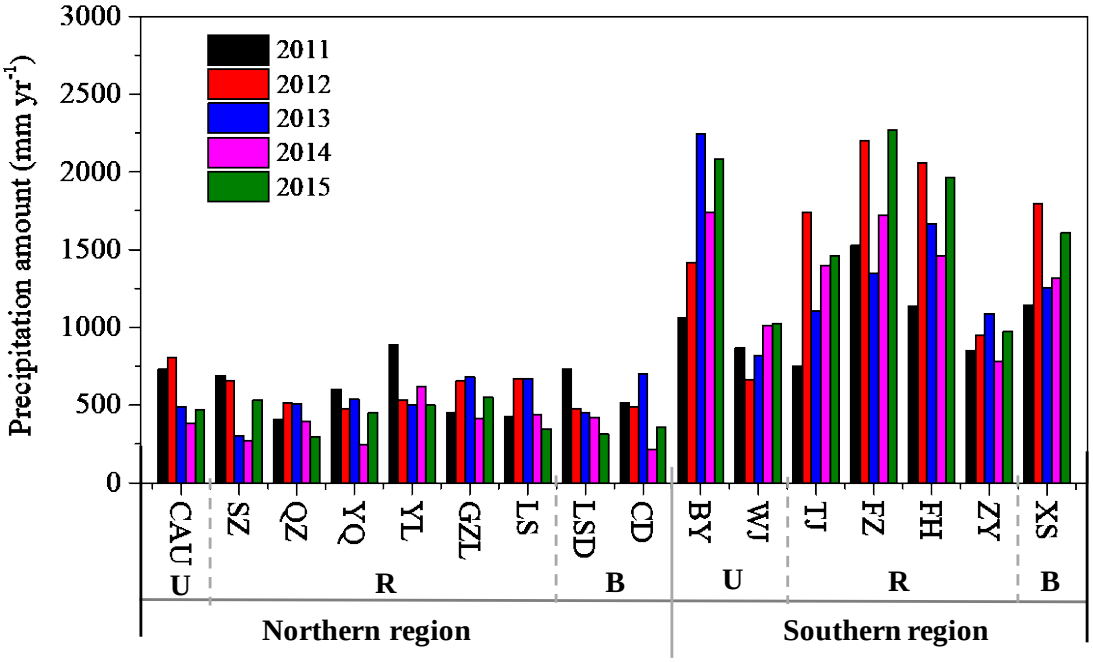
Precipitation amount (mm yr-1)
3000
2500
2000
1500
1000
500
0
2011
2012
2013
2014
2015
CAU
SZ
QZ
YQ
YL
GZL
LS
LSD
CD
BY
WJ
TJ
FZ
FH
ZY
XS
U
R
B
U
R
B
Northern region
Southern region

**Table S1.** Summary of the twenty-seven monitoring sites locations and periods.

| Site name | Land use type | Region | Coordinate | Monitoring period | |
|---|---|---|---|---|---|
| | | | | Dry deposition | Wet deposition |
| China Agricultural University (CAU) | Urban | Northern region | 116.28 º E, 40.02 º N | Jan. 2011-Dec. 2015 | Jan. 2011-Dec. 2015 |
| Zhengzhou (ZZ) | Urban | Northern region | 113.63 º E, 34.75 º N | Jan. 2011-Dec. 2015 | Jan. 2011-Dec. 2011 |
| Dalian (DL) | Urban | Northern region | 121.58 º E, 38.92 º N | Jan. 2011-Dec. 2015 | Jan. 2011-Dec. 2015 |
| Shangzhuang (SZ) | Rural | Northern region | 116.20 º E, 40.11 º N | Jan. 2011-Dec. 2015 | Jan. 2011-Dec. 2015 |
| Quzhou (QZ) | Rural | Northern region | 114.94 º E, 36.78 º N | Jan. 2011-Dec. 2015 | Jan. 2011-Dec. 2015 |
| Yangqu (YQ) | Rural | Northern region | 112.89 º E, 38.05 º N | Jan. 2011-Dec. 2015 | Jan. 2011-Dec. 2015 |
| Zhumadian (ZMD) | Rural | Northern region | 114.05 º E, 33.02 º N | Jan. 2011-Dec. 2015 | Jan. 2011-Dec. 2011<br>Jan. 2014-Dec. 2015 |
| Yanglin (YL) | Rural | Northern region | 108.01 º E, 34.31 º N | Jan. 2011-Dec. 2015 | Jan. 2011-Dec. 2015 |
| Yucheng (YC) | Rural | Northern region | 116.63 º E, 36.94 º N | Jan. 2013-Dec. 2015 | Jan. 2013-Dec. 2015 |
| Gongzhuling (GZL) | Rural | Northern region | 124.83 º E, 43.53 º N | Jan. 2011-Dec. 2015 | Jan. 2011-Dec. 2015 |
| Lishu (LS) | Rural | Northern region | 124.17 º E, 43.36 º N | Jan. 2011-Dec. 2015 | Jan. 2011-Dec. 2015 |
| Lingshandao (LSD) | Background | Northern region | 120.18 º E, 35.77 º N | Feb. 2011-Dec. 2015 | Feb. 2011-Dec. 2015 |
| Changdao (CD) | Background | Northern region | 120.75 º E, 37.93 º N | Jan. 2011-Dec. 2015 | Jan. 2011-Dec. 2015 |
| Nanjing (NJ) | Urban | Southern region | 118.85 º E, 31.84 º N | Jan. 2011-Dec. 2011<br>Jan. 2015-Dec. 2015 | Jan. 2011-Dec. 2011<br>Jan. 2015-Dec. 2015 |
| Baiyun (BY) | Urban | Southern region | 113.27 º E, 23.16 º N | Jan. 2011-Dec. 2015 | Jan. 2011-Dec. 2015 |
| Wenjiang (WJ) | Urban | Southern region | 103.84 º E, 30.55 º N | Jan. 2011-Dec. 2015 | Jan. 2011-Dec. 2015 |
| Wuxue (WX) | Rural | Southern region | 115.79 º E, 30.01 º N | Jan. 2012-Dec. 2015 | Jan. 2012-Dec. 2015 |
| Taojing (TJ) | Rural | Southern region | 111.97 º E, 28.61 º N | Jan. 2011-Dec. 2015 | Jan. 2011-Dec. 2015 |
| Fengyang (FYA) | Rural | Southern region | 117.56 º E, 32.88 º N | Feb. 2013-Dec. 2015 | Feb. 2014-Dec. 2015 |

| | | | | | |
|---|---|---|---|---|---|
| Zhanjiang (ZZ) | Rural | Southern region | 110.33 º E, 21.26 º N | Jan. 2011-Dec. 2015 | Jan. 2013-Dec. 2015 |
| Fuzhou (FZ) | Rural | Southern region | 119.36 º E, 26.17 º N | Jan. 2011-Dec. 2015 | Jan. 2011-Dec. 2015 |
| Fenghua (FH) | Rural | Southern region | 121.53 º E, 29.61 º N | Jan. 2011-Dec. 2015 | Jan. 2011-Dec. 2015 |
| Ziyang (ZY) | Rural | Southern region | 104.63 º E, 30.13 º N | Jan. 2011-Dec. 2015 | Jan. 2011-Dec. 2015 |
| Yanting (YT) | Rural | Southern region | 105.47 º E, 31.28 º N | Jan. 2012-Dec. 2013<br>Jan. 2015-Dec. 2015 | Jan. 2012-Dec. 2013 |
| Jiangjin (JJ) | Rural | Southern region | 106.18 º E, 29.06 º N | Jan. 2013-Dec. 2015 | Jan. 2013-Dec. 2015 |
| Huinong (HN) | Background | Southern region | 113.41 º E, 28.52 º N | Jan. 2011-Dec. 2015 | Jan. 2011-Dec. 2014 |
| Xishan (XS) | Background | Southern region | 113.31 º E, 28.61 º N | Jan. 2011-Dec. 2015 | Jan. 2011-Dec. 2015 |

**Table S2.** Summary of monthly mean $N_r$ concentrations measured during the 2011-2015 period.

| Site | $NH_3$ (μg N $m^{-3}$) | | | | $NO_2$ (μg N $m^{-3}$) | | | | $HNO_3$ (μg N $m^{-3}$) | | | | $pNH_4^+$ (μg N $m^{-3}$) | | | | $pNO_3^-$ (μg N $m^{-3}$) | | | |
|---|---|---|---|---|---|---|---|---|---|---|---|---|---|---|---|---|---|---|---|---|
| | Min | Max | Avg | N | Min | Max | Avg | N[a] | Min | Max | Avg | N | Min | Max | Avg | N | Min | Max | Avg | N |
| CAU | 2.86 | 22.43 | 11.21 | 60 | 6.35 | 24.03 | 12.87 | 60 | 0.36 | 4.93 | 1.98 | 60 | 1.96 | 19.40 | 8.72 | 60 | 1.01 | 13.38 | 5.34 | 60 |
| ZZ | 2.75 | 18.59 | 9.76 | 60 | 7.74 | 24.75 | 13.66 | 60 | 0.07 | 4.30 | 1.89 | 60 | 1.35 | 33.10 | 12.53 | 60 | 0.44 | 32.06 | 7.40 | 60 |
| DL | 0.27 | 8.53 | 3.40 | 60 | 2.54 | 21.04 | 8.60 | 60 | 0.10 | 2.58 | 1.00 | 60 | 0.65 | 9.54 | 4.45 | 60 | 0.01 | 7.16 | 2.53 | 60 |
| SZ | 1.00 | 21.23 | 9.44 | 60 | 3.96 | 16.27 | 8.16 | 60 | 0.29 | 3.50 | 1.54 | 60 | 1.48 | 15.95 | 6.95 | 60 | 1.00 | 9.43 | 3.53 | 60 |
| QZ | 1.36 | 34.80 | 15.43 | 60 | 3.23 | 19.48 | 7.97 | 60 | 0.14 | 4.40 | 1.59 | 60 | 1.89 | 57.20 | 19.68 | 60 | 0.22 | 20.78 | 6.06 | 60 |
| YQ | 0.58 | 13.81 | 4.88 | 60 | 3.62 | 13.61 | 6.98 | 60 | 0.04 | 2.73 | 1.18 | 60 | 0.99 | 10.69 | 5.11 | 60 | 0.21 | 7.26 | 2.72 | 60 |
| ZMD | 4.73 | 27.30 | 10.31 | 60 | 5.65 | 14.47 | 9.36 | 60 | 0.22 | 4.09 | 1.90 | 60 | 0.92 | 21.87 | 9.52 | 60 | 0.47 | 14.50 | 4.75 | 60 |
| YL | 1.91 | 19.77 | 8.30 | 60 | 4.30 | 17.64 | 7.55 | 60 | 0.14 | 3.73 | 1.35 | 60 | 0.59 | 21.55 | 5.56 | 60 | 1.07 | 16.22 | 4.29 | 60 |
| YC | 4.39 | 25.36 | 11.88 | 36 | 5.02 | 16.78 | 9.74 | 36 | 0.10 | 3.82 | 1.52 | 36 | 4.70 | 46.53 | 13.66 | 36 | 1.00 | 11.81 | 4.50 | 36 |
| GZL | 0.48 | 18.62 | 6.35 | 60 | 1.79 | 14.52 | 5.29 | 60 | 0.21 | 2.41 | 1.09 | 60 | 0.40 | 18.14 | 4.97 | 60 | 0.51 | 5.52 | 2.07 | 60 |
| LS | 1.42 | 38.89 | 11.79 | 60 | 0.55 | 9.45 | 4.16 | 60 | 0.22 | 3.27 | 1.00 | 60 | 1.61 | 26.67 | 7.51 | 60 | 0.29 | 5.79 | 1.93 | 60 |
| LSD | 0.30 | 16.02 | 5.30 | 59 | 1.32 | 16.97 | 5.31 | 59 | 0.08 | 1.69 | 0.92 | 59 | 0.39 | 20.69 | 5.34 | 59 | 0.21 | 6.15 | 2.05 | 59 |
| CD | 0.30 | 10.55 | 4.04 | 60 | 3.40 | 12.37 | 5.97 | 60 | 0.50 | 2.92 | 1.13 | 60 | 0.54 | 12.97 | 4.91 | 60 | 0.97 | 6.55 | 2.74 | 60 |
| NJ | 1.57 | 20.06 | 6.02 | 24 | 5.89 | 15.38 | 9.73 | 24 | 0.64 | 3.65 | 1.80 | 24 | 0.56 | 9.28 | 5.87 | 24 | 1.13 | 5.64 | 3.17 | 24 |
| BY | 1.13 | 17.22 | 7.86 | 60 | 4.75 | 14.97 | 8.86 | 60 | 0.16 | 2.58 | 1.38 | 60 | 0.60 | 8.57 | 3.81 | 60 | 0.73 | 4.62 | 2.62 | 60 |
| WJ | 3.53 | 39.57 | 12.47 | 60 | 2.52 | 29.06 | 7.58 | 60 | 0.09 | 3.27 | 1.70 | 60 | 2.00 | 32.21 | 14.09 | 60 | 1.09 | 11.50 | 3.04 | 60 |
| WX | 1.39 | 17.12 | 5.91 | 48 | 2.82 | 15.93 | 6.81 | 48 | 0.32 | 3.24 | 1.27 | 48 | 0.70 | 12.42 | 5.22 | 48 | 0.10 | 8.55 | 1.98 | 48 |
| TJ | 0.16 | 8.70 | 3.31 | 60 | 1.00 | 6.85 | 2.91 | 60 | 0.14 | 1.71 | 0.82 | 60 | 0.24 | 9.03 | 4.19 | 60 | 0.03 | 4.41 | 1.32 | 60 |
| FYA | 1.73 | 20.25 | 6.81 | 35 | 3.70 | 14.58 | 7.01 | 35 | 0.18 | 2.25 | 1.41 | 35 | 0.73 | 11.85 | 5.71 | 35 | 0.83 | 9.21 | 3.01 | 35 |
| ZJ | 1.07 | 14.80 | 6.68 | 60 | 1.84 | 7.41 | 4.52 | 60 | 0.09 | 1.68 | 0.77 | 60 | 0.39 | 10.23 | 3.58 | 60 | 0.19 | 9.83 | 2.23 | 60 |
| FZ | 0.19 | 7.20 | 1.77 | 60 | 0.57 | 6.15 | 3.05 | 60 | 0.05 | 1.62 | 0.45 | 60 | 0.17 | 3.79 | 2.22 | 60 | 0.22 | 2.20 | 1.20 | 60 |
| FH | 0.76 | 13.83 | 5.90 | 60 | 2.26 | 13.04 | 6.24 | 60 | 0.29 | 2.63 | 1.13 | 60 | 0.45 | 8.01 | 4.04 | 60 | 0.31 | 3.88 | 1.81 | 60 |

| | | | | | | | | | | | | | | | | | | |
|---|---|---|---|---|---|---|---|---|---|---|---|---|---|---|---|---|---|---|
| ZY | 1.16 | 12.46 | 5.12 | 60 | 1.45 | 6.85 | 3.83 | 60 | 0.22 | 2.24 | 0.96 | 60 | 0.11 | 16.08 | 4.99 | 60 | 0.11 | 5.53 | 1.78 | 60 |
| YT | 0.43 | 18.31 | 4.18 | 36 | 0.99 | 5.07 | 2.75 | 36 | 0.08 | 1.20 | 0.49 | 36 | 0.88 | 15.80 | 3.01 | 36 | 0.11 | 2.54 | 1.01 | 36 |
| JJ | 0.70 | 12.99 | 4.48 | 36 | 0.82 | 8.61 | 4.75 | 36 | 0.13 | 3.09 | 1.48 | 36 | 1.26 | 16.74 | 7.85 | 36 | 0.34 | 7.61 | 3.03 | 36 |
| HN | 0.64 | 18.86 | 3.78 | 60 | 0.89 | 9.59 | 4.31 | 60 | 0.12 | 2.68 | 0.74 | 60 | 0.44 | 12.58 | 4.21 | 60 | 0.16 | 14.77 | 1.62 | 60 |
| XS | 0.21 | 7.97 | 2.38 | 60 | 1.41 | 12.81 | 5.18 | 60 | 0.08 | 1.96 | 0.87 | 60 | 0.43 | 9.19 | 3.74 | 60 | 0.15 | 5.27 | 1.25 | 60 |

[a]Multiply by 3 to obtain a total numbers of $NO_2$ samples.

**Table S3.** Summary of monthly volume-weighted mean $N_r$ concentrations in precipitation measured during the 2011-2015 period.

| Site | $NH_4^+$-N (mg N $L^{-1}$) | | | | $NO_3^-$-N (mg N $L^{-1}$) | | | | TIN (mg N $L^{-1}$) | | | |
|---|---|---|---|---|---|---|---|---|---|---|---|---|
| | Min | Max | Avg | N | Min | Max | Avg | N | Min | Max | Avg | N |
| CAU | 0.16 | 19.15 | 3.91 | 47 | 0.22 | 15.75 | 4.20 | 47 | 0.46 | 32.37 | 8.10 | 47 |
| ZZ | 1.37 | 10.67 | 4.11 | 10 | 1.01 | 27.89 | 5.30 | 10 | 2.38 | 38.56 | 9.41 | 10 |
| DL | 0.13 | 15.93 | 2.94 | 53 | 0.70 | 14.40 | 4.22 | 53 | 1.13 | 25.57 | 7.15 | 53 |
| SZ | 0.44 | 13.08 | 3.21 | 42 | 0.40 | 8.99 | 2.86 | 42 | 0.84 | 19.52 | 6.08 | 42 |
| QZ | 0.16 | 16.60 | 3.76 | 47 | 0.21 | 14.40 | 3.04 | 47 | 0.53 | 29.27 | 6.80 | 47 |
| YQ | 0.16 | 17.56 | 2.79 | 48 | 0.22 | 12.45 | 3.18 | 48 | 0.69 | 30.01 | 5.96 | 48 |
| ZMD | 0.03 | 9.31 | 2.66 | 34 | 0.07 | 5.81 | 2.21 | 34 | 0.11 | 12.29 | 4.87 | 34 |
| YL | 0.46 | 10.51 | 3.29 | 53 | 0.07 | 8.32 | 2.83 | 53 | 0.55 | 17.86 | 6.12 | 53 |
| YC | 0.97 | 26.77 | 6.80 | 32 | 0.84 | 23.52 | 4.81 | 32 | 2.22 | 50.29 | 11.61 | 32 |
| GZL | 0.12 | 7.34 | 2.37 | 60 | 0.53 | 10.06 | 2.67 | 60 | 0.81 | 15.05 | 5.05 | 60 |
| LS | 0.27 | 12.72 | 2.22 | 48 | 0.28 | 9.46 | 2.61 | 48 | 0.55 | 14.73 | 4.82 | 48 |
| LSD | 0.29 | 8.44 | 2.38 | 45 | 0.14 | 11.10 | 2.41 | 45 | 0.54 | 17.67 | 4.80 | 45 |
| CD | 0.34 | 11.27 | 2.48 | 54 | 0.46 | 19.92 | 4.00 | 54 | 1.06 | 29.65 | 6.47 | 54 |
| NJ | 0.33 | 2.82 | 1.27 | 26 | 0.28 | 8.31 | 2.11 | 26 | 0.62 | 10.06 | 3.38 | 26 |
| BY | 0.01 | 13.88 | 0.97 | 53 | 0.11 | 6.23 | 1.70 | 53 | 0.34 | 19.98 | 2.67 | 53 |
| WJ | 0.19 | 13.62 | 2.65 | 52 | 0.10 | 28.92 | 4.75 | 52 | 0.91 | 34.64 | 7.41 | 52 |
| WX | 0.16 | 2.88 | 1.01 | 44 | 0.10 | 7.39 | 1.30 | 44 | 0.31 | 8.75 | 2.31 | 44 |
| TJ | 0.24 | 8.36 | 2.02 | 59 | 0.11 | 7.23 | 1.53 | 59 | 0.35 | 15.03 | 3.55 | 59 |
| FYA | 0.24 | 9.63 | 2.32 | 24 | 0.34 | 28.77 | 3.06 | 24 | 0.61 | 38.40 | 5.38 | 24 |
| ZJ | 0.10 | 2.04 | 0.42 | 29 | 0.07 | 3.77 | 0.79 | 29 | 0.23 | 4.16 | 1.21 | 29 |
| FZ | 0.04 | 4.96 | 0.74 | 60 | 0.09 | 4.93 | 0.85 | 60 | 0.22 | 8.88 | 1.59 | 60 |
| FH | 0.12 | 5.62 | 1.03 | 55 | 0.34 | 6.61 | 1.25 | 55 | 0.52 | 12.23 | 2.27 | 55 |
| ZY | 0.16 | 5.08 | 1.79 | 53 | 0.47 | 11.52 | 2.20 | 53 | 1.20 | 15.74 | 3.99 | 53 |
| YT | 0.16 | 3.81 | 1.31 | 32 | 0.16 | 3.13 | 1.17 | 32 | 0.54 | 6.27 | 2.48 | 32 |
| JJ | 0.35 | 12.73 | 3.27 | 36 | 0.26 | 10.31 | 2.63 | 36 | 0.61 | 23.04 | 5.89 | 36 |
| HN | 0.19 | 5.26 | 1.40 | 48 | 0.17 | 3.74 | 0.91 | 48 | 0.36 | 8.86 | 2.30 | 48 |
| XS | 0.03 | 3.78 | 1.22 | 60 | 0.06 | 3.52 | 0.81 | 60 | 0.09 | 6.09 | 2.03 | 60 |

**Table S4.** Seasonal average concentrations and deposition fluxes of gaseous $NH_3$ at twenty-seven monitoring sites in eastern China.

| Sites | Air concentrations | | | | Dry deposition fluxes | | | |
|---|---|---|---|---|---|---|---|---|
| | Spring | Summer | Autumn | Winter | Spring | Summer | Autumn | Winter |
| CAU | 12.1 ± 1.9b | 16.0 ± 2.4a | 11.2 ± 1.6b | 5.6 ± 1.5c | 3.8 ± 0.6b | 7.8 ± 1.1a | 4.1 ± 0.6b | 1.3 ± 0.3c |
| ZZ | 11.7 ± 1.4a | 12.2 ± 3.9a | 8.9 ± 3.2ab | 6.3 ± 1.1b | 3.4 ± 0.4a | 3.4 ± 1.1a | 2.2 ± 0.8ab | 1.5 ± 0.3b |
| DL | 3.8 ± 1.0a | 5.1 ± 1.2a | 3.5 ± 1.3a | 1.2 ± 0.4b | 4.2 ± 1.1a | 5.5 ± 1.3a | 4.1 ± 1.5a | 0.6 ± 0.2b |
| SZ | 9.7 ± 1.9b | 14.9 ± 2.5a | 9.0 ± 2.9b | 4.2 ± 1.4c | 3.1 ± 0.6b | 7.3 ± 1.2a | 3.4 ± 1.1b | 1.0 ± 0.3c |
| QZ | 17.4 ± 5.7a | 18.2 ± 4.6a | 13.3 ± 3.8a | 12.8 ± 8.8a | 4.8 ± 1.6a | 5.8 ± 1.5a | 3.7 ± 1.1a | 3.0 ± 2.1a |
| YQ | 7.7 ± 0.8a | 6.0 ± 0.6a | 3.1 ± 0.7b | 2.7 ± 2.1b | 2.0 ± 0.2a | 2.0 ± 0.2a | 0.9 ± 0.2b | 0.6 ± 0.5b |
| ZMD | 11.3 ± 4.0a | 9.8 ± 4.1a | 10.8 ± 2.9a | 9.3 ± 0.9a | 3.8 ± 1.3a | 3.1 ± 1.3a | 2.9 ± 0.8a | 2.2 ± 0.2a |
| YL | 7.6 ± 2.8a | 10.9 ± 6.3a | 8.5 ± 3.8a | 6.3 ± 2.1a | 2.4 ± 0.9ab | 4.3 ± 2.5a | 2.7 ± 1.3ab | 1.5 ± 0.5b |
| YC | 10.9 ± 2.2b | 17.0 ± 2.0a | 12.2 ± 2.3ab | 9.2 ± 2.1b | 2.6 ± 0.5b | 4.9 ± 0.6a | 3.1 ± 0.6b | 2.1 ± 0.5b |
| GZL | 7.3 ± 0.6b | 11.7 ± 2.4a | 5.2 ± 0.3b | 1.3 ± 0.6c | 1.8 ± 0.2b | 5.5 ± 1.2a | 1.8 ± 0.1b | 0.2 ± 0.1c |
| LS | 17.0 ± 3.5a | 13.2 ± 2.5ab | 11.9 ± 1.9b | 5.1 ± 1.7c | 4.0 ± 0.8b | 5.5 ± 1.1a | 3.6 ± 0.6b | 1.0 ± 0.4c |
| LSD | 5.0 ± 0.9b | 9.4 ± 2.4a | 4.8 ± 2.2bc | 1.9 ± 0.4c | 2.6 ± 0.5b | 5.2 ± 1.4a | 2.4 ± 1.1b | 0.5 ± 0.1c |
| CD | 4.9 ± 0.7b | 6.9 ± 1.2a | 3.3 ± 0.9b | 1.1 ± 0.5c | 3.6 ± 0.5ab | 4.8 ± 1.0a | 3.0 ± 0.8b | 0.6 ± 0.3c |
| NJ | 7.7 ± 1.7 | 10.2 ± 2.1 | 3.6 ± 1.1 | 3.8 ± 0.1 | 2.6 ± 0.6 | 3.8 ± 0.8 | 1.1 ± 0.3 | 0.9 ± 0.0 |
| BY | 7.4 ± 1.2b | 9.9 ± 2.0a | 9.4 ± 0.8ab | 4.7 ± 0.8c | 2.2 ± 0.4b | 3.1 ± 0.6a | 3.3 ± 0.3a | 1.4 ± 0.2c |
| WJ | 14.8 ± 3.8a | 16.2 ± 6.9a | 10.1 ± 3.8a | 8.8 ± 1.7a | 4.5 ± 1.1ab | 5.9 ± 2.5a | 2.6 ± 1.0b | 2.1 ± 0.4b |
| WX | 6.3 ± 1.9b | 9.6 ± 1.7a | 5.1 ± 0.9bc | 3.2 ± 0.5c | 1.9 ± 0.6b | 3.3 ± 0.6a | 1.8 ± 0.3b | 0.8 ± 0.1c |
| TJ | 4.0 ± 2.5ab | 5.3 ± 1.4a | 2.4 ± 1.2b | 1.5 ± 0.8b | 1.1 ± 0.7ab | 1.8 ± 0.5a | 0.9 ± 0.4b | 0.4 ± 0.2b |
| FYA | 6.4 ± 1.6ab | 11.2 ± 4.9a | 5.4 ± 0.2ab | 3.8 ± 0.5b | 2.1 ± 0.5ab | 3.6 ± 1.8a | 1.6 ± 0.0ab | 0.8 ± 0.3b |
| ZJ | 7.6 ± 1.5a | 9.3 ± 1.9a | 6.6 ± 1.6a | 3.3 ± 1.3b | 1.9 ± 0.4a | 2.6 ± 0.5a | 2.3 ± 0.6a | 0.8 ± 0.3b |
| FZ | 1.7 ± 0.5ab | 3.0 ± 1.2a | 1.4 ± 0.2b | 1.0 ± 0.6b | 1.2 ± 0.4b | 2.2 ± 0.9a | 1.1 ± 0.2b | 0.7 ± 0.4b |
| FH | 6.9 ± 2.3ab | 7.5 ± 2.5a | 5.9 ± 1.6ab | 3.4 ± 1.5b | 2.5 ± 0.9a | 3.1 ± 1.0a | 2.2 ± 0.6ab | 0.8 ± 0.4b |
| ZY | 7.7 ± 1.4a | 5.7 ± 2.0ab | 4.3 ± 1.2bc | 2.9 ± 0.5c | 2.0 ± 0.4a | 1.9 ± 0.6a | 1.1 ± 0.3b | 0.7 ± 0.1b |

| | | | | | | | | |
|---|---|---|---|---|---|---|---|---|
| YT | 3.3 ± 0.7b | 9.3 ± 0.8a | 2.6 ± 1.4b | 1.5 ± 0.7b | 1.0 ± 0.2b | 3.4 ± 0.2a | 0.8 ± 0.4b | 0.4 ± 0.2b |
| JJ | 7.1 ± 1.2a | 5.2 ± 2.1ab | 3.3 ± 0.8b | 2.4 ± 0.4b | 2.1 ± 0.4a | 1.9 ± 0.8a | 1.1 ± 0.3ab | 0.6 ± 0.1b |
| HN | 4.1 ± 0.7ab | 7.0 ± 2.8a | 2.2 ± 0.9b | 1.8 ± 0.6b | 1.4 ± 0.2b | 2.7 ± 1.1a | 0.9 ± 0.4b | 0.4 ± 0.2b |
| XS | 2.7 ± 1.3ab | 3.5 ± 1.3a | 1.8 ± 0.7ab | 1.5 ± 0.5b | 0.9 ± 0.5ab | 1.4 ± 0.5a | 0.7 ± 0.3ab | 0.4 ± 0.1b |

The data shown are the seasonal means ± standard deviations of observation periods (sampling period for each site are given in Table S1). Different letters in the columns of “air concentrations” and “dry deposition fluxes” indicate significant difference between the seasons at $p<0.05$. The full names of all the sites are presented in Table S1.

**Table S5.** Seasonal average concentrations and deposition fluxes of gaseous $NO_2$ at twenty-seven monitoring sites in eastern China.

| Sites | Air concentrations | | | | Dry deposition fluxes | | | |
|---|---|---|---|---|---|---|---|---|
| | Spring | Summer | Autumn | Winter | Spring | Summer | Autumn | Winter |
| CAU | 12.0 ± 1.7a | 12.7 ± 1.7a | 14.3 ± 3.3a | 12.5 ± 2.1a | 1.9 ± 0.2c | 4.2 ± 0.6a | 2.9 ± 0.8b | 0.3 ± 0.0d |
| ZZ | 12.5 ± 1.8a | 12.0 ± 2.2a | 15.0 ± 2.0a | 15.1 ± 2.3a | 1.9 ± 0.2a | 1.7 ± 0.3ab | 1.4 ± 0.2b | 0.7 ± 0.1c |
| DL | 9.1 ± 4.2a | 8.4 ± 4.4a | 8.6 ± 3.7a | 8.3 ± 3.8a | 0.1 ± 0.1a | 0.2 ± 0.1a | 0.2 ± 0.1a | 0.1 ± 0.0a |
| SZ | 8.8 ± 0.9a | 7.4 ± 1.0a | 7.4 ± 0.8a | 9.0 ± 2.1a | 1.4 ± 0.1b | 2.4 ± 0.3a | 1.3 ± 0.2b | 0.2 ± 0.0c |
| QZ | 6.8 ± 1.5b | 7.3 ± 1.5ab | 8.0 ± 0.9ab | 9.7 ± 1.7a | 0.9 ± 0.2a | 1.2 ± 0.2a | 0.9 ± 0.1a | 0.3 ± 0.1b |
| YQ | 6.7 ± 1.7a | 6.8 ± 1.6a | 7.5 ± 0.6a | 6.8 ± 1.8a | 0.6 ± 0.1b | 1.4 ± 0.3a | 0.8 ± 0.1b | 0.1 ± 0.0c |
| ZMD | 9.3 ± 0.9ab | 8.0 ± 0.5b | 9.5 ± 1.0ab | 10.5 ± 1.6a | 1.9 ± 0.2a | 1.5 ± 0.1b | 1.1 ± 0.1c | 0.7 ± 0.1d |
| YL | 7.2 ± 1.9ab | 5.9 ± 1.1b | 7.8 ± 0.4ab | 9.3 ± 1.8a | 1.3 ± 0.3a | 1.5 ± 0.3a | 1.1 ± 0.2a | 0.3 ± 0.1b |
| YC | 9.9 ± 2.9a | 8.5 ± 2.1a | 9.9 ± 2.2a | 11.3 ± 3.0a | 0.9 ± 0.2ab | 1.1 ± 0.3a | 0.8 ± 0.2ab | 0.3 ± 0.1b |
| GZL | 4.3 ± 1.0a | 5.8 ± 1.1a | 5.0 ± 0.5a | 6.0 ± 1.5a | 0.4 ± 0.1b | 1.9 ± 0.4a | 0.6 ± 0.2b | 0.04 ± 0.01c |
| LS | 3.8 ± 1.7a | 5.5 ± 0.6a | 3.8 ± 0.9a | 3.6 ± 1.0a | 0.3 ± 0.1b | 1.5 ± 0.2a | 0.4 ± 0.1b | 0.03 ± 0.01c |
| LSD | 4.5 ± 1.4bc | 3.4 ± 0.7c | 6.0 ± 2.4ab | 7.5 ± 0.3a | 0.4 ± 0.1a | 0.4 ± 0.1a | 0.5 ± 0.2a | 0.3 ± 0.0a |
| CD | 6.5 ± 0.5ab | 5.1 ± 0.5b | 5.2 ± 0.7b | 7.1 ± 1.6a | 0.04 ± 0.00a | 0.04 ± 0.00a | 0.04 ± 0.00a | 0.05 ± 0.01a |
| NJ | 12.0 ± 0.9 | 7.8 ± 0.7 | 8.5 ± 1.6 | 10.9 ± 0.8 | 1.5 ± 0.2 | 1.2 ± 0.1 | 1.1 ± 0.4 | 0.4 ± 0.0 |
| BY | 10.7 ± 2.0a | 9.4 ± 2.1ab | 7.6 ± 1.0b | 7.7 ± 0.7b | 1.0 ± 0.2a | 1.1 ± 0.2a | 1.1 ± 0.1a | 0.7 ± 0.1b |
| WJ | 7.4 ± 1.4ab | 5.9 ± 1.4b | 6.6 ± 0.6b | 10.4 ± 3.4a | 0.9 ± 0.2a | 1.1 ± 0.3a | 0.5 ± 0.1b | 0.5 ± 0.1b |
| WX | 6.8 ± 0.3a | 4.7 ± 0.7a | 8.0 ± 2.7a | 7.5 ± 1.4a | 0.8 ± 0.0ab | 0.8 ± 0.1ab | 1.2 ± 0.4a | 0.4 ± 0.1b |
| TJ | 2.6 ± 0.6bc | 1.9 ± 0.2c | 2.9 ± 0.3b | 4.3 ± 0.4a | 0.3 ± 0.1bc | 0.3 ± 0.0ab | 0.4 ± 0.1a | 0.2 ± 0.0c |
| FYA | 6.0 ± 1.3a | 5.7 ± 1.0a | 8.3 ± 0.8a | 8.4 ± 2.4a | 0.8 ± 0.2a | 0.9 ± 0.1a | 0.7 ± 0.2ab | 0.3 ± 0.1b |
| ZJ | 5.3 ± 0.4a | 3.2 ± 0.8b | 4.5 ± 0.8a | 5.1 ± 0.6a | 0.4 ± 0.0b | 0.4 ± 0.1b | 0.8 ± 0.1a | 0.4 ± 0.0b |
| FZ | 4.1 ± 0.5a | 3.4 ± 0.4b | 1.7 ± 0.2c | 3.0 ± 0.4b | 0.9 ± 0.1a | 0.8 ± 0.1a | 0.4 ± 0.1b | 0.4 ± 0.1b |
| FH | 6.7 ± 1.2b | 4.4 ± 1.1c | 5.5 ± 0.6bc | 8.4 ± 0.9a | 1.4 ± 0.3a | 1.2 ± 0.3ab | 1.2 ± 0.2ab | 0.8 ± 0.1b |
| ZY | 4.5 ± 0.8ab | 2.7 ± 0.4c | 3.5 ± 0.6bc | 4.6 ± 0.2a | 0.4 ± 0.1a | 0.4 ± 0.1a | 0.3 ± 0.1b | 0.2 ± 0.0c |

| | | | | | | | | |
|---|---|---|---|---|---|---|---|---|
| YT | 3.2 ± 0.7ab | 2.0 ± 0.4b | 2.4 ± 0.2ab | 3.5 ± 0.4a | 0.4 ± 0.1ab | 0.4 ± 0.1a | 0.3 ± 0.0ab | 0.2 ± 0.0b |
| JJ | 5.4 ± 0.7ab | 3.5 ± 0.4bc | 3.3 ± 0.9c | 6.8 ± 0.9a | 0.4 ± 0.1ab | 0.5 ± 0.1a | 0.4 ± 0.1ab | 0.2 ± 0.0b |
| HN | 3.8 ± 0.9bc | 2.7 ± 0.9c | 4.5 ± 0.4b | 6.1 ± 0.8a | 0.6 ± 0.1bc | 0.6 ± 0.2b | 0.9 ± 0.1a | 0.4 ± 0.0c |
| XS | 4.9 ± 1.2b | 2.8 ± 0.9b | 4.9 ± 0.8b | 8.2 ± 2.1a | 0.7 ± 0.2ab | 0.6 ± 0.2b | 1.0 ± 0.2a | 0.5 ± 0.1b |

The data shown are the seasonal means ± standard deviations of observation periods (sampling period for each site are given in Table S1). Different letters in the columns of “air concentrations” and “dry deposition fluxes” indicate significant difference between the seasons at $p<0.05$. The full names of all sites are presented in Table S1).

**Table S6.** Seasonal average concentrations and deposition fluxes of gaseous $HNO_3$ at twenty-seven monitoring sites in eastern China.

| Sites | Air concentrations | | | | Dry deposition fluxes | | | |
|---|---|---|---|---|---|---|---|---|
| | Spring | Summer | Autumn | Winter | Spring | Summer | Autumn | Winter |
| CAU | 1.9 ± 0.8a | 1.9 ± 0.2a | 1.8 ± 0.3a | 2.3 ± 0.8a | 3.5 ± 1.5b | 6.3 ± 0.6a | 4.6 ± 0.7b | 0.6 ± 0.2c |
| ZZ | 2.3 ± 0.5ab | 2.8 ± 0.5a | 1.5 ± 0.7bc | 1.0 ± 0.7c | 3.6 ± 0.7a | 3.9 ± 0.8a | 0.8 ± 0.4b | 0.2 ± 0.2b |
| DL | 1.1 ± 0.5a | 1.3 ± 0.4a | 1.0 ± 0.3a | 0.7 ± 0.4a | 1.2 ± 0.6a | 1.5 ± 0.4a | 1.3 ± 0.4a | 0.7 ± 0.4a |
| SZ | 1.3 ± 0.3b | 1.3 ± 0.5b | 1.5 ± 0.3ab | 2.0 ± 0.5a | 2.7 ± 0.6b | 4.3 ± 1.5a | 3.5 ± 0.6ab | 0.5 ± 0.1c |
| QZ | 1.8 ± 0.3a | 1.8 ± 0.8a | 1.2 ± 0.4a | 1.6 ± 0.6a | 2.7 ± 0.6a | 2.3 ± 1.0a | 1.0 ± 0.3b | 0.4 ± 0.2b |
| YQ | 1.3 ± 0.5a | 1.0 ± 0.4a | 1.0 ± 0.1a | 1.3 ± 0.5a | 1.0 ± 0.4ab | 1.6 ± 0.5a | 0.9 ± 0.2b | 0.2 ± 0.1c |
| ZMD | 1.6 ± 0.5a | 1.8 ± 0.3a | 2.0 ± 0.6a | 2.2 ± 0.7a | 2.9 ± 0.9a | 2.9 ± 0.6a | 1.5 ± 0.5b | 1.2 ± 0.3b |
| YL | 1.1 ± 0.2c | 1.2 ± 0.0bc | 1.5 ± 0.2ab | 1.7 ± 0.3a | 1.4 ± 0.2ab | 1.6 ± 0.0a | 1.1 ± 0.3b | 0.4 ± 0.1c |
| YC | 1.2 ± 0.1a | 1.9 ± 0.1a | 1.9 ± 1.1a | 1.3 ± 1.2a | 0.4 ± 0.0bc | 2.1 ± 0.1a | 1.1 ± 0.6b | 0.2 ± 0.2c |
| GZL | 0.9 ± 0.0a | 0.9 ± 0.1a | 1.2 ± 0.4a | 1.3 ± 0.4a | 0.6 ± 0.1b | 1.8 ± 0.1a | 1.4 ± 0.5a | 0.2 ± 0.0c |
| LS | 0.9 ± 0.2ab | 1.0 ± 0.4ab | 0.7 ± 0.2b | 1.4 ± 0.5a | 0.6 ± 0.1b | 2.0 ± 0.8a | 0.7 ± 0.3b | 0.2 ± 0.1b |
| LSD | 1.1 ± 0.1a | 0.9 ± 0.3ab | 0.7 ± 0.2b | 1.0 ± 0.2ab | 0.8 ± 0.1ab | 1.2 ± 0.4a | 0.6 ± 0.2b | 0.6 ± 0.2b |
| CD | 1.1 ± 0.2a | 1.2 ± 0.2a | 1.0 ± 0.2a | 1.2 ± 0.2a | 0.9 ± 0.2a | 0.8 ± 0.1a | 1.0 ± 0.2a | 1.1 ± 0.2a |
| NJ | 1.6 ± 0.4 | 1.8 ± 0.5 | 1.6 ± 0.6 | 2.2 ± 0.8 | 2.3 ± 0.3 | 2.8 ± 0.7 | 1.3 ± 0.5 | 0.5 ± 0.2 |
| BY | 1.4 ± 0.4a | 1.7 ± 0.4a | 1.2 ± 0.6a | 1.2 ± 0.2a | 1.2 ± 0.4bc | 2.3 ± 0.6a | 1.8 ± 0.8ab | 0.6 ± 0.2c |
| WJ | 2.0 ± 0.3a | 1.5 ± 0.2b | 1.5 ± 0.3ab | 1.8 ± 0.3ab | 2.0 ± 0.3a | 1.7 ± 0.2a | 0.7 ± 0.2b | 0.6 ± 0.1b |
| WX | 1.3 ± 0.2a | 1.3 ± 0.3a | 1.1 ± 0.5a | 1.4 ± 0.3a | 1.0 ± 0.2ab | 1.5 ± 0.3a | 1.1 ± 0.5a | 0.4 ± 0.1b |
| TJ | 0.9 ± 0.3a | 0.7 ± 0.1a | 0.7 ± 0.2a | 0.9 ± 0.1a | 0.8 ± 0.4a | 1.0 ± 0.2a | 0.9 ± 0.3a | 0.3 ± 0.0b |
| FYA | 1.3 ± 0.3a | 1.4 ± 0.2a | 1.4 ± 0.3a | 1.5 ± 0.3a | 1.9 ± 0.6a | 1.7 ± 0.3a | 1.0 ± 0.4ab | 0.4 ± 0.1b |
| ZJ | 0.8 ± 0.3a | 0.4 ± 0.1b | 0.9 ± 0.2a | 1.0 ± 0.1a | 0.5 ± 0.2b | 0.5 ± 0.1b | 1.4 ± 0.2a | 0.6 ± 0.1b |
| FZ | 0.5 ± 0.1ab | 0.6 ± 0.2a | 0.3 ± 0.2b | 0.3 ± 0.1ab | 0.8 ± 0.2a | 1.0 ± 0.3a | 0.6 ± 0.3a | 0.6 ± 0.2a |

| | | | | | | | | |
|---|---|---|---|---|---|---|---|---|
| FH | 1.1 ± 0.3ab | 0.9 ± 0.2b | 1.0 ± 0.3b | 1.5 ± 0.2a | 2.0 ± 0.5a | 1.5 ± 0.3a | 1.7 ± 0.6a | 2.1 ± 0.4a |
| ZY | 1.3 ± 0.5a | 0.6 ± 0.2b | 0.7 ± 0.3b | 1.2 ± 0.2ab | 0.7 ± 0.3a | 0.8 ± 0.3a | 0.5 ± 0.2ab | 0.2 ± 0.0b |
| YT | 0.6 ± 0.3a | 0.4 ± 0.1a | 0.4 ± 0.1a | 0.5 ± 0.2a | 0.6 ± 0.3a | 0.5 ± 0.1a | 0.4 ± 0.1a | 0.2 ± 0.0a |
| JJ | 1.7 ± 0.7a | 1.4 ± 0.8a | 1.2 ± 0.6a | 1.6 ± 0.4a | 0.7 ± 0.3ab | 1.9 ± 1.0a | 0.9 ± 0.5ab | 0.3 ± 0.1b |
| HN | 0.9 ± 0.3a | 0.6 ± 0.2a | 0.7 ± 0.2a | 0.7 ± 0.2a | 1.1 ± 0.4a | 1.0 ± 0.3a | 0.9 ± 0.3a | 0.4 ± 0.1b |
| XS | 0.8 ± 0.2a | 0.9 ± 0.4a | 0.9 ± 0.2a | 0.9 ± 0.4a | 1.0 ± 0.3ab | 1.3 ± 0.5a | 1.2 ± 0.3a | 0.5 ± 0.2b |

The data shown are the seasonal means ± standard deviations of observation periods (sampling period for each site are given in Table S1). Different letters in the columns of “air concentrations” and “dry deposition fluxes” indicate significant difference between the seasons at $p<0.05$. The full names of all sites are presented in Table S1.

**Table S7.** Seasonal average concentrations and deposition fluxes of particulate $NH_4^+$ at twenty-seven monitoring sites in eastern China.

| Sites | Air concentrations | | | | Dry deposition fluxes | | | |
|---|---|---|---|---|---|---|---|---|
| | Spring | Summer | Autumn | Winter | Spring | Summer | Autumn | Winter |
| CAU | 7.9 ± 3.6a | 10.4 ± 3.7a | 7.8 ± 2.0a | 8.8 ± 1.6a | 1.5 ± 0.7a | 2.0 ± 0.8a | 1.2 ± 0.3a | 1.0 ± 0.2a |
| ZZ | 8.2 ± 2.1b | 12.3 ± 4.5b | 10.7 ± 1.7b | 18.9 ± 4.6a | 1.6 ± 0.4a | 2.5 ± 0.9a | 1.6 ± 0.3a | 2.0 ± 0.5a |
| DL | 3.9 ± 0.8a | 4.5 ± 1.6a | 3.9 ± 0.3a | 5.5 ± 0.9a | 0.2 ± 0.1b | 0.3 ± 0.1ab | 0.3 ± 0.0ab | 0.4 ± 0.1a |
| SZ | 6.2 ± 2.2a | 8.7 ± 2.1a | 6.3 ± 1.9a | 6.6 ± 2.0a | 1.2 ± 0.4ab | 1.7 ± 0.4a | 0.9 ± 0.3b | 0.7 ± 0.2b |
| QZ | 15.3 ± 10.5a | 24.2 ± 12.2a | 15.7 ± 9.7a | 23.5 ± 12.6a | 2.9 ± 1.9a | 5.1 ± 2.6a | 2.2 ± 1.4a | 2.3 ± 1.3a |
| YQ | 4.6 ± 1.4a | 5.1 ± 0.6a | 5.0 ± 0.6a | 5.8 ± 1.4a | 0.9 ± 0.3ab | 1.2 ± 0.2a | 0.7 ± 0.1b | 0.6 ± 0.2b |
| ZMD | 11.5 ± 5.4ab | 12.7 ± 4.0a | 8.8 ± 4.2ab | 5.2 ± 0.7b | 2.1 ± 1.0a | 2.1 ± 0.6a | 1.3 ± 0.6ab | 0.6 ± 0.1b |
| YL | 4.8 ± 2.7a | 6.3 ± 2.4a | 4.1 ± 1.8a | 7.0 ± 4.2a | 0.9 ± 0.5a | 1.4 ± 0.6a | 0.6 ± 0.3a | 0.8 ± 0.5a |
| YC | 8.9 ± 0.8bc | 27.9 ± 1.9a | 7.3 ± 0.9c | 13.1 ± 2.8b | 1.6 ± 0.2b | 5.0 ± 0.3a | 1.0 ± 0.2c | 1.3 ± 0.2bc |
| GZL | 4.9 ± 2.3a | 6.1 ± 2.6a | 3.9 ± 0.8a | 5.0 ± 0.5a | 0.8 ± 0.3ab | 1.0 ± 0.5a | 0.4 ± 0.1b | 0.4 ± 0.1b |
| LS | 8.3 ± 5.1a | 9.8 ± 3.1a | 5.9 ± 1.0a | 6.0 ± 1.6a | 1.3 ± 0.8ab | 1.6 ± 0.5a | 0.6 ± 0.1b | 0.4 ± 0.1b |
| LSD | 4.8 ± 0.7a | 5.6 ± 3.3a | 4.5 ± 0.8a | 6.5 ± 1.4a | 0.6 ± 0.1a | 0.7 ± 0.4a | 0.5 ± 0.1a | 0.7 ± 0.2a |
| CD | 5.2 ± 0.8a | 5.5 ± 1.0a | 4.6 ± 1.5a | 4.3 ± 1.4a | 0.2 ± 0.0a | 0.3 ± 0.0a | 0.3 ± 0.1a | 0.3 ± 0.1a |
| NJ | 5.6 ± 2.4 | 4.4 ± 1.8 | 5.4 ± 0.3 | 7.8 ± 0.5 | 0.9 ± 0.3 | 0.5 ± 0.2 | 0.5 ± 0.0 | 0.9 ± 0.1 |
| BY | 3.6 ± 0.8a | 3.8 ± 0.8a | 3.4 ± 1.1a | 4.5 ± 0.3a | 0.5 ± 0.1a | 0.3 ± 0.1b | 0.3 ± 0.1b | 0.6 ± 0.0a |
| WJ | 8.9 ± 0.5a | 3.7 ± 1.5a | 6.5 ± 2.7b | 12.3 ± 1.3b | 4.3 ± 1.0a | 3.4 ± 0.6a | 1.0 ± 0.2b | 1.3 ± 0.5b |
| WX | 4.2 ± 1.3a | 4.6 ± 1.7a | 5.2 ± 0.6a | 6.5 ± 1.0a | 0.6 ± 0.2a | 0.4 ± 0.2a | 0.6 ± 0.1a | 0.7 ± 0.1a |
| TJ | 3.6 ± 1.3a | 3.3 ± 1.2a | 4.5 ± 1.1a | 5.4 ± 2.5a | 0.5 ± 0.2a | 0.4 ± 0.1a | 0.6 ± 0.2a | 0.7 ± 0.3a |
| FYA | 4.9 ± 1.3b | 4.4 ± 0.4b | 5.2 ± 1.2b | 8.7 ± 1.2a | 0.8 ± 0.2a | 0.6 ± 0.1a | 0.6 ± 0.1a | 0.8 ± 0.1a |
| ZJ | 3.6 ± 2.5a | 2.0 ± 0.3a | 4.1 ± 0.6a | 4.6 ± 1.6a | 0.5 ± 0.3a | 0.1 ± 0.0b | 0.4 ± 0.1ab | 0.6 ± 0.2a |

| | | | | | | | | |
|---|---|---|---|---|---|---|---|---|
| FZ | 2.8 ± 0.7a | 1.6 ± 0.3b | 2.1 ± 0.5ab | 2.4 ± 0.6ab | 0.3 ± 0.1a | 0.1 ± 0.0b | 0.2 ± 0.0ab | 0.2 ± 0.1ab |
| FH | 3.6 ± 1.0a | 4.2 ± 1.4a | 3.9 ± 1.5a | 4.5 ± 1.3a | 0.5 ± 0.1a | 0.4 ± 0.1a | 0.4 ± 0.2a | 0.5 ± 0.2a |
| ZY | 5.0 ± 2.1ab | 3.5 ± 1.3b | 4.2 ± 1.4b | 7.2 ± 1.4a | 1.0 ± 0.4a | 0.6 ± 0.2a | 0.6 ± 0.2a | 1.0 ± 0.2a |
| YT | 2.9 ± 1.1a | 2.7 ± 0.8a | 2.4 ± 0.9a | 2.7 ± 0.6a | 0.5 ± 0.2a | 0.4 ± 0.1a | 0.3 ± 0.1a | 0.4 ± 0.1a |
| JJ | 8.9 ± 0.5ab | 3.7 ± 1.5c | 6.5 ± 2.7bc | 12.3 ± 1.3a | 1.8 ± 0.1a | 0.6 ± 0.2b | 0.9 ± 0.4b | 1.9 ± 0.2a |
| HN | 3.5 ± 0.6a | 3.4 ± 1.4a | 4.5 ± 1.2a | 5.4 ± 1.3a | 0.5 ± 0.1ab | 0.3 ± 0.1b | 0.6 ± 0.2ab | 0.7 ± 0.2a |
| XS | 3.6 ± 0.7a | 3.2 ± 0.7a | 4.0 ± 1.5a | 4.1 ± 1.6a | 0.5 ± 0.1a | 0.3 ± 0.1a | 0.5 ± 0.2a | 0.5 ± 0.2a |

The data shown are the seasonal means ± standard deviations of observation periods (sampling period for each site are given in Table S1). Different letters in the columns of “air concentrations” and “dry deposition fluxes” indicate significant difference between the seasons at $p<0.05$. The full names of all sites are presented in Table S1.

**Table S8.** Seasonal average concentrations and deposition fluxes of particulate $NO_3^-$ at twenty-seven monitoring sites in eastern China.

| Sites | Air concentrations | | | | Dry deposition fluxes | | | |
|---|---|---|---|---|---|---|---|---|
| | Spring | Summer | Autumn | Winter | Spring | Summer | Autumn | Winter |
| CAU | 4.7 ± 1.6ab | 4.2 ± 1.2b | 5.9 ± 1.1ab | 6.5 ± 0.8a | 0.9 ± 0.3a | 0.8 ± 0.2a | 0.9 ± 0.2a | 0.7 ± 0.1a |
| ZZ | 4.8 ± 1.1b | 4.3 ± 0.5b | 7.1 ± 2.2b | 13.3 ± 4.5a | 0.9 ± 0.2a | 0.9 ± 0.1a | 1.0 ± 0.3a | 1.4 ± 0.5a |
| DL | 2.5 ± 1.3a | 2.1 ± 0.8a | 1.8 ± 0.9a | 3.6 ± 1.7a | 0.2 ± 0.1ab | 0.2 ± 0.1ab | 0.1 ± 0.1b | 0.3 ± 0.1a |
| SZ | 3.3 ± 0.7a | 2.9 ± 0.9a | 3.9 ± 0.6a | 4.0 ± 1.4a | 0.6 ± 0.1a | 0.5 ± 0.2a | 0.6 ± 0.1a | 0.5 ± 0.1a |
| QZ | 4.5 ± 2.3b | 3.7 ± 1.6b | 6.2 ± 2.8ab | 9.7 ± 4.0a | 0.9 ± 0.4a | 0.8 ± 0.3a | 0.9 ± 0.4a | 0.9 ± 0.4a |
| YQ | 2.7 ± 0.9a | 2.2 ± 0.6a | 2.9 ± 0.8a | 3.1 ± 1.3a | 0.5 ± 0.2a | 0.5 ± 0.2a | 0.4 ± 0.1a | 0.3 ± 0.1a |
| ZMD | 3.7 ± 0.7bc | 3.1 ± 0.6c | 5.4 ± 0.8ab | 6.8 ± 2.0a | 0.7 ± 0.1ab | 0.6 ± 0.1b | 0.8 ± 0.1a | 0.8 ± 0.2a |
| YL | 3.2 ± 0.7b | 2.4 ± 0.3b | 4.1 ± 0.7b | 7.5 ± 2.2a | 0.6 ± 0.1ab | 0.5 ± 0.1b | 0.5 ± 0.1ab | 0.8 ± 0.2a |
| YC | 4.1 ± 0.8ab | 3.0 ± 0.3b | 3.9 ± 1.2ab | 6.6 ± 1.5a | 0.7 ± 0.1a | 0.6 ± 0.1a | 0.5 ± 0.2a | 0.6 ± 0.1a |
| GZL | 1.7 ± 0.4a | 1.7 ± 0.3a | 2.3 ± 0.8a | 2.5 ± 0.8a | 0.3 ± 0.1a | 0.3 ± 0.0a | 0.2 ± 0.1a | 0.2 ± 0.0a |
| LS | 1.6 ± 0.8a | 1.7 ± 0.4a | 2.0 ± 0.5a | 2.4 ± 0.8a | 0.3 ± 0.1a | 0.3 ± 0.1a | 0.2 ± 0.1a | 0.2 ± 0.1a |
| LSD | 2.1 ± 0.4ab | 1.5 ± 0.3b | 1.5 ± 0.7b | 3.1 ± 0.9a | 0.3 ± 0.1a | 0.2 ± 0.0a | 0.2 ± 0.1a | 0.3 ± 0.1a |
| CD | 3.1 ± 0.4a | 2.4 ± 0.3a | 2.7 ± 0.5a | 2.7 ± 0.7a | 0.1 ± 0.0a | 0.1 ± 0.0a | 0.2 ± 0.0a | 0.2 ± 0.1a |
| NJ | 3.5 ± 0.8 | 2.5 ± 0.2 | 2.7 ± 0.9 | 3.8 ± 0.5 | 0.6 ± 0.0 | 0.2 ± 0.0 | 0.3 ± 0.1 | 0.4 ± 0.1 |
| BY | 3.0 ± 0.7a | 2.3 ± 0.4a | 2.2 ± 0.6a | 2.9 ± 0.2a | 0.4 ± 0.1a | 0.2 ± 0.0b | 0.2 ± 0.1b | 0.4 ± 0.0a |
| WJ | 2.7 ± 0.8b | 2.0 ± 0.7b | 2.8 ± 0.7ab | 4.6 ± 1.5a | 0.5 ± 0.2a | 0.4 ± 0.1a | 0.4 ± 0.1a | 0.6 ± 0.2a |
| WX | 1.7 ± 0.5a | 1.3 ± 0.4a | 1.9 ± 1.4a | 2.9 ± 0.6a | 0.2 ± 0.1ab | 0.1 ± 0.0b | 0.2 ± 0.2ab | 0.3 ± 0.1a |
| TJ | 0.9 ± 0.3b | 0.5 ± 0.0b | 1.3 ± 0.6b | 2.5 ± 1.0a | 0.1 ± 0.0b | 0.1 ± 0.0b | 0.2 ± 0.1ab | 0.3 ± 0.1a |
| FYA | 2.8 ± 0.4a | 2.1 ± 0.1a | 3.0 ± 1.4a | 4.5 ± 2.3a | 0.4 ± 0.1a | 0.3 ± 0.0a | 0.3 ± 0.2a | 0.4 ± 0.1a |
| ZJ | 2.3 ± 0.7ab | 1.1 ± 0.2b | 2.2 ± 0.4ab | 3.4 ± 1.5a | 0.3 ± 0.1ab | 0.1 ± 0.0c | 0.2 ± 0.0bc | 0.4 ± 0.2a |

| | | | | | | | | |
|---|---|---|---|---|---|---|---|---|
| FZ | 1.4 ± 0.1a | 1.1 ± 0.1a | 1.1 ± 0.5a | 1.2 ± 0.2a | 0.2 ± 0.0a | 0.1 ± 0.0a | 0.1 ± 0.0a | 0.1 ± 0.0a |
| FH | 1.9 ± 0.3ab | 1.1 ± 0.4c | 1.6 ± 0.7bc | 2.7 ± 0.4a | 0.3 ± 0.0ab | 0.1 ± 0.0c | 0.2 ± 0.1bc | 0.3 ± 0.0a |
| ZY | 1.6 ± 0.4bc | 0.7 ± 0.4c | 1.9 ± 1.0ab | 2.9 ± 0.5a | 0.3 ± 0.1a | 0.1 ± 0.1b | 0.3 ± 0.1ab | 0.4 ± 0.1a |
| YT | 1.3 ± 0.4a | 0.8 ± 0.1a | 0.9 ± 0.6a | 1.2 ± 0.3a | 0.2 ± 0.1a | 0.1 ± 0.0a | 0.1 ± 0.1a | 0.2 ± 0.0a |
| JJ | 2.9 ± 0.7ab | 1.7 ± 0.8b | 2.5 ± 1.6ab | 4.9 ± 0.8a | 0.6 ± 0.1a | 0.3 ± 0.1a | 0.4 ± 0.2a | 0.8 ± 0.1a |
| HN | 1.4 ± 0.3b | 0.6 ± 0.2b | 1.3 ± 0.5b | 3.2 ± 1.9a | 0.2 ± 0.0b | 0.1 ± 0.0b | 0.2 ± 0.1b | 0.4 ± 0.2a |
| XS | 1.2 ± 0.6ab | 0.7 ± 0.1b | 1.2 ± 0.4ab | 2.0 ± 1.0a | 0.2 ± 0.1a | 0.1 ± 0.0a | 0.2 ± 0.0a | 0.2 ± 0.1a |

The data shown are the seasonal means ± standard deviations of observation periods (sampling period for each site are given in Table S1). Different letters in the columns of “air concentrations” and “dry deposition fluxes” indicate significant difference between the seasons at $p<0.05$. The full names of all sites are presented in Table S1.

**Table S9.** Seasonal average concentrations and deposition fluxes of the total $N_r$ at twenty-seven monitoring sites in eastern China.

| Sites | Air concentrations | | | | Dry deposition fluxes | | | |
|---|---|---|---|---|---|---|---|---|
| | Spring | Summer | Autumn | Winter | Spring | Summer | Autumn | Winter |
| CAU | 38.6 ± 4.5ab | 45.3 ± 3.6a | 40.9 ± 4.2ab | 35.7 ± 3.0b | 11.7 ± 2.2b | 21.0 ± 0.3a | 13.6 ± 1.3b | 3.9 ± 0.7c |
| ZZ | 39.6 ± 2.9b | 43.6 ± 4.1b | 43.2 ± 2.0b | 54.6 ± 9.2a | 11.4 ± 1.2a | 12.5 ± 1.3a | 7.0 ± 1.0b | 5.9 ± 0.9b |
| DL | 20.5 ± 6.5a | 21.3 ± 7.1a | 18.9 ± 4.8a | 19.3 ± 4.7a | 5.9 ± 1.6a | 7.7 ± 1.7a | 6.0 ± 1.4a | 2.1 ± 0.2b |
| SZ | 29.4 ± 3.4ab | 35.2 ± 2.1a | 28.1 ± 5.2ab | 25.9 ± 4.4b | 9.0 ± 1.1b | 16.3 ± 1.3a | 9.6 ± 1.2b | 2.9 ± 0.6c |
| QZ | 45.9 ± 18.2a | 55.2 ± 16.5a | 44.5 ± 14.6a | 57.3 ± 22.6a | 12.2 ± 4.2ab | 15.2 ± 4.3a | 8.7 ± 2.6ab | 7.0 ± 3.6b |
| YQ | 23.0 ± 1.1a | 21.2 ± 2.2ab | 19.5 ± 1.1b | 19.7 ± 2.4b | 5.1 ± 0.5b | 6.6 ± 0.8a | 3.6 ± 0.2c | 1.9 ± 0.4d |
| ZMD | 37.4 ± 8.7a | 35.4 ± 7.2a | 36.6 ± 6.2a | 34.0 ± 3.7a | 11.3 ± 1.6a | 10.1 ± 1.2a | 7.7 ± 0.9b | 5.5 ± 0.6c |
| YL | 23.9 ± 6.7a | 26.6 ± 8.2a | 26.0 ± 4.3a | 31.7 ± 7.7a | 6.6 ± 1.7ab | 9.3 ± 2.9a | 6.0 ± 1.2b | 3.8 ± 1.0b |
| YC | 34.9 ± 5.2b | 58.4 ± 5.0a | 35.2 ± 3.1b | 41.6 ± 3.1b | 6.2 ± 0.7bc | 13.8 ± 0.8a | 6.5 ± 0.5b | 4.6 ± 0.2c |
| GZL | 19.1 ± 2.6b | 26.3 ± 3.0a | 17.5 ± 2.2b | 16.1 ± 1.7b | 3.9 ± 0.3b | 10.5 ± 1.0a | 4.4 ± 0.7b | 1.0 ± 0.1c |
| LS | 31.6 ± 8.0a | 31.2 ± 4.4a | 24.3 ± 2.9ab | 18.4 ± 2.3b | 6.5 ± 1.2b | 10.8 ± 1.7a | 5.5 ± 0.8b | 1.8 ± 0.3c |
| LSD | 17.5 ± 1.0a | 20.8 ± 4.4a | 17.5 ± 2.5a | 20.1 ± 2.3a | 4.7 ± 0.4b | 7.7 ± 1.8a | 4.2 ± 0.7bc | 2.4 ± 0.4c |
| CD | 20.7 ± 1.2ab | 21.1 ± 1.8a | 16.9 ± 2.6ab | 16.4 ± 3.4b | 4.9 ± 0.4ab | 6.0 ± 1.1a | 4.5 ± 0.7b | 2.3 ± 0.3c |
| NJ | 30.5 ± 2.0 | 26.8 ± 1.7 | 21.7 ± 1.4 | 28.5 ± 1.0 | 7.8 ± 0.4 | 8.6 ± 1.5 | 4.2 ± 0.8 | 3.1 ± 0.3 |
| BY | 26.2 ± 3.0a | 27.1 ± 1.8a | 23.8 ± 1.7ab | 21.0 ± 0.9b | 5.3 ± 0.8b | 7.0 ± 0.5a | 6.8 ± 0.6a | 3.6 ± 0.2c |
| WJ | 48.5 ± 4.1a | 44.7 ± 11.2a | 27.6 ± 3.9b | 34.7 ± 9.0ab | 12.2 ± 0.8a | 12.5 ± 3.3a | 5.2 ± 1.2b | 5.1 ± 1.2b |
| WX | 20.3 ± 2.6a | 21.4 ± 2.4a | 21.2 ± 4.2a | 21.6 ± 1.1a | 4.5 ± 0.8b | 6.2 ± 0.6a | 4.9 ± 0.6b | 2.6 ± 0.2c |
| TJ | 12.0 ± 2.3a | 11.8 ± 1.1a | 11.8 ± 2.3a | 14.6 ± 2.7a | 2.9 ± 0.8ab | 3.7 ± 0.4a | 3.0 ± 0.8a | 1.8 ± 0.3b |
| FYA | 21.5 ± 3.7a | 24.8 ± 4.2a | 23.3 ± 3.2a | 26.9 ± 3.8a | 6.0 ± 0.2ab | 7.0 ± 1.5a | 4.1 ± 0.7bc | 2.7 ± 0.4c |
| ZJ | 19.6 ± 4.3a | 15.9 ± 1.6a | 18.2 ± 2.7a | 17.4 ± 3.1a | 3.5 ± 0.8b | 3.7 ± 0.5b | 5.0 ± 0.7a | 2.8 ± 0.4b |
| FZ | 10.6 ± 1.3a | 9.6 ± 1.3ab | 6.7 ± 0.6c | 7.9 ± 1.5bc | 3.3 ± 0.6ab | 4.3 ± 1.0a | 2.4 ± 0.3bc | 2.0 ± 0.6c |
| FH | 20.2 ± 3.7a | 18.0 ± 2.2a | 17.9 ± 2.1a | 20.5 ± 1.9a | 6.6 ± 1.5a | 6.2 ± 1.2ab | 5.6 ± 0.7ab | 4.5 ± 0.4b |

| | | | | | | | | |
|---|---|---|---|---|---|---|---|---|
| ZY | 20.1 ± 2.3a | 13.2 ± 3.4c | 14.6 ± 3.0bc | 18.8 ± 1.8ab | 4.5 ± 0.6a | 3.8 ± 1.1ab | 2.8 ± 0.7b | 2.6 ± 0.3b |
| YT | 11.2 ± 2.1b | 15.2 ± 1.3a | 8.6 ± 0.3b | 9.6 ± 0.6b | 2.7 ± 0.8b | 4.9 ± 0.4a | 1.9 ± 0.2bc | 1.2 ± 0.1c |
| JJ | 25.9 ± 1.4ab | 15.5 ± 4.6c | 16.8 ± 5.3bc | 28.0 ± 1.6a | 5.5 ± 0.5a | 5.2 ± 1.9a | 3.6 ± 1.2a | 3.7 ± 0.3a |
| HN | 13.7 ± 1.3b | 14.3 ± 2.2ab | 13.2 ± 2.1b | 17.3 ± 1.5a | 3.7 ± 0.5a | 4.6 ± 1.0a | 3.5 ± 0.9ab | 2.2 ± 0.2b |
| XS | 13.2 ± 1.3ab | 11.0 ± 2.4b | 12.7 ± 1.7ab | 16.7 ± 3.6a | 3.3 ± 0.7ab | 3.7 ± 1.1a | 3.6 ± 0.5a | 2.1 ± 0.2b |

The data shown are the seasonal means ± standard deviations of observation periods (sampling period for each site are given in Table S1). Different letters in the columns of “air concentrations” and “dry deposition fluxes” indicate significant difference between the seasons at $p<0.05$. The full names of all sites are presented in Table S1.

**Table S10.** Seasonal volume-weighted mean concentrations and wet/bulk deposition fluxes of $NH_4^+$-N in precipitation at twenty-seven monitoring sites in eastern China.

| Sites | Volume-weighted mean concentrations | | | | Wet/bulk deposition fluxes | | | |
|---|---|---|---|---|---|---|---|---|
| | Spring | Summer | Autumn | Winter | Spring | Summer | Autumn | Winter |
| CAU | 2.8 | 2.6 | 2.9 | 3.9 | 1.7 ± 0.9b | 10.8 ± 6.8a | 2.5 ± 2.0b | 0.4 ± 0.3b |
| ZZ | 4.5 | 3.2 | 1.6 | 3.8 | 2.6 | 8.0 | 4.5 | 1.3 |
| DL | 2.5 | 0.8 | 1.1 | 5.2 | 1.8 ± 0.9ab | 3.1 ± 0.7a | 1.2 ± 0.4b | 1.2 ± 1.1b |
| SZ | 3.2 | 2.2 | 1.8 | 6.1 | 1.5 ± 1.0b | 7.6 ± 3.9a | 1.8 ± 1.6b | 0.3 ± 0.4b |
| QZ | 3.0 | 4.0 | 2.6 | 3.8 | 2.2 ± 1.5b | 10.5 ± 5.4a | 1.9 ± 0.9b | 0.5 ± 0.9b |
| YQ | 2.8 | 2.1 | 1.5 | 2.7 | 2.0 ± 0.6b | 5.0 ± 1.6a | 2.2 ± 1.4b | 0.2 ± 0.1b |
| ZMD | 2.0 | 2.2 | 2.1 | 3.8 | 2.6 ± 0.2a | 5.8 ± 3.8a | 5.8 ± 5.9a | 1.5 ± 0.9a |
| YL | 2.2 | 2.3 | 2.1 | 6.6 | 2.8 ± 0.9ab | 5.6 ± 3.9a | 4.9 ± 3.7ab | 0.5 ± 0.4b |
| YC | 4.5 | 3.3 | 2.8 | 10.7 | 2.5 ± 1.8b | 10.4 ± 3.1a | 1.5 ± 0.6b | 3.2 ± 3.1b |
| GZL | 2.6 | 1.1 | 1.1 | 2.9 | 2.4 ± 1.3ab | 3.7 ± 0.8a | 1.1 ± 0.2bc | 0.7 ± 0.1c |
| LS | 2.0 | 1.3 | 1.9 | 4.2 | 1.6 ± 0.5b | 4.2 ± 0.9a | 1.7 ± 1.4b | 0.3 ± 0.2b |
| LSD | 2.1 | 1.9 | 1.9 | 1.6 | 1.9 ± 2.4b | 4.8 ± 0.4a | 2.0 ± 1.9b | 0.6 ± 0.4b |
| CD | 2.0 | 1.2 | 0.9 | 3.9 | 1.2 ± 0.3b | 3.7 ± 1.3a | 0.5 ± 0.3b | 1.0 ± 0.8b |
| NJ | 1.1 | 1.6 | 0.7 | 0.9 | 1.1 ± 0.3 | 11.0 ± 1.2 | 1.0 ± 0.2 | 0.6 ± 0.1 |
| BY | 0.6 | 0.3 | 0.4 | 1.0 | 3.5 ± 1.3a | 2.2 ± 0.6ab | 0.7 ± 0.4b | 1.1 ± 1.0b |
| WJ | 2.0 | 1.2 | 1.3 | 6.7 | 3.2 ± 1.4b | 6.4 ± 2.7a | 2.4 ± 0.9b | 1.0 ± 0.9b |
| WX | 1.0 | 1.2 | 1.0 | 1.0 | 3.8 ± 0.8ab | 5.1 ± 2.1a | 2.0 ± 1.3bc | 0.8 ± 0.6c |
| TJ | 2.8 | 2.6 | 2.9 | 3.9 | 5.7 ± 1.4a | 3.7 ± 1.4a | 3.7 ± 1.4a | 5.3 ± 2.8a |
| FYA | 1.2 | 0.8 | 2.0 | 3.4 | 2.2 ± 0.2 | 3.3 ± 0.6 | 2.5 ± 3.3 | 1.7 ± 0.6 |
| ZJ | 0.3 | 0.3 | 0.5 | 0.3 | 0.7 ± 0.6ab | 1.7 ± 0.3a | 1.5 ± 0.6a | 0.1 ± 0.1b |

| | | | | | | | | |
|---|---|---|---|---|---|---|---|---|
| FZ | 0.7 | 0.4 | 0.5 | 0.5 | 3.1 ± 1.2a | 3.1 ± 1.1a | 1.8 ± 2.3a | 1.1 ± 0.4a |
| FH | 0.9 | 0.4 | 0.4 | 1.6 | 2.8 ± 0.8a | 2.8 ± 0.6a | 1.5 ± 1.0a | 3.4 ± 2.2a |
| ZY | 1.9 | 1.0 | 1.0 | 3.3 | 3.7 ± 2.3ab | 5.5 ± 2.0a | 1.8 ± 1.0b | 1.0 ± 1.0b |
| YT | 1.0 | 1.0 | 0.8 | 1.1 | 2.2± 0.2 | 5.8±0.8 | 2.2±0.1 | 0.3±0.3 |
| JJ | 2.5 | 1.3 | 1.5 | 5.6 | 6.0 ±1.5a | 6.4±2.4a | 2.9±1.8a | 3.7±3.3a |
| HN | 1.0 | 0.9 | 0.9 | 1.4 | 5.1±1.3b | 3.9±2.3ab | 2.1±1.1a | 2.4±1.3a |
| XS | 1.1 | 0.5 | 1.0 | 1.6 | 6.3±4.8b | 2.4±1.2a | 2.3±1.4a | 2.6±0.7ab |

The data on wet/bulk deposition fluxes are the seasonal means ± standard deviations of observation periods (sampling periods at all sites are given in Table S1). Different letters in the “wet/bulk deposition fluxes” column indicate significant difference between the seasons at $p<0.05$. The full names of all sites are presented in Table S1.

**Table S11.** Seasonal volume-weighted mean concentrations and wet/bulk deposition fluxes of $NO_3^-$-N in precipitation at twenty-seven monitoring sites in eastern China.

| Sites | Volume-weighted mean concentrations | | | | Wet/bulk deposition fluxes (Mean ± SD) | | | |
|---|---|---|---|---|---|---|---|---|
| | Spring | Summer | Autumn | Winter | Spring | Summer | Autumn | Winter |
| CAU | 3.5 | 2.0 | 3.5 | 4.0 | 2.1 ± 0.6bc | 8.3 ± 2.2a | 3.1 ± 1.5b | 0.4 ± 0.3c |
| ZZ | 4.6 | 2.1 | 1.6 | 2.8 | 2.7 | 5.1 | 4.4 | 0.9 |
| DL | 2.7 | 1.6 | 3.3 | 5.5 | 1.9 ± 0.7bc | 6.0 ± 1.8a | 3.3 ± 0.9b | 1.3 ± 0.9c |
| SZ | 2.3 | 2.4 | 1.8 | 3.0 | 1.1 ± 0.6b | 8.4 ± 6.1a | 1.8 ± 1.4b | 0.1 ± 0.2b |
| QZ | 2.7 | 2.1 | 2.0 | 4.5 | 1.9 ± 2.0b | 5.5 ± 1.6a | 1.5 ± 1.0b | 0.6 ± 1.1b |
| YQ | 2.7 | 1.9 | 2.7 | 3.6 | 2.0 ± 0.5ab | 4.5 ± 1.5a | 3.8 ± 2.7a | 0.2 ± 0.2b |
| ZMD | 2.2 | 1.7 | 1.9 | 2.6 | 2.9 ± 1.5a | 4.5 ± 1.8a | 5.3 ± 6.2a | 1.0 ± 0.2a |
| YL | 1.8 | 1.4 | 1.3 | 4.3 | 2.3 ± 0.9a | 3.2 ± 2.7a | 3.0 ± 1.7a | 0.3 ± 0.3a |
| YC | 4.0 | 2.0 | 2.7 | 4.2 | 2.3 ± 1.8ab | 6.4 ± 3.2a | 1.5 ± 0.9ab | 1.3 ± 0.8b |
| GZL | 2.6 | 1.4 | 1.5 | 2.8 | 2.5 ± 1.0ab | 4.6 ± 2.5a | 1.5 ± 0.5b | 0.6 ± 0.1b |
| LS | 2.8 | 1.1 | 1.5 | 6.0 | 2.3 ± 0.6b | 3.6 ± 0.9a | 1.4 ± 0.4bc | 0.4 ± 0.5c |
| WW | 3.8 | 1.4 | 1.6 | 2.8 | 0.8 ± 0.8ab | 1.0 ± 0.4a | 0.3 ± 0.2ab | 0.1 ± 0.1b |
| LSD | 1.4 | 1.2 | 1.9 | 1.2 | 1.2 ± 0.7ab | 3.1 ± 1.6a | 2.0 ± 1.7ab | 0.4 ± 0.2b |
| CD | 3.2 | 1.3 | 1.6 | 6.1 | 1.9 ± 0.6b | 3.9 ± 0.9a | 1.0 ± 0.5b | 1.6 ± 1.0b |
| NJ | 1.4 | 1.7 | 1.2 | 1.4 | 1.4 ± 0.7 | 11.6 ± 2.1 | 1.7 ± 0.9 | 1.4 ± 0.2 |
| BY | 0.8 | 0.9 | 1.5 | 1.7 | 4.7 ± 1.8ab | 6.9 ± 2.8a | 3.0 ± 1.1b | 1.7 ± 0.6b |
| WJ | 4.8 | 1.0 | 1.8 | 7.3 | 7.8 ± 2.2a | 5.4 ± 3.2ab | 3.2 ± 0.8bc | 1.1 ± 0.7c |
| WX | 0.9 | 1.0 | 0.8 | 1.0 | 3.4 ± 0.7a | 4.1 ± 3.9a | 1.7 ± 0.5a | 0.8 ± 0.6a |
| TJ | 3.5 | 2.0 | 3.5 | 4.0 | 4.0 ± 1.1a | 1.9 ± 0.7a | 3.1 ± 1.4a | 4.0 ± 2.0a |
| FYA | 1.0 | 0.9 | 1.9 | 2.5 | 1.8 ± 0.5 | 3.8 ± 1.7 | 2.4 ± 2.2 | 1.3 ± 0.6 |

| | | | | | | | | |
|---|---|---|---|---|---|---|---|---|
| ZJ | 0.6 | 0.3 | 0.7 | 2.3 | 1.2 ± 0.9a | 1.9 ± 0.3a | 2.1 ± 0.6a | 0.8 ± 1.0a |
| FZ | 0.8 | 0.3 | 0.6 | 0.6 | 3.6 ± 2.0a | 2.8 ± 1.5a | 2.1 ± 1.8a | 1.3 ± 0.6a |
| FH | 1.0 | 0.5 | 0.7 | 1.9 | 3.1 ± 1.2a | 3.7 ± 0.7a | 2.5 ± 0.4a | 4.0 ± 2.9a |
| ZY | 2.0 | 1.0 | 1.3 | 3.5 | 3.8 ± 1.2ab | 5.1 ± 1.8a | 2.2 ± 0.6bc | 1.0 ± 0.7c |
| YT | 0.7 | 0.5 | 0.5 | 2.2 | 1.5 ± 0.4 | 3.0 ± 0.2 | 1.5 ± 0.6 | 0.7 ± 0.6 |
| JJ | 1.5 | 0.7 | 1.0 | 4.4 | 3.6 ± 0.3a | 3.4 ± 1.4a | 2.0 ± 1.2a | 3.0 ± 1.2a |
| HN | 0.6 | 0.4 | 0.6 | 1.1 | 2.9 ± 0.8a | 1.6 ± 0.4a | 1.5 ± 0.8a | 1.9 ± 1.0a |
| XS | 0.5 | 0.3 | 0.6 | 1.2 | 3.1 ± 1.8a | 1.3 ± 0.5a | 1.5 ± 0.8a | 1.9 ± 0.8a |

The data on wet/bulk deposition fluxes are the seasonal means ± standard deviations of observation periods (sampling periods at all sites are given in Table S1). Different letters in the “wet/bulk deposition fluxes” column indicate significant difference between the seasons at $p<0.05$. The full names of all sites are presented in Table S1.

**Table S12.** Seasonal volume-weighted mean concentrations and wet/bulk deposition fluxes of TIN (the sum of $NH_4^+$-N and $NO_3^-$-N) in precipitation at twenty-seven monitoring sites in eastern China.

| Sites | Volume-weighted mean concentrations | | | | Wet/bulk deposition fluxes (Mean ± SD) | | | |
|---|---|---|---|---|---|---|---|---|
| | Spring | Summer | Autumn | Winter | Spring | Summer | Autumn | Winter |
| CAU | 6.3 | 4.6 | 6.4 | 7.9 | 3.9 ± 1.2b | 19.1 ± 8.9a | 5.6 ± 2.9b | 0.8 ± 0.6b |
| ZZ | 9.1 | 5.3 | 3.2 | 6.6 | 5.2 | 13.1 | 8.9 | 2.2 |
| DL | 5.2 | 2.4 | 4.4 | 10.7 | 3.7 ± 1.1b | 9.2 ± 1.3a | 4.5 ± 1.3b | 2.4 ± 1.9b |
| SZ | 5.5 | 4.6 | 3.6 | 9.1 | 2.7 ± 1.5b | 16.0 ± 9.8a | 3.6 ± 3.0b | 0.4 ± 0.6b |
| QZ | 5.7 | 6.1 | 4.6 | 8.3 | 4.1 ± 3.0b | 16.0 ± 6.3a | 3.4 ± 1.7b | 1.1 ± 2.0b |
| YQ | 5.5 | 4.0 | 4.2 | 6.3 | 4.0 ± 1.0bc | 9.6 ± 2.9a | 6.0 ± 3.8ab | 0.4 ± 0.3c |
| ZMD | 4.2 | 3.9 | 4.0 | 6.4 | 5.5 ± 1.3a | 10.3 ± 5.3a | 11.0 ± 12.0a | 2.5 ± 1.1a |
| YL | 4.0 | 3.7 | 3.4 | 10.9 | 5.0 ± 1.6ab | 8.8 ± 6.6a | 7.9 ± 5.1ab | 0.7 ± 0.7b |
| YC | 8.5 | 5.3 | 5.5 | 14.9 | 4.8 ± 3.6b | 16.8 ± 6.0a | 3.0 ± 1.4b | 4.4 ± 3.9b |
| GZL | 5.2 | 2.5 | 2.6 | 5.7 | 4.9 ± 2.3ab | 8.3 ± 3.0a | 2.6 ± 0.5bc | 1.3 ± 0.2c |
| LS | 4.8 | 2.4 | 3.4 | 10.2 | 3.9 ± 1.0b | 7.8 ± 0.6a | 3.1 ± 1.7b | 0.6 ± 0.8c |
| WW | 8.9 | 4.9 | 4.9 | 7.4 | 1.8 ± 1.5ab | 3.6 ± 1.2a | 1.1 ± 0.7b | 0.3 ± 0.3b |
| LSD | 3.5 | 3.1 | 3.8 | 2.8 | 3.1 ± 2.7b | 7.9 ± 1.8a | 4.0 ± 3.6ab | 1.0 ± 0.5b |
| CD | 5.2 | 2.5 | 2.5 | 10.0 | 3.1 ± 0.9b | 7.6 ± 2.0a | 1.5 ± 0.7b | 2.6 ± 1.8b |
| NJ | 2.5 | 3.3 | 1.9 | 2.3 | 2.6 ± 1.0 | 22.6 ± 3.3 | 2.6 ± 0.7 | 2.0 ± 0.3 |
| BY | 1.4 | 1.2 | 1.9 | 2.7 | 8.2 ± 2.2a | 9.1 ± 2.8a | 3.8 ± 1.3b | 2.7 ± 0.8b |
| WJ | 6.8 | 2.2 | 3.1 | 14.0 | 11 ± 2.9a | 11.8 ± 4.1a | 5.6 ± 1.5b | 2.1 ± 1.6b |
| WX | 1.9 | 2.2 | 1.8 | 2.0 | 7.3 ± 1.5ab | 9.1 ± 4.9a | 3.7 ± 1.8ab | 1.6 ± 1.2b |
| TJ | 6.3 | 4.6 | 6.4 | 7.9 | 9.7 ± 2.5a | 5.6 ± 2.0a | 6.8 ± 2.8a | 9.2 ± 4.8a |
| FYA | 2.2 | 1.7 | 3.9 | 5.9 | 4.1 ± 0.6 | 7.1 ± 2.3 | 4.9 ± 5.4 | 3.0 ± 1.2 |
| ZJ | 0.9 | 0.6 | 1.2 | 2.6 | 1.9 ± 0.9ab | 3.6 ± 0.3a | 3.5 ± 1.0a | 0.9 ± 1.1b |
| FZ | 1.5 | 0.7 | 1.1 | 1.1 | 6.7 ± 3.0a | 5.9 ± 2.5a | 3.9 ± 4.1a | 2.4 ± 0.9a |

| | | | | | | | | |
|---|---|---|---|---|---|---|---|---|
| FH | 1.9 | 0.9 | 1.1 | 3.5 | 5.9 ± 1.8a | 6.6 ± 1.1a | 4.0 ± 1.0a | 7.5 ± 5.0a |
| ZY | 3.9 | 2.0 | 2.3 | 6.8 | 7.5 ± 2.4ab | 10 ± 3.0a | 4.3 ± 1.0bc | 2.0 ± 1.7c |
| YT | 1.7 | 1.5 | 1.3 | 3.3 | 3.7 ± 0.6b | 8.8 ± 1.0a | 3.7 ± 0.7b | 1.0 ± 0.9b |
| JJ | 4.0 | 2.0 | 2.5 | 10.0 | 9.6 ± 1.8a | 9.8 ± 3.7a | 4.9 ± 3.0a | 6.7 ± 3.3a |
| HN | 1.6 | 1.3 | 1.5 | 2.5 | 8.1 ± 2.0a | 5.5 ± 2.7a | 3.6 ± 1.8a | 4.3 ± 2.2a |
| XS | 1.6 | 0.8 | 1.6 | 2.8 | 9.4 ± 6.4a | 3.7 ± 1.6a | 3.8 ± 1.9a | 4.5 ± 1.5a |

The data on wet/bulk deposition fluxes are the seasonal means ± standard deviations of observation periods (sampling periods at all sites are given in **Table S1**). Different letters in the "wet/bulk deposition fluxes" column indicate significant difference between the seasons at $p<0.05$. The full names of all sites are presented in **Table S1**.

**Table S13**. Annual $NH_3$ and $NO_x$ emissions over Eastern China and its contribution to total emissions in China (Tg N $a^{-1}$)

| | Source Type | Eastern China | Eastern China/China |
|---|---|---|---|
| $NH_3$ | Fertilizer[a] | 7.3 | 93% |
| | Livestock | 1.8 | 76% |
| | Human waste | 1.4 | 93% |
| | Fuel combustion[b] | 0.6 | 93% |
| | Natural | 0.4 | 81% |
| | Total | 11.6 | 90% |
| $NO_x$ | Industry | 3.1 | 92% |
| | Power | 2.5 | 88% |
| | Transportation | 2.1 | 91% |
| | Residential | 0.3 | 90% |
| | Natural[c] | 0.5 | 68% |
| | Total | 8.5 | 89% |

[a]Fertilizer $NH_3$ emissions include both chemical fertilizer and manure fertilizer.

[b]$NH_3$ emissions from fuel combustion in power plant, industry, transportation and residential.

[c]Natural $NO_x$ emissions from soil, lighting and biomass burning.